

Low-complexity Performance Evaluation Methodologies for OFDMA-based Packet-Switched Wireless Networks

Dem Fachbereich 18
Elektrotechnik und Informationstechnik
der Technischen Universität Darmstadt
zur Erlangung der Würde eines
Doktor-Ingenieurs (Dr.-Ing.)
vorgelegte Dissertation

von
Dipl.-Ing. Andreas Fernekeß
geboren am 03.07.1977 in Frankfurt am Main

Referent:	Prof. Dr.-Ing. Anja Klein
Korreferent:	Prof. Dr.-Ing. Thomas Kürner
Tag der Einreichung:	26. März 2010
Tag der mündlichen Prüfung:	...

Kurzfassung

Zellulare Funknetzwerke müssen sorgfältig geplant werden, um sowohl Servicequalität (QoS) für den Endnutzer zu garantieren als auch Ertrag für den Betreiber zu erzielen. Deswegen werden für eine optimale Planung Abschätzungen für Key Performance Indicators (KPIs) in Abhängigkeit von Parametern wie dem Nutzerscheduling, Datenverkehr und der Datenverkehrslast benötigt. Heutige zellulare Funknetzwerke verwenden Orthogonalen Frequenzteil Vielfachzugriff (OFDMA) und besitzen eine paketvermittelte Netzwerkarchitektur wie zum Beispiel Worldwide Interoperability for Microwave Access (WiMAX) oder Long Term Evolution (LTE) des Universal Mobile Telecommunications System (UMTS). OFDMA und eine paketvermittelte Netzwerkarchitektur werden gebraucht, um einige Anforderungen heutiger zellulärer Funknetzwerke zu erfüllen, wie eine große Systembandbreite um hohe Datenraten zu ermöglichen oder die Verwendung verschiedener Datenverkehrsdienste. Ressourcen in Form von Bandbreite und Zeit können flexibel zur Datenübertragung zugewiesen werden und Endnutzer werden zum Beispiel auf Grund von Kanalinformationen oder QoS Anforderungen für die Datenübertragung ausgewählt. Die Berücksichtigung all dieser Parameter zur Untersuchung von KPIs führt zu einem hohen Rechenaufwand. Normalerweise werden System-Ebene-Simulationen mit Simulationsdauern von Tagen benötigt um genau KPI Ergebnisse zu erhalten.

In dieser Arbeit werden Rahmenbedingungen für die Untersuchung von KPIs in OFDMA basierten paketvermittelten Funknetzwerken aufgestellt. Mit Hilfe dieser Rahmenbedingungen werden zwei neuartige Auswertungsmethodologien aufgestellt. Zuerst wird eine ausschnitt-basierte simulative System-Ebene-Analyse Methodologie vorgeschlagen. Kurze und voneinander unabhängige Ausschnitte werden für die Untersuchung von KPIs berücksichtigt. Für jeden Ausschnitt wird angenommen, dass die Position des Endnutzers sich nicht wesentlich verändert, so dass Ausbreitungsverluste auf Grund von großer räumlicher Distanz nur einmal pro Ausschnitt berechnet werden müssen. Um unabhängige Ausschnitte zu erzeugen, welche zufällig aus der Hauptverkehrsstunde ausgewählt sind, werden Randbedingungen in dieser Arbeit hergeleitet, die beispielsweise die Anzahl aktiver Endnutzer und die Pufferfüllstände beschreiben. Wahrscheinlichkeitsdichtefunktionen (pdfs) für Randbedingungen der Ausschnitte und unter Berücksichtigung von verschiedenen Datenverkehrsmodellen werden in dieser Arbeit aufgestellt. Für jeden Ausschnitt werden die Ankunft von Datenpaketen im Sender, das Endnutzerscheduling und der frequenzselektive und zeitvariante Kanal detailliert modelliert. Die simulative System-Ebene-Analyse Methodologie wird für ein zelluläres Funknetzwerk, verschiedene Kanalmodelle und Endnutzer mit verschiedenen Datenverkehrsdiensten untersucht. Ergebnisse für KPIs werden mit der

simulativen System-Ebene-Analyse Methodologie unter Verwendung eines normalen Arbeitsplatzcomputers schon nach einigen Stunden erreicht im Gegensatz zu Simulationsdauern von mehr als einem Tag mit herkömmlichen dynamischen System-Ebene-Simulationen. Die Genauigkeit der KPI Ergebnisse unter Verwendung der simulativen System-Ebene-Analyse Methodologie ist vergleichbar mit der Genauigkeit, die mit herkömmlichen dynamischen System-Ebene-Simulationen erzielt werden kann.

Als zweites wird in dieser Arbeit eine analytische System-Ebene-Bewertungsmethodologie definiert, welche analytische Berechnungen von KPIs für paketvermittelte Funknetzwerke beinhaltet, so dass Ergebnisse für KPIs noch schneller als mit der vorgeschlagenen simulativen System-Ebene-Analyse Methodologie erzielt werden können. Basierend auf den entwickelten Rahmenbedingungen für die Bewertung von KPIs in paketvermittelten Funknetzen, werden Eigenschaft in OFDMA basierten paketvermittelten Funknetzwerken analytisch beschrieben. Beispielsweise werden Herleitungen für pdfs der Anzahl aktiver Nutzer, der Veränderung des Signal zu Interferenz Verhältnisses (SIR) und der Anzahl allozierter Ressourcen auf Grund des Endnutzerschedulings gegeben, so dass KPIs analytisch berechnet werden können. Eine Untersuchung der analytischen System-Ebene-Bewertungsmethodologie für ein zellulares Funknetzwerk zeigt, dass KPI Ergebnisse innerhalb von Sekunden erzielt werden auf Kosten von einem Fehler in den KPI Ergebnissen, der kleiner als 15 % verglichen mit System-Ebene-Simulationen ist. Deswegen ist die analytische System-Ebene-Bewertungsmethodologie fähig Planungswerkzeuge für OFDMA basierte paketvermittelte Funknetzwerke zu verbessern, indem sie schnell Werte für die KPIs berechnet. Gleichwohl sollten System-Ebene-Simulationen verwendet werden um präzise KPIs für den endgültigen Netzwerkaufbau zu erhalten.

Der Einfluss von Datenverkehr und Endnutzerscheduling auf KPIs wird mit Hilfe der entwickelten Methodologien untersucht. Unter anderem wird gezeigt, dass der mittlere Durchsatz pro Endnutzer fast proportional zu dem Kehrwert der mittleren Anzahl aktiver Nutzer ist beziehungsweise dass ähnliche Ergebnisse für den durchschnittlichen Durchsatz pro Zelle erreicht werden, wenn das Verhältnis der mittleren Anzahl aktiver Nutzer und der Serverdatenrate konstant bleibt. Desweiteren werden Grenzwerte bestimmt, welche die erreichbare Performanz für drei unterschiedliche Endnutzerschedulingstrategien beschreiben. Letztendlich werden KPI Ergebnisse für ein frei zugängliches Referenzszenario präsentiert, welches reale Umgebungsdaten von europäischen Großstädten beinhaltet, um zu zeigen, dass die entwickelte simulative System-Ebene-Analyse Methodologie und die entwickelte analytische System-Ebene-Bewertungsmethodologie beide fähig sind KPIs für reale Umgebungszenarien zu untersuchen und deswegen auch in der Planung OFDMA basierter paketvermittelter Funknetze eingesetzt werden können.

Abstract

Cellular wireless networks have to be accurately planned to provide Quality of Service (QoS) to the user and to achieve revenue for the operator. Therefore, estimates of key performance indicators (KPIs) depending on parameters like the user scheduling, the data traffic and the data traffic load are necessary for planning of cellular wireless networks. Today's cellular wireless networks are based on orthogonal frequency division multiple access (OFDMA) and a packet-switched network architecture like in, e.g., Worldwide Interoperability for Microwave Access (WiMAX) or Long Term Evolution (LTE) of Universal Mobile Telecommunications System (UMTS). OFDMA and a packet-switched network architecture are suitable for many challenges that today's cellular wireless networks have to cope with, e.g., a large system bandwidth to provide high data rates or different traffic services. Resources in terms of bandwidth and time can be allocated for transmission of data in a very flexible manner and users are scheduled for transmission, e.g., depending on channel state information or QoS requirements. The consideration of all these parameters for evaluation of KPIs leads to a high computational complexity. Usually, system level simulations are required with simulation durations of days to obtain accurate results for KPIs.

In this work, a framework is derived for evaluation of KPIs in OFDMA based packet-switched wireless networks. Based on this framework, this thesis gives two novel evaluation methodologies. At first, a snapshot based simulative system level analysis methodology is proposed. Short and independent snapshots are considered for the evaluation of KPIs. During each snapshot, it is assumed that the location of a user does not change significantly so that large-scale propagation loss only has to be calculated once per snapshot. To get independent snapshots that are randomly selected from the busy hour, constraints are derived in this thesis, e.g., for the number of active users and the buffer occupancy at snapshot start. Probability density functions (pdfs) are given in this thesis for the constraints considering different data traffic models. During each snapshot, the arrival of data packets in the transmitter, user scheduling and the frequency selective and time variant small scale fading channel are modelled in detail. The simulative system level analysis methodology is evaluated assuming a cellular wireless network, different channel models for the transmission of data and users that utilise different data traffic services. It only takes several hours to achieve KPI results with the simulative system level analysis methodology using a standard personal computer instead of more than a day with state-of-the-art dynamic system level simulations. The accuracy of the KPI results using the simulative system level analysis methodology is comparable to the accuracy achieved with state-of-the-art dy-

namic system level simulations. The simulative system level analysis methodology is suitable for accurate performance evaluation of a specific network configuration.

Secondly, an analytical system level evaluation methodology is defined in this thesis that contains an analytical calculation of KPIs for packet-switched wireless networks so that results for KPIs are achieved even faster than with the proposed simulative system level analysis methodology. Based on the developed framework for evaluation of KPIs in packet-switched wireless networks, properties in OFDMA based packet-switched wireless networks are described analytically. Derivations for pdfs of, e.g., the number of active users, the change in signal to interference ratio (SIR) and the number of allocated resources due to user scheduling are derived in this thesis so that KPIs are calculated analytically. Evaluations of the analytical system level evaluation methodology assuming a cellular wireless network indicate that KPI results are obtained within seconds at the expense of an error in KPI results below 15 % compared to system level simulations. Therefore, the analytical system level evaluation methodology is able to enhance planning tools for OFDMA based packet-switched wireless networks by providing fast estimates for KPIs. Nevertheless, system level simulations shall be used to obtain precise KPIs for the final network layout.

The impact of data traffic and user scheduling on KPIs is evaluated using the developed methodologies. Among others, it is shown that the average user throughput is almost proportional to the inverse of the average number of active users or that for a constant ratio between the average number of active users and the server data rate similar average cell throughput results are achieved. Furthermore, thresholds are derived indicating the performance that can be achieved for three different user scheduling strategies. Finally, KPI results are presented for a public reference scenario representing real world scenarios for European cities indicating that the developed simulative system level analysis methodology and the developed analytical system level evaluation methodology are both able to give KPIs for real world scenarios and can be applied in the planning process of OFDMA based packet-switched wireless networks.

Contents

1	Introduction	1
1.1	OFDMA based packet-switched wireless networks	1
1.2	Performance evaluation of cellular wireless networks	4
1.3	State-of-the-art	8
1.4	Problem statement	12
1.5	Thesis overview and contributions	14
2	Scenario assumptions	17
2.1	Introduction	17
2.2	User distribution	18
2.3	Channel model	20
2.4	Data traffic model	22
2.5	Resource unit definition	26
2.6	User scheduling	27
2.7	Key performance indicators (KPIs)	30
3	Simulative system level analysis methodology	33
3.1	Snapshot based system level simulation methodology	33
3.2	User placement and large-scale propagation loss calculation	36
3.3	Data traffic generation	37
3.3.1	Introduction	37
3.3.2	Speech traffic	39
3.3.3	Download traffic	40
3.3.4	Web browsing traffic	42
3.4	Effective resource unit performance	44
3.5	User scheduling	48
3.6	KPI measurements	49
3.7	Performance and complexity evaluation	50
3.7.1	Introduction	50
3.7.2	Number of snapshots	54
3.7.3	Snapshot duration	57
3.7.4	Effective SIR calculation	63
3.8	Conclusion	68
4	Analytical system level evaluation methodology	71
4.1	Introduction	71
4.2	User placement and large-scale propagation loss calculation	74

4.3	Data traffic consideration	76
4.3.1	General problem statement	76
4.3.2	Speech traffic	77
4.3.3	Download and web browsing traffic	80
4.3.4	Resource unit utilisation	81
4.4	Resource unit consideration	84
4.5	User scheduling	85
4.5.1	General problem formulation	85
4.5.2	SIR gain	87
4.5.2.1	General problem formulation	87
4.5.2.2	Fair resource scheduling	87
4.5.2.3	Proportional fair scheduling	88
4.5.2.4	Fair throughput scheduling	89
4.5.3	Number of allocated resource units	90
4.5.3.1	General problem formulation	90
4.5.3.2	Fair resource scheduling	90
4.5.3.3	Proportional fair scheduling	91
4.5.3.4	Fair throughput scheduling	92
4.6	KPI measurements	95
4.7	Performance and complexity evaluation	99
4.7.1	Introduction	99
4.7.2	Approximation of SIR due to large-scale propagation loss	100
4.7.3	Number of active users during the session duration	101
4.7.4	Effective small-scale fading model	106
4.8	Conclusion	108
5	Impact of user scheduling and data traffic on network capacity	111
5.1	Introduction	111
5.2	System parameter assumptions	111
5.3	Impact of data traffic on the network capacity	113
5.3.1	Introduction	113
5.3.2	User performance	115
5.3.3	Cell performance	118
5.3.4	Network performance	119
5.3.5	Rules for the impact of data traffic on the network capacity	120
5.4	Impact of scheduling on the network capacity	121
5.4.1	Introduction	121
5.4.2	User performance	122
5.4.3	Cell performance	125

5.4.4	Network performance	126
5.4.5	Rules for the impact of user scheduling on the network capacity	128
5.5	Real world scenarios	130
6	Conclusions	135
	Appendix	139
A.1	Numerical solution of the mutual information formula	139
A.2	Derivation of state transition probabilities in an $M/M/\infty$ queueing system	141
	List of Acronyms	145
	List of Symbols	149
	Bibliography	151

Chapter 1

Introduction

1.1 OFDMA based packet-switched wireless networks

One major challenge for wireless networks nowadays and in future is the ubiquitous demand for high data rates combined with many different data traffic services that are utilised in such networks [PGL⁺97, UMT99, ITU00, WDK⁺09]. In contrast to prior wireless networks, higher system bandwidth, adaptive modulation schemes and adaptive coding rates are necessary to achieve higher data rates. Furthermore, different data traffic services including, e.g., speech traffic, download traffic or web browsing traffic, can be served more efficiently in packet-switched than in circuit-switched networks.

A high system bandwidth leads to sensitivity to frequency-selective channel variations. To combat frequency-selective channel variations, Orthogonal Frequency Division Multiplexing (OFDM) is used where the available system bandwidth is divided into several small bands that are called subcarriers and that are orthogonal to each other [Bin90, vNP00, HP03]. A multiple access scheme can be used based on OFDM called Orthogonal Frequency Division Multiple Access (OFDMA) [vNP00, PY04]. In OFDMA, a fraction of the available bandwidth is allocated for transmission. Due to the possibility to change the allocation of the bandwidth after a certain number of OFDM symbols, a mixture of OFDMA and Time Division Multiple Access (TDMA) can be used allocating a specific fraction of the available bandwidth for a specific time duration. OFDMA is also a promising candidate for future wireless networks [PY04, WDK⁺09]. To reduce complexity in realistic networks, resource units are formed which are transmitted using one modulation scheme and one coding rate. Each resource unit contains a number of subcarriers and a number of OFDM symbols. For Long Term Evolution (LTE) of Universal Mobile Telecommunications System (UMTS), resource units are termed physical resource blocks [3GP06] and for Worldwide Interoperability for Microwave Access (WiMAX), resource units are termed slots [IEE05]. The data rate of the transmission is adapted to the channel state information using different modulation schemes and coding rates so that high data rates can be achieved in good channel conditions while still a successful transmission is guaranteed in bad channel conditions [JL03, ZL04, LZ06].

Furthermore, an increasing utilisation of data traffic services like web browsing or download traffic will be observed in future networks [PGL⁺97,UMT99]. Data traffic services have a bursty characteristic, where intervals can be observed when a high amount of data has to be transmitted and intervals with only small amount of data to be transmitted. Therefore, packet-switched networks are more suitable than circuit-switched networks due to allocating resources, e.g., bandwidth and time, flexibly depending on the amount of data that has to be transmitted [ZL04,LZ06]. In circuit-switched networks, resources are reserved for the whole duration when the connection is established and resources are wasted in intervals for which only small amount of data is available. Especially in networks using OFDMA, resource units can be assigned for each transmission in a very flexible manner. The flexible allocation of resource units can be performed in different ways considering for instance channel state information or Quality of Service (QoS) requirements. The decision which user is allowed for transmission of data packets on certain resource units termed user scheduling, plays a major role in packet-switched wireless networks [YL00,LZ06].

Cellular wireless networks play a major role nowadays. Networks like LTE or WiMAX which are the focus of this work are currently under development and under standardisation by 3rd Generation Partnership Project (3GPP) [3GP08b] and Institute of Electrical and Electronic Engineers (IEEE) [IEE05], respectively. Compared with existing wireless networks like Global System for Mobile Communications (GSM), networks like LTE or WiMAX provide high data rates and are designed to handle different data traffic services. In contrast to ad hoc networks like Wireless Local Area Networks (WLANs), cellular wireless networks require infrastructure [Rap02]. For instance, base stations (BSs) and controlling entities for the BSs, e.g., Radio Network Controllers, have to be placed, the core network including, e.g., home location register or mobile switching centres has to be designed and backbone connections to the internet or telephone networks have to be established [Mis04]. Cellular wireless networks are usually controlled by an operator. Users have to pay to utilise services and to establish connections. Therefore, users expect, e.g., to be able to establish and maintain a connection everytime and everywhere. Cellular wireless networks have to be planned accurately for two main reasons. At first, key performance indicators (KPIs) have to be met. KPIs represent user, cell or network performance. Secondly, costs for building the infrastructure and operating the network should be minimised. Expenses are necessary, e.g., to buy BSs or Radio Network Controllers. Furthermore, operational expenses occur, e.g., due to power supply or the rent for the site, where the BS is located. Accurate estimates of KPIs are required to be able to setup an optimal network infrastructure, e.g., locations of BSs [Kür98,MOM03b].

The planning of cellular wireless networks is usually conducted in two steps. At first,

coverage planning is performed to ensure that a minimum received power is guaranteed at every location within the network. Secondly, capacity planning is performed so that the load due to data traffic can be transmitted and, e.g., enough bandwidth is available so that each user is able to achieve the required QoS, e.g., in terms of throughput or delay [Mis04]. In wireless communication, the signal power decreases with increasing distance between the transmitter and the receiver due to propagation loss [Rap02]. Considering effects that are able to increase the power, e.g., antenna pattern with gain in a specific direction compared to an isotropic transmitter, and effects that decrease the power, e.g., cable or feeder loss, a maximum propagation loss can be calculated so that a minimum received power is achieved considering the thermal noise power spectral density. This is called link budget calculation, e.g. [LW01, HT02]. Assuming a specific propagation loss model, a maximum cell radius can be derived based on the maximum propagation loss calculated in the link budget calculation. To consider also worst case scenarios in link budget calculations, margins are introduced, e.g., for shadow fading or fast fading as well as for interference due to varying traffic load [HT02, HB02]. These margins account for scenarios where, e.g., losses due to shadowing effects behind buildings or fast fading conditions are not favourable.

During capacity planning, the traffic load is taken into account. The network has to be planned so that each user can establish a connection and get access to the resources and that QoS is fulfilled during the connection. In circuit-switched wireless networks like GSM, the Erlang B formula can be used to determine the capacity of a cell [Erl17, Kle75, Ang01]. The Erlang B formula describes an analytical relationship between the probability that a new user does not get access to the network, the number of available resource units and the traffic load. In packet-switched networks, immediate access to resources is not necessary since packets can be buffered in the transmitter to a certain extent. However, QoS requirements demand that, e.g., a certain delay is not exceeded for transmitting packets or a certain throughput is achieved. Furthermore, packet-switched wireless networks have more properties that have to be considered as described above, like different data traffic services and their properties, scheduling or the flexible allocation of bandwidth and time. Therefore, it is a challenge to accurately obtain the capacity of cells in OFDMA based packet-switched wireless networks like LTE or WiMAX, i.e., how many users the cell can serve while guaranteeing QoS, e.g., a certain user throughput. Since the setup of a testbed is very expensive, simulations on system level are suitable to achieve estimates of the capacity of OFDMA based packet-switched wireless networks. Due to the circumstance that data traffic has an asymmetric characteristic and a higher traffic load usually is observed for the transmission from the BS to the user which is named downlink [UMT99, ITU00], usually the downlink is considered.

1.2 Performance evaluation of cellular wireless networks

The evaluation of the performance of cellular wireless networks like LTE or WiMAX is described in this section. A framework of aspects that have to be considered in the performance evaluation of wireless cellular networks is given in Figure 1.1. For evaluating the performance of cellular wireless networks, users are placed in the investigation area and large-scale propagation loss is calculated based on the distance between the BSs and the user. Data traffic services can be considered by application of appropriate data traffic models [ETS98, WiM07, WIN06]. Properties of the applied network have to be considered like the setup of the frame, e.g., how resources can be allocated depending on the multiple access scheme or which bandwidth is available. The modelling of fast variations of the channel transfer function due to multipath fading is considered together with the frame setup in the framework given by Figure 1.1 due to interactions that can be observed. The channel transfer factors have to be calculated for subcarriers that are included in the frame. The scheduling of the users is essential for packet-switched networks. During scheduling it has to be determined which connection shall transmit data and what resources, e.g., bandwidth or time, shall be used for the transmission. Finally, KPI measurements are performed, e.g., of user, cell or network performance, to get estimates of the capacity of the network.

System level simulations can be classified in two approaches, namely static system level simulations and dynamic system level simulations [LWNH01, NBL05]. Table 1.1 com-

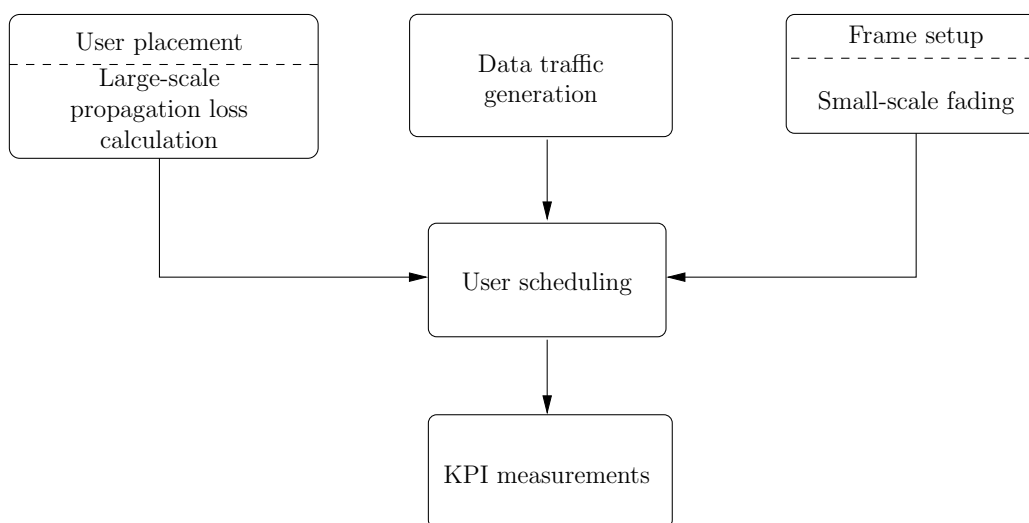


Figure 1.1. Framework for performance evaluation of wireless cellular networks

compares features of static and dynamic system level simulations based on the framework presented in Figure 1.1. For static system level simulations, users are placed into the investigation area so that the probability density function (pdf) of user locations is fulfilled. For each user location, the large-scale propagation loss has to be calculated depending on the distance between transmitter and receiver [Rap02]. As indicated by the name, static system level simulation do not consider user movement. To consider user movement, dynamic system level simulations have to be used. In dynamic system level simulations, user locations are determined as the result of the applied mobility model [CBD02]. In contrast to static system level simulations, user positions need to be updated due to the movement. Large-scale propagation loss also needs to be calculated for the new position. The update of the user position and the large-scale propagation loss increases the complexity of dynamic system level simulations compared to static ones.

In static system level simulations, no realistic data traffic is considered. Rather, it is assumed that each user has always enough data available for transmission which is known as full buffer traffic model [HSVC03]. The consequence is that the network is fully loaded and a worst case scenario is assumed in terms of signal to interference plus noise ratio (SINR). However, the full buffer traffic model also leads to cell performance results that are too optimistic compared with realistic data traffic models [FKWD06]. Realistic traffic models can be considered in dynamic system level simulations by modelling the session arrival process as well as the session duration in detail. However, the generation of data traffic is very complex, e.g., an initialisation is necessary at the beginning of the investigation. If a network with zero active users is assumed for the beginning of the investigation, it takes a certain time until reliable measurements can be obtained [Kle75]. Furthermore, the number of active users may vary only very slowly in time so that a long time duration has to be observed. Therefore, a long simulation duration is necessary.

The frame setup and the small-scale fading are considered together in the framework presented in Figure 1.1. In static system level simulations, no temporal dependency, e.g., of the small-scale fading channel is considered so that the frame structure of the considered network is also not important. Rather, the average SINR is calculated for each symbol assuming that all BSs transmit with the maximum transmit power and the average SINR is considered for the whole OFDM symbol [NBL05]. Therefore, static system level simulations are not able to consider effects of varying channel transfer factors due to frequency-selective fading and only average values of the channel transfer factors are taken into account. In dynamic system level simulation, the frequency-selective and time varying fading channel is modelled in detail and the channel transfer factor is derived for each subcarrier [WiM07]. Furthermore, the frame structure is also

built in detail and used during the scheduling decision [WiM07,LJZ09]. Especially, the calculation of the channel transfer factor for each subcarrier leads to a high complexity of dynamic system level simulations. OFDMA based networks like LTE or WiMAX may contain several hundreds of subcarriers [3GP06, WiM07].

User scheduling is very essential in the performance evaluation of OFDMA based packet-switched wireless networks [CL01, FKWD06, PKM06]. However, static system level simulations cannot consider sophisticated user selection and only a random user selection can be considered [BHIM05]. Therefore, multiuser diversity due to user scheduling is not observed in static system level simulations [KH95, BHIM05]. Dynamic system level simulations are used to investigate the impact of user scheduling on network and user performance and scheduling is investigated on time slot or frame basis [PKM06, LJZ09]. The modelling of the scheduling in dynamic system level simulations is very complex due to decisions that have to be done for each resource unit, e.g., which user is selected for transmission, which modulation scheme and coding rate shall be used or which transmit power is used.

Finally, performance measurements can be obtained with both dynamic and static system level simulations. However, the accuracy of the results differ. Static system level simulations are very suitable to obtain results on received power and SINR at the receiver due to large-scale propagation loss. Throughput results are achieved by mapping, e.g., SINR values onto average throughput results obtained by simulations considering the link between one transmitter and one receiver, e.g. [HSH⁺97, BHIM05]. Nevertheless, there are effects considered in static system level simulations that have impact on the accuracy of the throughput results. The consideration of full buffer traffic leads to throughput results that are higher than throughput results if realistic data traffic is considered [FKWD06]. Sophisticated scheduling algorithms are able to increase the throughput compared to random user scheduling as considered in static system level simulations, e.g. [KH95, VTL02, BHIM05]. Dynamic system level simulation are also able to achieve results on the SINR at the receiver. In contrast to static system level simulations, not only the average SINR is measured but also the actual SINR for a certain subcarrier and the temporal development of the SINR due to small-scale fading and user movement is measured. SINR values are mapped to block error probability (BLEP) values for the resource units [BSC⁺04, DS04, BAS⁺05, SGLV09] and the throughput is calculated by the ratio of the data that is successfully received and the time duration needed for the transmission. The consideration of all aspects of the framework presented in Figure 1.1 in detail in the dynamic system level simulation leads to very high computational complexity and very long simulation durations that could take many days.

Table 1.1. Overview of system level simulation methodologies

Part of the simulator structure	Static system level simulation		Dynamic system level simulation	
	Modelling	Disadvantages	Modelling	Disadvantages
User placement and large-scale propagation loss calculation	Fix user locations as samples of user location pdf in the cellular environment	No movement of the users possible	Location of a user determined based on the applied mobility model	User position and large-scale propagation loss has to be updated during the movement
Data traffic generation	No realistic data traffic is considered, each user has always enough data available for transmission	Network is fully loaded, worst case SINR considered	Session start and whole session modelled in detail, user vanishes after session end	Traffic generation is complex, initialisation phase in the beginning, number of active users varies slowly in time
Frame setup and small-scale fading	Only whole OFDMA symbols are considered, average SINR is calculated, all BSs transmit with maximum transmit power	Only consideration of the average value of the channel transfer factors	Frequency-selective and time varying fading modelled in detail, channel transfer factor for each subcarrier, frame structure is built in detail due to scheduling decision	Complex due to consideration of the channel transfer factors in detail, SINR has to be calculated for each subcarrier and OFDMA symbol
User scheduling	Only random user scheduling	No multiuser diversity	Modelled in detail for different scheduling algorithms and on frame or time slot basis	Complex due to making a scheduling decision for each resource unit, adaptive allocation of resource units, power, modulation and coding
KPI measurements	E.g., receiver SINR, average user/cell throughput	No QoS measurement, e.g., of the delay of transmitted packets	E.g., receiver SINR, user and cell throughput, QoS measurements, modulation and coding scheme utilisation	Long simulation time

1.3 State-of-the-art

This section gives a review of the state-of-the-art of the planning and the performance evaluation of wireless networks.

Planning of wireless cellular networks is performed in two steps, namely coverage planning and capacity planning [LW01, LWN02, Mis04]. During coverage planning, link budget calculations are used to determine the maximum possible propagation loss so that a minimum SINR is guaranteed at the receiver [LWN02, HT02, Mis04]. Margins are included to consider worst case scenarios, e.g., due to shadowing effects behind buildings. Furthermore, margins are added in Code Division Multiple Access (CDMA) networks like UMTS to consider load dependent interference [HB02]. Due to imperfect autocorrelation and crosscorrelation properties of the spreading sequences, intra-cell and inter-cell interference increases if the number of users increases [Rap02]. In networks using OFDMA, intra-cell interference can be avoided due to using orthogonal subcarriers. When transmitting subcarriers that are distributed over the whole system bandwidth as it is proposed for the uplink of LTE and the default transmit modes of WiMAX, interference averaging can be observed if subcarriers are distributed differently in neighboring cells [MFK⁺06]. In [FKW⁺08], a load dependent interference margin is derived for OFDMA networks that are only partially loaded.

Besides the maximum cell radius which is the result of the coverage planning, it is necessary to be aware of the traffic load each cell can cope with. In circuit-switched networks, users get one resource unit allocated for the whole session duration and a reliable transmission can be guaranteed. However, it may happen that all available resource units are allocated when a new user arrives in the network so that this user has to be blocked. Blocking a user leads to unsatisfaction because this user is not able to establish a connection. The Erlang B formula describes an analytical relationship between the blocking probability, the number of available resource units and the traffic load [Erl17, Kle75, Ang01]. For circuit-switched networks, the Erlang B formula is used to determine, e.g., how many resource units are necessary to cope with a given traffic load of a specific area and a predefined blocking probability. Speech traffic is assumed so that the number of active users is given by a random variable with Poisson distribution and each user utilises one resource unit during the whole session duration. In [HS04], it is shown that also web browsing traffic leads to a number of active users that is given by a random variable with Poisson distribution so that the capacity of networks with web browsing users can also be determined using the Erlang B formula. However, it is assumed in [HS04] that each web browsing user utilises one resource unit during the whole session which is only valid in circuit-switched networks.

For packet-switched networks, there is no work that gives a similar description for the amount of traffic load one cell is able to cope with as the Erlang B formula. Usually, system level simulations are used to derive, e.g., the spectral efficiency of a cell in a packet-switched network which is an indicator for the traffic load that can be handled [LW01, LWN02, Mis04]. In the following, a review of system level simulations in the literature is given and the state-of-the-art for parts of the framework presented in Figure 1.1 is discussed.

A static system level simulator for planning issues of wideband CDMA networks is described in [WLSJ99]. The simulator considers the network scenario and different user distributions and presents results, e.g., on the signal to interference ratio (SIR) and is suitable for coverage predictions. Another static simulator is presented in [TH01] which is optimised for evaluation of small cells in indoor environments. The performance of static simulators for wideband CDMA is described in [NBL05] showing that widely used propagation models have some limitations with respect to measurements. However, static system level simulations are widely used, especially for coverage planning because the computational complexity is acceptable [WLSJ99, LWS00, LW01, LWN02].

Dynamic system level simulations gained great attention with the introduction of packet-switched wireless networks due to the different aspects that have to be considered in detail as indicated in the framework presented in Figure 1.1. In [HHS99], a dynamic system level simulator is proposed for wideband CDMA networks. The proposed simulator considers the modelling of the propagation channel, of the user movement, of the data traffic and of user scheduling in detail and is able to give results, e.g., on the transmit power of a BS as function of the time. The simulator proposed in [HDP⁺04, HPD⁺04] is also able to evaluate the performance of UMTS networks. Data traffic is modelled in detail. A special configuration is used for cells at the border to avoid border effects. A simulator for performance evaluation of scheduling in LTE is presented in [PKM06] which models user scheduling and the frame setup in detail but applies only a simple traffic model with a fixed download size. Only one cell is simulated in detail and additional cells are created to generate a realistic interference scenario for the investigation.

Simulators for WiMAX networks are presented, e.g., in [WGL⁺05, BHIT05a, BHIT05b, LJZ09]. The simulator proposed in [WGL⁺05] considers the WiMAX frame structure in detail and models realistic web browsing traffic. Multipath channel models are used to generate frequency-selective and time varying small-scale fading. An effective SINR is calculated for each OFDM symbol using the exponential function. The BLEP corresponding to the effective SINR as obtained from simulations considering only one connection are used to derive the BLEP of the packets. The authors in [BHIT05a,

[BHIT05b] describe a system level simulation model for various scenarios. Cells are wrapped onto a torus to avoid border effects. User scheduling and data traffic are modelled in detail. Different mobility models can be applied to the users so that fixed and mobile users experience different channel models. The dynamic system level simulator presented in [LJZ09] contains the generation of data packets so that realistic data traffic is modelled. Various scheduling algorithms and QoS classifications are implemented. The simulator contains different methodologies how a fraction of the bandwidth can be allocated for transmission, namely an allocation of neighboured subcarriers or an allocation of subcarriers that are distributed over the whole system bandwidth.

In the following, properties of the framework presented in Figure 1.1 are discussed in detail. In dynamic system level simulations, the user movement increases computational complexity due to location updates that are necessary during the simulation duration. There are investigations, e.g., in [BHIT05a] where only users with fix location are assumed which reduces the computational complexity but this is an assumption that cannot be drawn for every investigation. To derive large-scale propagation loss based on the location of the user, different analytical large-scale propagation loss models can be used [Kür05]. An overview is given, e.g., in [Rap02, Mol05]. The analytical large-scale propagation loss models may have limitations compared to real world scenarios as shown in [NBL05] but are well established for evaluation of wireless cellular networks. Border effects occur during the evaluation of wireless cellular networks due to a finite investigation area. BSs at the border of the investigation area have less neighbours than BSs in the centre of the investigation area. In [HDP⁺04, HPD⁺04], a special configuration is proposed for cells at the cell border, which are excluded from the measurements. It is also possible to extend the investigation area by mapping the investigation area onto a torus [ZK01, BHIT05a, BHIT05b]. If the investigation area is mapped onto a torus, measurements can be obtained from all cells.

For the generation of data traffic, different models are proposed that reflect the properties of different data traffic services, e.g., of speech, download or web browsing traffic. Models for data traffic services are based on random variables, e.g., to derive file sizes or session durations as given in [ETS98, WIN06, WiM07, NGM08] and to consider the protocol stack as given by the Open Systems Interconnection (OSI) reference model [II94]. To reduce the computational complexity of the evaluation, data traffic is assumed with a constant file size, e.g., in [BHIT05a] or a predefined arrival rate of packets in the transmitter is assumed as proposed in [ETS98] and higher layers of the OSI reference model are omitted from the investigation. Further reduction of the computational complexity is achieved using the full buffer traffic model as described in [HSVC03] assuming that always data is available for transmission.

To evaluate the performance of a cellular wireless network, the frame setup used in the network has to be modelled in detail, cf. for instance [WIN06,WiM07]. Channel transfer factors due to frequency-selective and time varying small-scale fading are calculated for each subcarrier and OFDM symbol as described in [WGL⁺05].

User scheduling also has to be modelled in detail. Instead of optimal scheduling algorithms with high computational complexity, the performance using suboptimal scheduling algorithms is often investigated that provide low computational complexity [YL00,ZL04,LZ06]. Furthermore, random user scheduling can be used which provides very low computational complexity at the expense of results that are lower compared to adaptive user scheduling as discussed in [Hah91,LBS99,BHIT05b,FKWD06].

Different KPI measurements are obtained using dynamic system level simulations like the development of the transmit power over time [HHS99], the user throughput [BHIT05a,BHIT05b,WGL⁺05,PKM06], the cell throughput [WGL⁺05,PKM06], the blocking probability [BHIT05a,BHIT05b] or packet loss and packet delay [LJZ09]. The consideration of the performance of each connection between transmitter and receiver in a dynamic system level simulation is too complex [HSH⁺97]. Therefore, look-up tables are used to obtain, e.g., BLEP from SIR values derived in the system level simulations as described in [HSH⁺97,BSC⁺04,DS04,TW05,WGL⁺05] to obtain KPI measurements.

Despite many approaches to reduce the computational complexity, dynamic system level simulations still suffer from long simulation durations. Therefore, an application in the network planning process is hardly possible. Dynamic system level simulations are used to analyse the performance of packet-switched wireless cellular networks [WGL⁺05,BHIT05b,PKM06,LJZ09] or to verify planning prediction methods as proposed in [LWNH01]. Only little work is done to analytically describe the performance of OFDMA based packet-switched networks in detail. A comparison of the cell capacity of packet-switched and circuit-switched networks is given in [SDLY00] considering voice traffic. However, only results on the blocking probability are given. Rules for dimensioning of GSM/General Packet Radio Service (GPRS) networks are derived in [SP01] based on results that are taken from system level simulations. In [BHIM05], a method is provided for estimating the cell capacity using simulated link level performance results and cell SIR distribution results. Two different traffic models are assumed, on the one hand traffic with constant download duration, e.g., streaming traffic and on the other hand traffic with constant file size, e.g., download traffic. However, only a random user scheduling is considered. An approach using the exponentially effective SINR is used in [GM09,GLMS09] to describe the relationship between outage probability, minimum required signal to noise ratio (SNR) and the number of required

subcarriers. Finally, a first methodology for calculating the cell capacity considering various scheduling algorithms is presented by our work in [FKWD09a,FKWD09b].

1.4 Problem statement

In this section, open problems coming from the review of existing literature with respect to the evaluation of OFDMA based packet-switched wireless networks are summarised.

On the one hand, static system level simulations are already applied during the planning of cellular wireless networks. However, important issues of packet-switched cellular wireless networks can hardly be considered. Data traffic and scheduling are only taken into account by means of very simple models. The impact of user scheduling and small-scale fading is considered only by average values.

On the other hand, accurate performance evaluations of packet-switched wireless networks can be performed using dynamic system level simulations. All aspects of the framework given in Figure 1.1 can be modelled in detail using dynamic system level simulations. However, dynamic system level simulations can hardly be applied in the planning process of wireless networks due to high computational complexity and a long simulation duration although dynamic system level simulations are necessarily required if, e.g., the traffic load has to be determined accurately that one cell in a packet-switched wireless network is able to handle.

A system level simulation methodology is required that reduces the computational complexity compared to state-of-the-art dynamic system level simulation. However, all important issues that have influence on the capacity of packet-switched cellular wireless networks have to be considered so that a comparable accuracy as in state-of-the-art dynamic system level simulations is achieved during KPI measurement. Open problems for such a system level simulation methodology are summarised as follows:

1. The location update due to the user movement leads to high computational complexity in dynamic system level simulations. However, it is not sufficient to consider only static scenarios if KPI measurements are performed for packet-switched wireless networks. A system level simulation methodology is necessary for low complexity performance evaluation of packet-switched networks that is able to consider scenarios with moving users but avoids continuous location updates of the users during the simulation.

2. Realistic modelling of data traffic and user scheduling is required so that accurate KPI measurements are obtained from system level simulation. However, realistic modelling of, e.g., the data traffic leads to a number of active users that varies very slow in time so that long simulations are necessary to achieve statistical reliability. A methodology is required that is able to reduce the simulation duration by eliminating time intervals that have high correlation, e.g., due to the same users that are active.
3. The consideration of the frequency-selective small-scale fading channel in the system level simulation of OFDMA based wireless networks has high computational complexity due to the channel transfer factor that has to be derived for each subcarrier. Furthermore, it is necessary to derive an effective SIR value for the fraction of the available bandwidth and the time duration that is allocated for transmission in OFDMA based wireless networks. A methodology has to be derived that simplifies the calculation of the effective SIR of the fraction of the available bandwidth and the time duration that is allocated for transmission in OFDMA based wireless networks. Adaptive user scheduling based on channel state information has to be possible.

In circuit-switched networks, the Erlang B formula gives an analytical relationship between the blocking probability, the number of available resource units and the traffic load. For packet-switched wireless networks, no analytical expression is available that describes the impact of, e.g., traffic load of different data traffic services, the frame setup and the user scheduling on KPIs for user, cell and network performance. An analytical evaluation methodology is required for KPI estimations of packet-switched cellular wireless networks which can be applied to the capacity planning process. The methodology has to give fast and accurate performance and QoS results. It is expected that a methodology that is based on analytical equations is able to provide results of the performance of packet-switched wireless networks very fast. Open problems for an analytical system level evaluation methodology are summarised as follows:

1. The mixture of different data traffic services in packet-switched wireless networks is an important characteristic that has to be considered during the performance evaluation of packet-switched wireless networks. An analytical methodology is necessary to accurately describe the development of the number of active users over time for different realistic data traffic models modelling, e.g., speech, download and web browsing traffic.
2. Link to system level interfaces are used mapping SIR values derived in the system level simulation to results for, e.g., BLEPs from simulations considering one link

between transmitter and receiver so that error probabilities for received packets in the system level simulation are derived. An analytical expression is required that describes an effective SIR that represents the performance that can be achieved transmitting data with a fraction of the available bandwidth and in a specific time interval in an OFDMA based wireless network. The effective SIR has to include properties of the frequency-selective and time varying small-scale fading channel without calculating, e.g., the channel transfer factor for each subcarrier.

3. User scheduling has influence on KPIs in packet-switched wireless networks so that the modelling of user scheduling is an essential part when evaluating the performance of packet-switched wireless networks. An analytical expression is required that describes the number of subcarriers and the time duration that is allocated for transmission of data from the transmitter to the receiver. Furthermore, an analytical expression is necessary that describes the influence of user scheduling on the channel transfer factor and the SIR that are observed if only specific subcarriers are used for transmission. A methodology has to be developed that describes the difference of the SIR that is observed during transmission assuming a random user scheduling compared to the SIR that is observed during transmission assuming adaptive user scheduling considering channel state information and QoS requirements.

1.5 Thesis overview and contributions

This section gives an overview of the thesis and summarises the main contributions. Two methodologies are derived. The first methodology aims at reducing the complexity of system level simulations compared to state-of-the-art dynamic system level simulation so that KPI results are obtained faster. The accuracy of the results is comparable to state-of-the-art dynamic system level simulations. The second methodology aims at providing KPI results within a couple of seconds so that the methodology can be applied during the network planning process. Reliable results are obtained considering all effects of OFDMA based packet-switched cellular networks.

In Chapter 3, a new system level simulation methodology is proposed that provides lower complexity than state-of-the-art dynamic system level simulations and achieves comparable accuracy in terms of KPI measurements. Instead of considering a long time duration during the evaluation of OFDMA based packet-switched wireless networks as in dynamic system level simulations, the proposed system level simulation methodology is based on a number of short snapshots. Constraints, e.g., the number of active users

and their locations, are fulfilled so that each snapshot represents a short time interval of the investigated busy hour, i.e., a duration of one hour where the maximum traffic load is observed. The snapshots are independent of each other. One snapshot is short enough so that simplifications are assumed that reduce the computational complexity compared to state-of-the-art dynamic system level simulations, e.g., a user location that does not change during the snapshot and a location update due to user movement is not necessary. However, parts of the framework given in Figure 1.1 with fast changes in time like small-scale propagation loss and the user scheduling are considered in each snapshot. Thus, results of KPIs can be obtained with similar accuracy as in dynamic system level simulations. The open problems identified in Section 1.4 are solved as follows:

1. Due to the assumption of a constant user location in the considered snapshot based system level simulation methodology, computational complexity is significantly reduced. No update of user locations and large-scale propagation loss is necessary during the snapshot. A large user pool can be generated offline to further reduce the computational complexity. User locations and the large-scale propagation loss values between the BSs and the user locations are taken randomly from the user pool. The user pool can be used for performance evaluations as long as the network setup, i.e., the locations of the BSs, the large-scale propagation loss model and the distribution of the users in the network does not change.
2. The snapshots considered in the snapshot based system level simulation methodology have to represent short intervals that are randomly taken from the investigated busy hour. Random variables are derived in this thesis that describe constraints, e.g., the number of active users at the beginning of the snapshot or the time instants during the snapshot when the transmission is terminated. Derivations are given in this thesis that describe constraints by means of different random variables so that, e.g., realistic data traffic models can be considered in the snapshot based system level simulation methodology.
3. During each snapshot, frequency-selective small-scale propagation loss is considered. State-of-the-art solutions that calculate the channel transfer factor for each subcarrier have high computational complexity. A methodology is derived in this thesis that reduces the computational complexity compared to state-of-the-art solutions by approximating the pdf of the channel transfer factors and derives an effective SIR for a fraction of the available bandwidth that is used for transmission with one modulation scheme and one coding rate.

In Chapter 4, a novel system level evaluation methodology is proposed that is based on analytical derivations and describes the framework for performance evaluation of packet-switched wireless networks given in Figure 1.1 and relationships between parts of the framework analytically. Compared with state-of-the-art system level simulations, pdfs are derived for the random variables of the framework instead of performing simulations where many realisations of the random variable are generated to achieve KPI measurements. In this thesis, analytical equations are derived so that KPIs can be calculated analytically. Therefore, KPI results are achieved very fast and the proposed performance evaluation methodology is able to improve the planning of packet-switched wireless networks. The pdf of the SIR due to large-scale propagation loss considering the distribution of the users in the network is modified considering the impact of, e.g., small-scale propagation loss and scheduling resulting into a pdf that describes a random variable that indicates the SIR in the network if only subcarriers that are transmitted between transmitter and receiver are considered. The pdf of a random variable that indicates the fraction of the available bandwidth and the time duration that is allocated to transmit to each user is derived, e.g., considering the user scheduling and the number of users that are active in the network. Combining these two random variables, the pdfs of KPIs are calculated.

Chapter 5 presents how the derived methodologies can be applied during capacity planning of OFDMA based packet-switched cellular wireless networks. The impact of data traffic and user scheduling on KPIs is investigated. Results of KPIs are presented for scenarios with a network based on hexagonal cells and scenarios that represent real world scenarios. Uniformly distributed user locations are considered as well as user distributions that represent real environment scenarios. Different data traffic scenarios are considered as well as different user scheduling strategies. KPIs are investigated representing user, cell and network performance. Rules are derived that can be applied when planning cellular wireless networks showing the impact of data traffic and user scheduling on the performance of the network.

Chapter 2

Scenario assumptions

2.1 Introduction

This chapter summarises assumptions for the scenario used throughout this work. A general scenario is described that is used during capacity planning of cellular wireless networks. However, certain requirements are considered that usually apply to capacity planning scenarios. The assumed scenario is able to model among others realistic packet-switched networks, realistic propagation loss, realistic data traffic and realistic user scheduling algorithms, cf. Figure 1.1.

Realistic cellular wireless networks are investigated in this work like WiMAX or LTE. Thus, the scenario assumptions have to cope with features, e.g., regarding the frame setup of those networks. OFDMA as currently deployed in WiMAX or the downlink of LTE is assumed as multiple access scheme. Furthermore, OFDMA is also a promising candidate for multiple access of future wireless networks [PY04]. It is assumed that BS locations are given, e.g., as the results of a coverage planning or pre-planning phase. A realistic propagation model has to be assumed. In contrast to cells in rural environments where the cell radius is limited by received signal strength requirements [Mis04], urban areas are mostly considered during capacity planning where a dense user penetration can be observed. The cell radius is reduced in urban areas compared to rural areas to cope with the traffic load. Urban area scenarios are considered in this work and it is assumed that the network is interference limited and noise is omitted.

Realistic data traffic models have to be considered including Voice over IP (VoIP), download and web browsing traffic. Except VoIP, those traffic types show asymmetric traffic load behaviour. Higher traffic load can be observed in the downlink, i.e., transmitted from the BS to the user compared to the uplink, i.e., transmitted from the user to the BS. The downlink performance will limit the capacity of cellular wireless networks [UMT99,ITU00]. Throughout this work only the downlink is considered.

There are scenarios proposed for networks like WiMAX [WiM07], LTE [NGM08] and the IST Wireless World Initiative New Radio (WINNER) project [WIN06] that shall be used when evaluating those networks. The scenario assumed throughout this work follows these proposals. Some specific assumptions are drawn due to the application

of capacity planning of cellular wireless networks. The remainder of the chapter is organised as follows. In Section 2.2, the cellular environment and the distribution of user locations is described. Section 2.3 presents the used channel model. The modelling of data traffic is depicted in Section 2.4. Resource units needed for transmission of data are defined in Section 2.5. Section 2.6 gives an overview of the scheduling of users. Finally, KPIs are defined in Section 2.7.

2.2 User distribution

In this section, the distribution of users in the cellular environment is described. Two different scenarios are described in the following. Scenario one is often used in scientific investigations. The second scenario reflects a more realistic situation.

In many scientific investigations a scenario is assumed that assumes hexagonal cells with equidistant site-to-site distance D_{sts} [ZK01, Rap02]. The site-to-site distance describes the distance between two neighboring BSs. BSs are located in the cell centre and placed such that each BS has six neighbours with equal D_{sts} . If users are assigned to a BS based on the smallest distance, hexagonal cell areas are formed as depicted in Figure 2.1. In Figure 2.1, 12 cells are depicted. The circles represent the different BSs and the border of the cells are marked by the hexagons. Depending on the antenna pattern and the number of transceiver entities, sectors can be formed that serve part of the cell. Unless otherwise stated, it is assumed that BSs are equipped with omnidirectional antennas and there is only one sector per cell throughout this work. An extension towards cellular networks with directional antennas and sectorisation is straight forward.

Users are placed randomly into the investigation area $\mathcal{A}_{\text{area}}$. The size of the investigation area consisting of hexagonal cells depends on the number N_{BS} of BSs and is given by

$$A_{\text{area}} = N_{\text{BS}} \frac{3}{8} D_{\text{sts}}^2 \sqrt{3}. \quad (2.1)$$

In a hexagonal cellular network as described above, often a uniform user distribution is assumed [SBEM90, AE99, Tim05, EFK⁺06]. The location $U_i(x, y)$ of user i is taken from a uniformly distributed random variable with pdf given by

$$f_U(U_i(x, y)) = \begin{cases} \frac{1 \text{ m}^2}{A_{\text{area}}} & \text{for } (x, y) \in \mathcal{A}_{\text{area}} \\ 0 & \text{else} \end{cases} \quad (2.2)$$

where x and y are the x- and y-position within the investigation area, respectively.

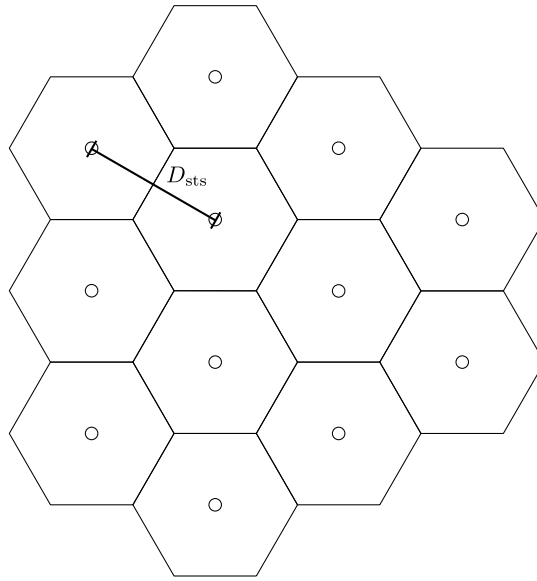


Figure 2.1. Hexagonal cell layout

However, a hexagonal cell area and a uniform user distribution does not reflect a realistic user distribution. In reality, the cell shape depends on the environment [Mis04]. The location of users depends on the environment and the daytime. Users will be located in streets, buildings and public places. During working time, users will be located mostly in industrial and business areas. In the evening and during the weekend, users will be mostly located in residential areas or areas with cultural or event character [MLTS97]. Therefore, a second scenario is taken into account that is based on realistic environments. Realistic scenarios are defined, e.g., within the IST MOMENTUM project [MOM03a] or the SIG A of the COST 2100 action [FB08]. In these scenarios, BS locations are given among others depending on the environment and user distribution. The site-to-site distance and therefore the size of the area one BS serves is not constant. Furthermore, a specific user distribution is defined in these scenarios that is mainly based on environmental properties, e.g., placing more users in urban areas than in rural areas [FB08, MOM03a].

A problem arises during the investigation of cellular wireless networks at the borders of the investigation area. The number of neighboring BSs is smaller at the border compared to the centre of the investigation area. Instead of removing the cells at the border from the evaluation, a technique is applied in this work that enlarges the investigation area by mapping the investigation area onto a torus. Therefore, cells at the right border of the investigation area get neighbours of cells at the left border and cells on the upper border get neighbours of cells at the lower border, respectively [ZK01].

2.3 Channel model

This section describes the channel model for the radio propagation assumed throughout this work. The channel model describes the attenuation of the transmit signal power P_S . Two different effects can be distinguished: large-scale propagation loss and small-scale propagation loss [Rap02]. Large-scale propagation loss describes the attenuation between transmitter and receiver due to the distance. Small-scale propagation loss describes the rapid fluctuation due to multipath propagation and user movement [Rap02].

Large-scale propagation loss, which is termed α_{PL} in the following, models the loss due to the natural expansion of the wave front. The received signal power is reduced with increasing distance d between transmitter and receiver. In non-line of sight (NLOS) scenarios three basic mechanisms can be observed, i.e., reflection, diffraction and scattering [Rap02, Par01]. It is shown that α_{PL} is expressed as a function of the distance d and a pathloss exponent n by

$$\alpha_{\text{PL}} \propto \left(\frac{d}{d_0} \right)^n \quad (2.3)$$

where d_0 represents a reference distance [Rap02]. An overview of different large-scale propagation loss models for both indoor and outdoor scenarios can be found, e.g., in [Rap02, Kür05]. Throughout this work, a model is assumed that was proposed by M. Hata [Hat80] who fitted measurements made by Y. Okumura [OOKF68] in Tokyo into a mathematical model. The Hata model provides logarithmic propagation loss in urban areas valid for frequencies f_c from 150 MHz to 1500 MHz using parameters resulting into

$$a_{\text{PL,dB}} = A + B \cdot \log_{10} \left(\frac{d}{1 \text{ m}} \right) \quad (2.4)$$

where A and B are functions of f_c , BS height and height of the device of the user. There are several extensions of Hata's propagation model for suburban and rural areas [Rap02] as well as an extensions to frequencies higher than 1500 MHz [COS91, Kür01], but all extensions can be reduced into the form given by (2.4) by adapting the parameters A and B .

However, $a_{\text{PL,dB}}$ as calculated in (2.4) represents only an average value. Surrounding environmental clutter is different for locations with equal distance between transmitter and receiver, thus different propagation loss values are observed [Rap02]. It is shown in [CMN84] and [Ber87] that the large-scale propagation loss at any value d is random and can be modelled by a lognormally distributed random variable α_{SF} . This is called shadow fading.

The total large-scale propagation loss $\alpha_{\text{ls,dB}}$ in dB is then given by

$$\alpha_{\text{ls}} = a_{\text{PL,dB}} + \alpha_{\text{SF,dB}} \quad (2.5)$$

with the pdf of $\alpha_{\text{SF,dB}} = 10 \log_{10}(\alpha_{\text{SF}})$ given by

$$f_{\alpha_{\text{SF,dB}}}(a_{\text{SF,dB}}) = \frac{1}{\sqrt{2\pi}\sigma_{\text{SF}}} \exp\left(-\frac{a_{\text{SF,dB}}}{2\sigma_{\text{SF}}^2}\right). \quad (2.6)$$

$\exp(x)$ denotes the exponential function e^x throughout this work. In realistic scenarios, the shadow fading is spatially correlated as explained in [ZK01].

Small-scale propagation loss, which is also known as small-scale fading, results in effects like rapid changes of the signal strength over a short travel distance, random frequency modulation due to different Doppler shifts and time dispersion [Rap02]. The main reason for those rapid changes lies in NLOS propagation over multiple independent paths and the superposition of different signals at the receiver [Pro01,Pät02]. A tapped-delay-line model with N_{taps} is assumed modelling small-scale fading. Tap i for $i = 1, \dots, N_{\text{taps}}$ has a relative delay τ_i compared to the first tap and a time variant channel impulse response $h_i(t)$. The channel impulse response at time t and delay τ of the frequency-selective radio channel is given by

$$h(\tau, t) = \sum_{i=1}^{N_{\text{taps}}} h_i(t) \cdot \delta(\tau - \tau_i) \quad (2.7)$$

where $\delta(\cdot)$ represents the dirac-distribution.

Applying the Discrete Fourier Transform (DFT) on (2.7) results in the channel transfer factors as

$$H(t, f_k) = \sum_{i=1}^{N_{\text{taps}}} h_i(t) e^{-j2\pi f_k \tau_i} \quad (2.8)$$

where f_k represents the frequency of subcarrier k . It is assumed in the following that the channel transfer factor is constant for the bandwidth given by the subcarrier spacing $f_k - f_{k-1}$ and for one OFDM symbol duration.

Throughout this work, fast fading models are used that are specified by the International Telecommunication Union (ITU) for pedestrian and vehicular test environments [ITU97]. The specified parameters can be found in Table 2.1.

Table 2.1. ITU tapped-delay-line parameters [ITU97]

Tap	Pedestrian test environment				Vehicular test environment			
	Channel A		Channel B		Channel A		Channel B	
	Relative delay in ns	Average power in dB	Relative delay in ns	Average power in dB	Relative delay in ns	Average power in dB	Relative delay in ns	Average power in dB
1	0	0	0	0	0	0	0	-2.5
2	110	-9.7	200	-0.9	310	-1.0	300	0
3	190	-19.2	800	-4.9	710	-9.0	8900	-12.8
4	410	-22.8	1200	-8.0	1090	-10.0	12900	-10.0
5	-	-	2300	-7.8	1730	-15.0	17100	-25.2
6	-	-	3700	-23.9	2510	-20.0	20000	-16.0

2.4 Data traffic model

Cellular wireless networks like WiMAX or LTE have to deal with several different real-time and non-real-time services [BFM⁺97, PGL⁺97, Sam98]. Therefore, the transmission of data packets has to be modeled accurately during the investigation of the network performance. This section provides an overview how data traffic, i.e., the transmission of data is modeled.

Besides the conversational service, services like file download and web browsing are expected to become important traffic services in networks like WiMAX or LTE and future wireless networks [ITU00]. For the evaluation and also for the planning of cellular wireless networks, the busy hour traffic load is considered [Yac93, Flo97]. The busy hour is the interval of the day with a length of one hour when the highest traffic load, e.g., amount of data, is observed.

In the following, the interval from the generation of the first data packet until the reception of the last data packet in the receiver is called session. When modelling sessions, several aspects have to be considered. First, the process when a new session starts has to be modelled. During the session several protocols are involved in the transmission which are described by the OSI reference model [Zim80, II94] defined by the International Organization for Standardization (ISO). Throughout this work, effects due to layer 7 - 3 are modelled for each session by defining, e.g., the size and the number of the data packets or when data packets are available for transmission. Effects on layer 2 and 1 are taken into account in the simulation methodology.

The start of telephone calls in a telephone network can be modeled by a Poisson process [Kle75]. Throughout this work, it is also assumed that the time instant of the beginning of a new session is modeled according to a Poisson process. The Poisson process describes a birth process with independent and Poisson distributed arrival samples. The average arrival rate λ of the Poisson process is given by the average number of arrivals per time interval.

In the following, properties of the Poisson process that are important for this work are discussed. The Poisson process is memoryless and the time duration Δt_1 until the next session arrives starting from an arbitrary time instant is given by an exponentially distributed random variable [Kle75]. The pdf of Δt_1 is given by

$$f_{\Delta t_1}(\Delta t_1) = \lambda \cdot \exp(-\lambda \Delta t_1), \quad (2.9)$$

[Kle75]. The time interval Δt_k until the k -th session arrives starting from an arbitrary time instant is given by an Erlang-K distribution with the pdf of $\Delta t, k$ given by

$$f_{\Delta t_k}(\Delta t_k) = \frac{(\lambda \Delta t_k)^{k-1}}{(k-1)!} \cdot \lambda \cdot \exp(-\lambda \Delta t_k), \quad (2.10)$$

[Kle75]. The probability that l sessions arrive in the arbitrary time duration T is given by

$$P(l|T) = \frac{(\lambda T)^l}{l!} \cdot \exp(-\lambda T), \quad (2.11)$$

[Kle75].

Upon arrival of a new session, the traffic service and the effects due to higher layers in the OSI reference model have to be modeled accurately. Throughout this work, the behaviour of the application, presentation and session layers, i.e. layer 7 - 5, is combined together to model the structure of a session in terms of, e.g., duration or file size. The behaviour of the transport and network layer, i.e., layer 3 and 4, is also modeled together, e.g., by defining the size of individual packets and the arrival of packets at the BS.

- Speech traffic:

Speech traffic is a model for conversational services. In packet-switched networks, VoIP using Real-time Transport Protocol (RTP) [SCFJ03] on application layer is used for conversational services. The duration T_{speech} of a speech traffic session

is modelled by an exponentially distributed random variable [ETS98]. The pdf of T_{speech} is given by

$$f_{T_{\text{speech}}}(T_{\text{speech}}) = \mu_{\text{speech}} \exp(-\mu_{\text{speech}} T_{\text{speech}}) \quad (2.12)$$

with $\frac{1}{\mu_{\text{speech}}}$ the average duration of one speech traffic session. Using a speech codec the data is segmented into packets with equal size [New08]. The transmission using User Datagram Protocol (UDP) [Pos80] and Internet Protocol (IP) [Inf81a] is modeled by a constant stream of packets arriving at the BS that have to be transmitted using the air interface which comprises layers 1 and 2 of the OSI reference model in cellular wireless networks [FN00]. Size S_{speech} and arrival rate r_{sam} of the packets are defined by the codec and header overhead added by the protocols. Features like silence suppression [BSS⁺97] are not considered so that the stream is constant over the whole session duration. Services like video conferencing can also be modelled with the speech traffic model.

- Download traffic:

Download traffic represents the download of one file using for instance File Transfer Protocol (FTP) on application layer. The download is finalised if all data is transmitted. The file size $S_{f,\text{dl}}$ is a random variable taken from a lognormal distribution [AB73]. The pdf of $S_{f,\text{dl}}$ is given by

$$f_{S_{f,\text{dl}}}(S_{f,\text{dl}}) = \frac{1}{\sigma_L \sqrt{2\pi} S_{f,\text{dl}}} \exp\left(-\frac{(\ln(S_{f,\text{dl}}) - \mu_L)^2}{2\sigma_L^2}\right) \quad (2.13)$$

where σ_L and μ_L are the parameters of the lognormal distribution defining the expectation value and the standard deviation [Pap84]. Due to the transmission using Transmission Control Protocol (TCP) and IP [Inf81b, Ste94], the file is segmented into packets with a maximum packet size $S_{p,\text{dl}}$ which is usually smaller than $S_{f,\text{dl}}$. Algorithms used in TCP like, e.g., congestion avoidance [APS99] are not considered in this work. It is rather assumed that TCP provides a regular stream of packets, when a predefined server data rate r_{serv} is reached. The time interval $t_{\text{intera},\text{dl}}$ between two consecutive packets is taken from an exponential distribution where the arrival time interval is given by

$$E\{t_{\text{intera},\text{dl}}\} = \frac{S_{p,\text{dl}}}{r_{\text{serv}}}. \quad (2.14)$$

- Web browsing traffic:

Web browsing traffic describes the browsing through the internet using for instance Hypertext Transfer Protocol (http) on application layer. A web browsing session reflects the following situation [Mah97, ETS98, CL99, RGC⁺99]: A browser

is opened by the user and a web page is accessed which is referred as packet call. After reading the content of the web page for a duration called reading time, a new web page is visited by starting a new packet call. This continues until the browser is closed and the session is finalised after transmission of the last packet call. An example web browsing session is depicted in Figure 2.2. The file size S_{pc} transmitted in each packet call is taken from a Pareto distribution [ETS98]. The pdf of S_{pc} is given by

$$f_{S_{pc}}(S_{pc}) = \frac{a \cdot k^a}{S_{pc}^{a+1}} \quad (2.15)$$

where a and k are the parameters of the Pareto distribution resulting into the expectation value and the standard deviation [ETS98]. The transmission of the packet call data using TCP and IP is modeled in the same way as for download traffic as described above. The number N_{pc} of packet calls, i.e., the number of web pages that are accessed during one session, is obtained from a geometrical distribution. The probability for $N_{pc} = l$ packet calls in one session is given by

$$P(N_{pc} = l) = p_{pc}(1 - p_{pc})^l \quad (2.16)$$

where the average number of packet calls is given by

$$E\{N_{pc}\} = \frac{1 - p_{pc}}{p_{pc}}. \quad (2.17)$$

The duration between two consecutive packet calls when the user reads the content of the web page is called reading time T_{RT} . The reading time is also taken from a geometrical distribution. During the reading time no data is transmitted [ETS98].

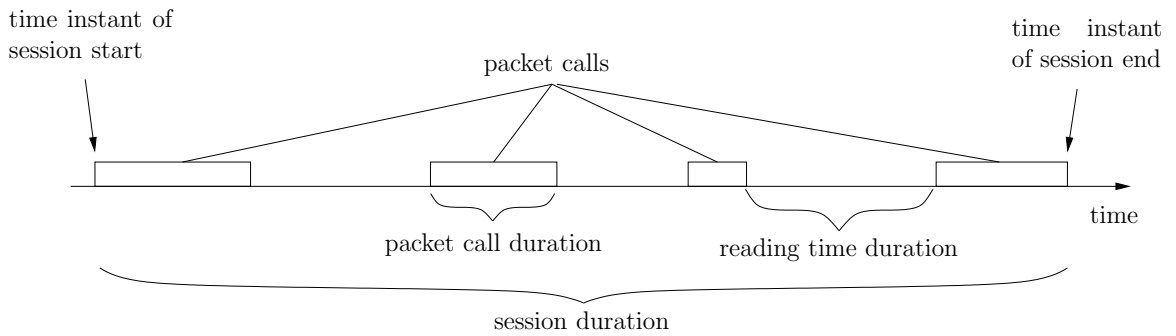


Figure 2.2. Example web browsing session

2.5 Resource unit definition

This section describes how resource units are defined in the system model that are used for data transmission. OFDMA which is assumed as multiple access scheme throughout this work is a very promising candidate multiple access scheme for future cellular wireless networks. OFDMA is currently used in networks according to the IEEE 802.16 [IEE05] as well as 802.20 standard [BXG07, GKT⁺08] or in networks according to 3GPP LTE. OFDMA is based on OFDM where the available system bandwidth is divided into orthogonal and narrowband subcarriers [vNP00, Mol05]. The relationship between system bandwidth B_{sys} , Fast Fourier Transform (FFT) size N_{FFT} and subcarrier frequency spacing f_{sc} is given as follows:

$$f_{\text{sc}} = \frac{B_{\text{sys}}}{N_{\text{FFT}}}. \quad (2.18)$$

The OFDMA symbol duration T_{sym} is given by

$$T_{\text{sym}} = \frac{1}{f_{\text{sc}}} + T_{\text{g}} \quad (2.19)$$

where the first summand is the useful symbol duration given by the inverse of f_{sc} and the second summand represents a guard interval that has to be inserted to avoid inter-symbol interference [vNP00, HP03].

OFDMA provides a very flexible way of allocating bandwidth and time to users. In networks like WiMAX or LTE, frames are created for resource allocation. A typical frame structure is depicted in Figure 2.3. The frame contains the whole available bandwidth and a certain number of OFDMA symbols leading to the frame duration T_{fr} . In each frame, subcarriers and OFDMA symbols can be allocated to users. Many different ways to allocate subcarriers and OFDMA symbols are possible. To reduce complexity, cellular wireless networks are designed so that N_{sc} subcarriers and N_{sym} OFDMA symbols are allocated together to one user. This logical entity is called resource unit throughout this work. A resource unit is the smallest unit in frequency and time domain that can be allocated to one user. A resource unit is used with one modulation scheme and one coding rate. In WiMAX, a resource unit represents one slot [IEE05], in IST WINNER, resource units are called chunks [WIN08, WDK⁺08, WDK⁺09] and in LTE, resource units are named physical resource blocks [3GP06]. The time duration T_{ru} of the resource unit and the separation f_{ru} in frequency domain from one resource units to another are given by

$$T_{\text{ru}} = N_{\text{sym}} \cdot T_{\text{sym}} \quad (2.20)$$

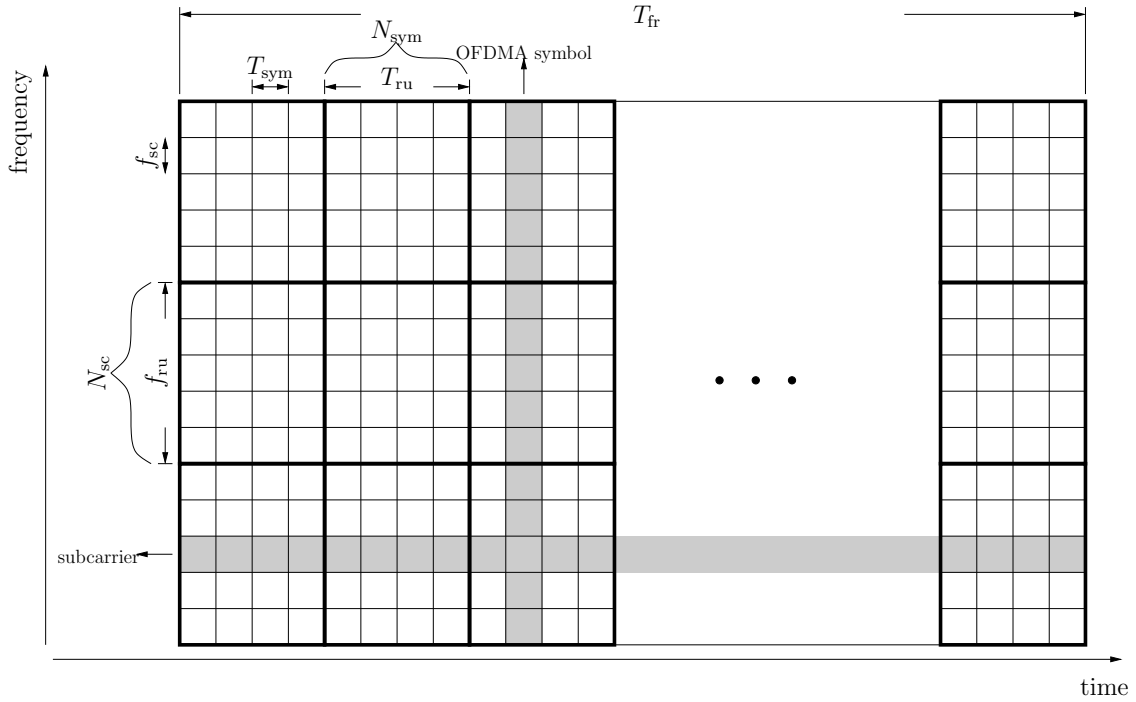


Figure 2.3. Frame structure for OFDMA transmission

and

$$f_{\text{ru}} = N_{\text{sc}} \cdot f_{\text{sc}}. \quad (2.21)$$

Subcarriers that are combined in one resource unit can be physically neighbored or distributed over the whole system bandwidth. Throughout this work a distributed subcarrier allocation is assumed where subcarriers of one resource unit are distributed over the whole frequency bandwidth using pseudo-noise permutation schemes [IEE05] or frequency-hopping patterns [vNP00]. This is used for instance in the Partial Usage of Subchannels (PUSC) and Full Usage of Subchannels (FUSC) mode of WiMAX and proposed for IST WINNER [WDK⁺08, WDK⁺09]. A distributed subcarrier allocation provides frequency diversity [FKCS05, PKM06, SFF⁺07]. If different permutation schemes are used in neighboring cells, interference averaging can be observed [EKL05, MFK⁺06, JZY⁺07, FKW⁺07].

2.6 User scheduling

This section describes the user scheduling assumed during this work. In contrast to cellular wireless networks of the second generation, no dedicated channels are avail-

able in networks like WiMAX or LTE. These networks are packet-switched instead of circuit-switched. Thus, shared channels are used [HT06, Ort07]. Therefore, users have to compete for medium access. An entity with knowledge about, e.g., buffer occupancies or channel quality information decides during the user scheduling which user shall transmit during the frame duration and which resource units are allocated to these users for transmission. The latter is often referred as resource allocation. Besides the user scheduling two other issues have to be determined for each transmission, i.e.,

- which transmit power is used, i.e., power allocation,
- and which modulation and coding scheme is used for the transmission, i.e., link adaptation.

The focus of this thesis is on the impact of scheduling on the network performance and power allocation and link adaptation is considered only in a very simple way. However, the maximum transmit power is limited and it is assumed that constant transmit power is used per subcarrier. If all subcarriers are used for transmission, the maximum transmit power is divided equally among all subcarriers. Otherwise, the sum transmit power is reduced compared to the maximum transmit power. One modulation and coding scheme is selected per resource unit. Which modulation and coding scheme is determined based on a look-up table that defines which modulation and coding scheme is selected based on the SIR of the resource unit. The scheduling entity determines an appropriate user that is allowed to transmit using a given resource unit. Resource units are considered one after another. For each resource unit in one cell, only one user can be selected.

In the following, the scheduling problem is described as optimisation problem in a general way. Central point of the optimisation problem is the objective function for the resource unit with index k

$$j(k) = \arg \max_i \{f_i(k)\} \quad (2.22)$$

where $f_i(k)$ is the utility function of user i and resource unit k . This objective function has to be solved for each resource unit. Depending on the scheduling strategy that is applied, the utility function in (2.22) is a function depending on channel state information, user throughput conditions, number of already allocated resource units and so on. State of the art strategies that are often pursued aim at

- maximising the network performance, e.g., by maximising the sum throughput in each cell [YL00, JL03, ZL04, CLC04, LZ06],

- guaranteeing a minimum performance to each user, e.g., by maximising the minimum user throughput [Hah91, RC00] or
- providing fairness among the users, e.g., by allocating equal number of resource units to each user or providing proportional fairness [GP99, JPP00, CL01, VTL02].

Three state-of-the-art scheduling strategies are considered throughout this work that are applicable for real cellular wireless networks. State-of-the-art scheduling strategies are selected that provide fairness by allocating equal number of resource units, improve the sum throughput while providing proportional fairness and guarantee the same throughput to all users. Strategies that maximise the sum throughput are not considered due to the fact that QoS can hardly be achieved for most of the users. The three strategies are described in the following.

A way to perform scheduling with low complexity is obtained by using fair resource scheduling [Hah91, LBS99, KFM02]. Fair resource scheduling is also known as round robin scheduling. According to the scheduling list, resource units are allocated to the users in a consecutive way. The objective function for resource unit k in (2.22) results in

$$j(k) = \arg \max_i \{n_{\text{alloc}}^{(i)}(k)\} \quad (2.23)$$

where $n_{\text{alloc}}^{(i)}(k)$ represents the number of resource units that are allocated to user i until resource unit k divided by the time interval from the session start of user i to the time resource unit k shall be transmitted. (2.23) is solved for resource unit k subject to

$$\gamma^{(j)}(k) > \gamma_{\text{low}} \quad (2.24)$$

where $\gamma^{(j)}(k)$ represents the SIR of resource unit k when the selected user j transmits and γ_{low} is the minimal required SIR that a reliable transmission can be guaranteed. Thus, (2.24) prevents the allocation of a resource unit to a user which is not able to transmit data with the resource unit so that it can be decoded in the receiver with acceptable error probability. Fair resource scheduling is one scheduling strategy that provides fairness among the users.

The second scheduling strategy considered in this thesis is an opportunistic scheduling algorithms that takes channel state information into account when allocating users to resource units and is able to increase cell throughput compared to fair resource scheduling [KH95, VTL02]. Of practical relevance are scheduling algorithms that do not only maximise the network performance but also provide a certain degree of fairness among the users. Proportional fair scheduling is one algorithm that is used for instance

in high data rate networks [JPP00,Hol01,Kol03,KKHY04]. Proportional fair scheduling provides high sum throughput in each cell and achieves fairness among the users. With proportional fair scheduling, the utility function represents the ratio between the actual possible throughput $r_{\text{user}}^{(i)}(k)$ of user i when transmitting resource unit k and the average achieved throughput $\bar{r}_{\text{user}}^{(i)}(k)$ of user i over a past time interval. Therefore, the objective function in (2.22) results into

$$j(k) = \arg \max_i \left\{ \frac{r_{\text{user}}^{(i)}(k)}{\bar{r}_{\text{user}}^{(i)}(k)} \right\}. \quad (2.25)$$

It can be seen in (2.25) that actual information about the rate that can be achieved per resource unit is required to perform proportional fair scheduling. The average user throughput is updated after transmission of the resource unit.

The third algorithm provides absolute fairness among the users by modifying (2.25) so that

$$j(k) = \arg \max_i \left\{ \frac{1}{\bar{r}_{\text{user}}^{(i)}(k)} \right\} \quad (2.26)$$

resulting into a fair throughput scheduling. A resource unit is always allocated to the user that has the lowest average throughput over a past time interval. In the long term, all users will get equal average throughput. This algorithm represents scheduling strategies that aim at allocating a minimum throughput to all users. To prevent that resource units are allocated to users despite a reliable transmission is not possible, again the side condition (2.24) has to be fulfilled.

2.7 Key performance indicators (KPIs)

This section describes the key performance indicators (KPIs) that are selected for the investigation. KPIs are a measure to evaluate the performance of cellular wireless networks. To evaluate the network and user performance of cellular wireless networks, several KPIs can be chosen reflecting the behaviour of the network during operation. Throughout this work, KPIs are selected that reflect the performance from different points of view, i.e., from point of view of a specific user, from point of view of a cell and from point of view of the entire network. Of course, different KPIs can be selected, however, the KPIs that are described in the following give a good overview on the performance of the cellular wireless network and focus on aspects that are important for both operators, e.g., efficient utilisation of resource units, and users, e.g., maintaining QoS requirements.

The performance from the perspective of a specific user within the network is evaluated by the average user throughput. The average user throughput $\bar{r}_{\text{user}}^{(i)}$ of user i is given by the sum data $d_{\text{user}}^{(i)}$ in bits that is transmitted by user i and the time duration $T_{\text{active}}^{(i)}$ where user i has data for transmission available as:

$$\bar{r}_{\text{user}}^{(i)} = \frac{d_{\text{user}}^{(i)}}{T_{\text{active}}^{(i)}}. \quad (2.27)$$

The time duration $T_{\text{active}}^{(i)}$ where user i has data for transmission available is obtained by subtracting durations like the reading time, when no data is transmitted, from the session duration. The user throughput can be linked to QoS requirements if a minimum user throughput has to be fulfilled. Among others, the user throughput depends on the location of the user within the network. Areas with low average user throughput where QoS requirements cannot be fulfilled shall be avoided in well planned networks.

The performance from the view point of one cell is evaluated by the cell throughput that is obtained during the busy hour in one cell. Assuming that user i for $i = 1, \dots, N_{\text{user}}^{(j)}$ is served by cell j and $N_{\text{user}}^{(j)}$ is the number of users that are served by cell j during the busy hour duration T_{BH} , the average cell throughput $r_{\text{cell}}^{(j)}$ is calculated using the sum data $d_{\text{user}}^{(i)}$ in bits that is transmitted by user i during the busy hour as:

$$r_{\text{cell}}^{(j)} = \frac{\sum_{i=1}^{N_{\text{user}}^{(j)}} d_{\text{user}}^{(i)}}{T_{\text{BH}}}. \quad (2.28)$$

The cell throughput indicates how much data is transmitted by each cell and how efficient each cell deals with the available resource units. If the average cell throughput is significantly lower than the ratio of data arriving at the BS within the busy hour divided by the time duration, packets get stored in the BS and overload conditions may occur in terms of buffer overflow.

Finally, the performance from network point of view is evaluated considering the number of unsatisfied users. A user gets unsatisfied if its QoS requirement is not fulfilled. The QoS requirement depends on the service type that is used. For voice services, ITU has specified delay classifications so that a one-way delay of more than 400 ms is unacceptable for the user [ITU03]. 3GPP additionally has specified user expectations for services that are usually considered as background or interactive traffic without QoS requirements [ETS98], e.g., data transfer or web browsing. Throughout this work, all QoS requirements are transformed into a user throughput requirement. Based on the server data rate r_{serv} as introduced in Section 2.4, a service dependent minimum user throughput requirement r_{req} is derived that has to be fulfilled in a given time interval. This is described in the following for the traffic models described in Section 2.4.

In case of interactive and background transmission, [3GP08a] states that, e.g., a web page has to be transmitted within less than 4 s. Therefore, a QoS requirement as described in [ETS98] is assumed throughout this work. A background or interactive user gets unsatisfied if the average user throughput is below a required average user throughput r_{req} . In [ETS98], it is stated that r_{req} is 10 % of the server data rate r_{serv} which is also adapted in this work.

For conversational traffic, the delay requirement is transformed into a throughput requirement. A constant stream of packets is required in the receiving entity and it is assumed that small delay variations can be compensated by a jitter buffer in the receiver [HNA00, Goo02]. Furthermore, packets cannot be buffered for a long time in the BS otherwise the maximum delay will be exceeded. Therefore, the required user throughput r_{req} for conversational traffic has to be close to the server data rate r_{serv} . However, for short time intervals a smaller user throughput is acceptable due to the jitter buffer. With τ_{jitter} the maximum delay that can be compensated by the jitter buffer and T_{sam} the sampling duration of the voice codec given by the packet size divided by r_{serv} , the minimum required throughput $r_{\text{req}}(m)$ obtained over an time interval of length $(m + 1)T_{\text{sam}}$ for $m = 1, 2, \dots$ is given by

$$r_{\text{req}}(m) \geq \frac{T_{\text{sam}} \cdot r_{\text{serv}}}{T_{\text{sam}} + \frac{\tau_{\text{jitter}}}{m}}. \quad (2.29)$$

It can be seen that $r_{\text{req}}(m)$ can be smaller than r_{serv} for short time intervals while $r_{\text{req}}(m)$ approaches towards r_{serv} for long time intervals.

The number of users with $\bar{r}_{\text{user}}^{(i)} < r_{\text{req}}$ with $\bar{r}_{\text{user}}^{(i)}$ the average user throughput of user i gives the number of unsatisfied users N_{unsat} . The outage probability is calculated by

$$p_{\text{out}} = \frac{N_{\text{unsat}}}{N_{\text{user}}} \quad (2.30)$$

where N_{user} is the number of active users in the network. The network is in outage if p_{out} is higher than a predefined threshold. Usually, the outage probability is in the order of 0.01 up to 0.05 [Yac93].

Chapter 3

Simulative system level analysis methodology

3.1 Snapshot based system level simulation methodology

This chapter gives an overview of the system level simulation methodology developed to evaluate the performance of cellular wireless networks during the capacity planning process. It is stated in Chapter 1 that static system level simulations are widely used during planning of cellular wireless networks. However, static system level simulations do not consider effects like user scheduling or different data traffic models during the evaluation. Those effects can only be considered using dynamic system level simulations as described in Chapter 1 and it is necessary to consider those effects if reliable results of KPIs shall be obtained. However, dynamic system level simulations show a very high computational complexity. Thus, simulations take too long to be applicable in the network planning process. The aim of this work is to derive a new system level simulation methodology that provides lower computational complexity than state-of-the-art dynamic system level simulations but still shows the same accuracy in terms of performance results.

Main issues that lead to a long duration of dynamic system level simulations are identified as follows. Due to the movement of users, large-scale propagation loss has to be updated based on the new position of the user [HHS99, LJZ09]. This is time-consuming and an increasing complexity is observed with increasing number of users and BSs. Modelling of data traffic using the Poisson process for session arrivals and data traffic models leads to high correlations in time [HHS99, BHIT05b]. Conditions, e.g., the number of active users, change only with a low frequency. Thus, a long time duration has to be considered. Furthermore, an initialisation duration is necessary at the beginning of the investigation until stable conditions are achieved. No reliable results are obtained in the initialisation duration. Small-scale fading models have to be considered to achieve accurate results but the calculation of channel transfer factors for each subcarrier is very complex [WGL⁺05, BAS⁺05, WiM07]. Table 3.1 gives an overview of these problems. Solutions are proposed in this work that reduce the computational complexity while achieving accurate results that are comparable to conventional dynamic system level simulations. These solutions are described in detail in the following

Table 3.1. Overview of snapshot based system level simulation methodology

Part of the investigation	Identified problem	Proposed solution
Large-scale propagation loss calculation	Update necessary if the user moves through the area	Consideration of independent and short time intervals, the user location does not change significantly during the time interval
Data traffic generation	Temporal dependencies during data traffic modelling	
Small-scale fading	Channel transfer factor for each subcarrier needed, one performance value per resource unit required	Using statistical properties of the small-scale fading channel

The proposed snapshot based system level simulation methodology consists of several independent short time intervals which are called snapshots in the following. Due to the short duration of each snapshot, it is assumed that the user position is nearly constant during the snapshot duration. Within each snapshot, data traffic and small-scale fading are modelled on a time slot or OFDMA symbol duration basis. For calculating small-scale fading, not each subcarrier is considered but statistical properties are taken into account and the pdf of the channel transfer factor is approximated by a finite number of samples.

In the following, the impact of the snapshot based system level simulation methodology on different parts of the investigation model is shortly summarised. A detailed elaboration is given in the following sections. An overview of the snapshot based system level simulation methodology and advantages as well as restrictions that can be observed compared with state-of-the-art dynamic system level simulations is given in Table 3.2.

It is assumed that the duration of one snapshot is short enough so that the position of the user and therefore the large-scale propagation loss does not change significantly. Hence, only one large-scale propagation loss calculation is necessary per user-BS pair and per snapshot. For a given scenario, the calculation can be done in advance of the simulation to reduce the complexity. By generating many independent snapshots taken randomly from the investigated time interval, accurate results can be achieved. However, handover procedures due to the movement of users cannot be investigated. Each user remains allocated to one BS during the entire snapshot, cf. Section 3.2. Due to the short duration of one snapshot, errors due to not performing handovers can be neglected.

Table 3.2. Comparison of snapshot based system level simulation methodology with dynamic system level simulations

Part of the investigation	Novel snapshot-based system level simulation	Advantage compared to dynamic system level simulation	Differences compared to dynamic system level simulation
User placement and large-scale propagation loss	User position assumed to be fix during one snapshot, independent snapshots generated by taking users from a large pool	No update of large-scale propagation loss necessary during one snapshot, large-scale propagation loss can be calculated in advance	No investigation of handover protocols possible
Data traffic generation	Generate data traffic by considering statistics, e.g., for active users at snapshot start, new arriving users, vanishing users	Low complexity consideration of data traffic by applying statistics	Consideration of statistics instead of state-of-the-art models
Small-scale fading	Approximated statistical properties of the channel transfer factors in frequency domain and calculation of an effective performance value based on a finite number of samples	Complexity reduction by considering statistical properties and using a finite number of samples	Accuracy reduced compared to a consideration of all subcarriers
KPI measurements	Analyse throughput and QoS performance considering the snapshot method	Performance measurements are possible for throughput and QoS as in dynamic simulations	Performance measurements limited to snapshot duration

The snapshots are too short to apply state-of-the-art data traffic modelling using the Poisson process and data traffic models. Instead, statistical properties are derived in Section 3.3 describing the conditions at the beginning of the snapshot and the development during the snapshot, i.e., whether new users arrive or active user leave. Using statistical properties of the data traffic removes temporal correlation, e.g., in the number of active users and reduces the complexity. No initialisation phase is necessary in the proposed methodology.

As stated before, small-scale fading is considered on OFDMA symbol basis. To reduce complexity, not each individual subcarrier is considered. Instead, statistical properties

are obtained using a sample version of the channel transfer factors to derive its pdf which is used to determine an effective channel transfer factor for each resource unit, cf. Section 3.4.

User scheduling is omitted in Table 3.2 due to a state-of-the-art consideration as in dynamic system level simulations. A short description can be found in Section 3.5.

Measurement of KPIs is affected by the snapshot based system level simulation methodology. However, all KPIs as depicted in Section 2.7 can be obtained using the described methodology. It is not possible to achieve temporal results, e.g., of throughput development over the entire session duration due to a maximal measurement duration of one snapshot. Nevertheless, throughput and QoS results, as needed to identify the performance of the network, are achieved very accurately and with consideration of the impact of, e.g., user scheduling and data traffic, cf. Section 3.6.

3.2 User placement and large-scale propagation loss calculation

This section describes how users are placed into the investigation area and large-scale propagation loss is calculated. It is stated in Table 3.1 that conventional dynamic system level simulations get complex due to a changing user position and large-scale propagation loss updates that are necessary due to the movement of the users [HHS99, LJZ09]. Large-scale propagation loss varies very slow due to the movement of the users. Therefore, long time durations have to be considered in dynamic system level simulations so that statistical reliability is achieved. This results in high complexity and a long simulation duration. The proposed snapshot based methodology overcomes this problem by considering only short time interval called snapshots so that a constant large-scale propagation loss can be assumed during the whole snapshot. Additionally, those snapshots are independent of each other representing uncorrelated situations taken randomly from a scenario where moving users in a cellular wireless network are considered.

The actual user placement is carried out so that statistics regarding the user distribution are fulfilled. Assuming that n_{active} users are considered during the snapshot, the large-scale propagation loss between user i for $i = 1, 2, \dots, n_{\text{active}}$ and BS j for $j = 1, 2, \dots, N_{\text{BS}}$ is given by $\alpha_{\text{ls},i,j}$ which is calculated according to (2.5) once per snapshot. To reduce the complexity, a large user pool with N_{pool} user positions is generated

in advance of the investigation where $N_{\text{pool}} \gg n_{\text{active}}$. The large-scale propagation loss values for each user position are combined into the matrix

$$\mathbf{A}_{\text{ls}} = \begin{bmatrix} \alpha_{\text{ls},1,1} & \alpha_{\text{ls},1,2} & \cdots & \alpha_{\text{ls},1,N_{\text{BS}}} \\ \alpha_{\text{ls},2,1} & \alpha_{\text{ls},2,2} & \cdots & \alpha_{\text{ls},2,N_{\text{BS}}} \\ \vdots & \vdots & \ddots & \vdots \\ \alpha_{\text{ls},N_{\text{pool}},1} & \alpha_{\text{ls},N_{\text{pool}},2} & \cdots & \alpha_{\text{ls},N_{\text{pool}},N_{\text{BS}}} \end{bmatrix}. \quad (3.1)$$

\mathbf{A}_{ls} has the dimension $N_{\text{pool}} \times N_{\text{BS}}$.

For each snapshot, n_{active} users are selected randomly from the user pool and the large-scale propagation loss values are taken from the appropriate rows of \mathbf{A}_{ls} . This selection is comparable to an urn problem, where, e.g., balls are taken from an urn [JK77]. The number of different combinations of active users is given by

$$n_{\text{comb}} = \binom{N_{\text{pool}}}{n_{\text{active}}} = \frac{N_{\text{pool}}!}{(N_{\text{pool}} - n_{\text{active}})!n_{\text{active}}!}. \quad (3.2)$$

If a scenario with a specific user distribution and large-scale propagation loss model is investigated, e.g., for different data traffic scenarios or user scheduling algorithms, the same user pool can be used.

Compared with state-of-the-art dynamic system level simulations, it can be seen that the large-scale propagation loss calculation has lower complexity. Only one large-scale propagation loss value is necessary per user position, BS and snapshot. No update is required due to the movement of the users. The temporal dependencies due to the movement are resolved due to the assumption of independent snapshots. While large-scale propagation loss is calculated on demand in conventional dynamic system level simulations and updates are necessary depending on the changing positions due to the applied mobility model, the snapshot-based system level simulation methodology only requires the calculation of large-scale propagation loss for a sufficiently large user pool. The calculated large-scale propagation loss values can be reused if another investigation is made assuming the same user distribution and large-scale propagation loss model.

3.3 Data traffic generation

3.3.1 Introduction

This section treats the generation of data traffic in the snapshot based system level simulation methodology. Conventional dynamic system level simulations generate data

traffic using the Poisson process and data traffic models [HHS99,BHIT05b]. Properties due to data traffic, e.g., the number of users wanting to transmit data, change only slowly and long simulation durations are necessary to obtain reliable results. Furthermore, an initialisation phase is necessary at the beginning of the investigation until stable conditions are achieved. No reliable results can be achieved during the initialisation phase leading to simulation overhead. With the snapshot based system level simulation methodology, short snapshots are formed. Thus, an application of state-of-the-art data traffic generation is not possible. However, an accurate modelling of data traffic is necessary due to its impact on, e.g., the network performance.

As stated in Section 3.1, each snapshot is randomly selected from the investigated time interval and the statistics of the data traffic have to be fulfilled. For the snapshot based system level simulation methodology, statistical properties of the data traffic are derived summarised by the following questions:

- How many sessions are active at the beginning of the snapshot?
- How large is the buffer occupancy for all active sessions at the beginning of the snapshot in the transmitting entities?
- How many sessions start during the snapshot and when do they start?
- When do packets arrive in the transmitting entity during the snapshot?
- How many sessions terminate and when do they terminate during the snapshot?

The statistical properties of different data traffic services are derived in the following sections.

To answer the five questions, statistics are derived for each snapshot for the number of users that are active at the beginning of the snapshot and for the buffer occupancy in the transmitting entities. Statistics are derived when new sessions start and users become active. The arrival of data packets in the transmitting entity is defined based on the traffic model definition. Finally, statistics are given for the time instants when sessions are terminated during the snapshot. Each user is mapped to one position as described in Section 3.2.

Compared with conventional dynamic system level simulations, data traffic generation is carried out before the snapshot in the snapshot based methodology. Instead of determining the session start time and applying data traffic models as given by the

literature, statistics of the data traffic are derived and applied to each snapshot. By designing independent snapshots, e.g., in terms of active users, simulation duration is reduced. Furthermore, the initialisation phase becomes unnecessary due to using statistics of the data traffic generation. The network is already in a stable condition at snapshot start and the statistics of the data traffic are fulfilled.

3.3.2 Speech traffic

This section gives answers how speech traffic is considered in the snapshot based system level simulation methodology.

With a Poisson process as arrival process and an exponentially distributed session duration, speech traffic can be modelled as $M/M/\infty$ queueing model in Kendall's notation [Kle75, Ken51]. At the beginning of the snapshot which represents an arbitrary time instant, the probability of n_{active} active speech users is therefore given by

$$P(n_{\text{active}} = k) = \begin{cases} \frac{N_{\text{speech}}^k}{k!} \exp(-N_{\text{speech}}) & \text{for } k \geq 0 \\ 0 & \text{else} \end{cases} \quad (3.3)$$

with N_{speech} the average number of active speech users given by the arrival rate λ_{speech} and the average session duration $\frac{1}{\mu_{\text{speech}}}$ as

$$N_{\text{speech}} = \frac{\lambda_{\text{speech}}}{\mu_{\text{speech}}}. \quad (3.4)$$

Speech traffic demands challenging requirements on, e.g., delay so that a high amount of buffered data cannot be tolerated, cf. Section 2.7. Therefore, it is assumed that the buffers of users that are already active at the beginning of the snapshot are not filled with data. New packets arrive in a regular time interval as specified by the speech traffic model.

New sessions start during the snapshot based on the Poisson process. The time instant $t^{(i)}$ when session i for $i = 1, 2, \dots, N_{\text{max}}$ starts is modelled by an exponentially distributed random variable with pdf given by

$$f_{t^{(i)}}(t^{(i)}) = \begin{cases} \lambda_{\text{speech}} \exp(-\lambda_{\text{speech}} \cdot (t^{(i)} - t^{(i-1)})) & \text{for } t^{(i)} \geq t^{(i-1)} \\ 0 & \text{else} \end{cases} \quad (3.5)$$

with $t^{(0)} = 0$ the beginning of the snapshot. The Poisson process is memoryless so that everything that happens after the snapshot start is independent of conditions before the snapshot starts [Pap84].

During the snapshot, new packets of active sessions arrive according to the traffic model as described in Section 2.4.

According to the traffic model, sessions terminate after an exponentially distributed session duration T_{speech} as given in (2.12). The time instant $t_{\text{term}}^{(i)}$ when session i for $i = 1, 2, \dots$ ends is given by a random variable with exponential distribution and depends on the time instant $t_{\text{term}}^{(i-1)}$ where session i ends and the number n_{active} of active users at session start. The pdf of $t_{\text{term}}^{(i)}$, using the fact that the process is memoryless, is given by

$$f_{t_{\text{term}}} \left(t_{\text{term}}^{(i)} + t_{\text{term}}^{(i-1)} \right) = \begin{cases} (n_{\text{active}} - i + 1) \mu_{\text{speech}} \cdot \dots \cdot \exp \left(-(n_{\text{active}} - i + 1) \mu_{\text{speech}} t_{\text{term}}^{(i)} \right) & \text{for } 0 \leq t_{\text{term}}^{(i)} \\ 0 & \text{else} \end{cases} \quad (3.6)$$

Session i that ends at time $t_{\text{term}}^{(i)}$ is selected randomly out of the sessions that are active at snapshot start. The time $t_{\text{term}}^{(0)}$ is the time when the snapshot started.

3.3.3 Download traffic

This section derives statistics for download traffic as used in the snapshot based system level simulation methodology.

Download traffic can be treated as queueing model with state dependent session duration. As described in Section 2.4, a file size $S_{\text{f,dl}}^{(i)}$ in byte is chosen randomly for user i . The session duration $T_{\text{dl}}^{(i)}$ depends on the average user throughput $\bar{r}_{\text{user}}^{(i)}$ in bit per second of user i as follows:

$$T_{\text{dl}}^{(i)} = \frac{S_{\text{f,dl}}^{(i)} \cdot 8 \frac{\text{bits}}{\text{byte}}}{\bar{r}_{\text{user}}^{(i)}}. \quad (3.7)$$

The following relationship can be observed between the number of active users and the average user throughput due to the limited number of resource units. If the number of active users is high only a small number of resource units can be allocated to each user. Therefore, the average user throughput will decrease if the number of active users increases if all other parameters remain constant. This leads to an increase in the session duration if the number of active users increases assuming a constant arrival rate for the queueing model. In Kendall's notation the queueing model for the number of active users is given by $M/SD/\infty$ indicating a Markovian arrival process and a state dependent ending process.

The average number of active users can be obtained using Little's law [Lit61] that states that the average number of active users is given by the product of the arrival

rate λ_{dl} and the average session duration $E\{T_{dl}\}$ independent of the arrival or ending processes, thus,

$$E\{n_{active,dl}\} = \lambda_{dl} \cdot E\{T_{dl}\}. \quad (3.8)$$

Using (3.7), the average session duration of downlink traffic is given by

$$E\{T_{dl}\} = E\{S_{f,dl}\} \cdot 8 \frac{\text{bits}}{\text{byte}} \cdot E\left\{\frac{1}{d_{res}}\right\} E\left\{\frac{1}{n_{alloc}}\right\} \quad (3.9)$$

where d_{res} represents the number of bits that can be transmitted using one single resource unit and n_{alloc} represents the number of resource units a user gets allocated during one second. The expectation value of the reciprocal of the allocated resource units is proportional to the expectation value of the active users divided by the number of available resource units per second N_{res} as follows:

$$E\left\{\frac{1}{n_{alloc}}\right\} = \frac{E\{n_{active,dl}\} + 1}{N_{res}}. \quad (3.10)$$

Using (3.8), (3.9) and (3.10), the average number of active users is given by

$$E\{n_{active,dl}\} = \frac{\lambda_{dl} E\{S_{f,dl}\} \cdot 8 \frac{\text{bits}}{\text{byte}} \cdot E\left\{\frac{1}{d_{res}}\right\} \frac{1}{N_{res}}}{1 - \lambda_{dl} E\{S_{f,dl}\} \cdot 8 \frac{\text{bits}}{\text{byte}} \cdot E\left\{\frac{1}{d_{res}}\right\} \frac{1}{N_{res}}}. \quad (3.11)$$

The probability for $n_{active,dl}$ active download sessions at snapshot start is given by

$$P(n_{active,dl} = k) = \begin{cases} \frac{1}{1 + E\{n_{active,dl}\}} \cdot \left(1 + \frac{1}{E\{n_{active,dl}\}}\right)^{-k} & \text{for } k \geq 0 \\ 0 & \text{else.} \end{cases} \quad (3.12)$$

The buffer level of user i at the beginning of the snapshot depends on the file size $S_{f,dl}^{(i)}$ at the beginning of the session, the average throughput $\bar{r}_{user}^{(i)}$ of the user and the interval $\Delta t^{(i)}$ between the session start and the snapshot start and is given by

$$S_{buffer}^{(i)} = S_{f,dl}^{(i)} - \bar{r}_{user}^{(i)} \cdot \Delta t^{(i)}. \quad (3.13)$$

$\Delta t^{(i)}$ can assumed to be uniformly distributed in the interval

$$0 \leq \Delta t^{(i)} \leq \frac{S_{f,dl}^{(i)}}{\bar{r}_{user}^{(i)}} \quad (3.14)$$

if $\bar{r}_{user}^{(i)}$ does not change significantly over the time. For simplicity reasons, the user index i is skipped for the following investigation. The calculated pdf is valid for all users with

an active download session. Applying random variable transformation [Pap84] results into the pdf of the buffer level given by

$$f_S(S_{\text{buffer}}) = \begin{cases} g_S(S_{\text{buffer}}) & \text{for } S_{\text{buffer}} > 0 \\ 0 & \text{else} \end{cases} \quad (3.15)$$

with

$$g_S(S_{\text{buffer}}) = \frac{1}{2\sigma_L} \left(\frac{\exp\left(-\frac{(\ln(S_{\text{buffer}})-\mu_L)^2}{2\sigma_L^2}\right) \cdot \sigma_L}{S_{\text{buffer}} \sqrt{\pi} \sigma_L} + \exp\left(-\mu_L + \frac{\sigma_L^2}{2}\right) \cdot \left(\operatorname{erfc}\left(\frac{\ln(S_{\text{buffer}}) + \mu_L + \sigma_L}{\sqrt{2}\sigma_L}\right) - \frac{\exp\left(\frac{(\ln(S_{\text{buffer}})+\mu_L+\sigma_L)^2}{2\sigma_L^2}\right) \sqrt{2}}{\sqrt{\pi}\sigma_L} \right) \right) \quad (3.16)$$

where μ_L and σ_L are parameters of the lognormally distributed file size, cf. Section 2.4. $\operatorname{erfc}(x)$ is the complementary error function given by

$$\operatorname{erfc}(x) = \frac{2}{\sqrt{\pi}} \int_x^{\infty} \exp\{-t^2\} dt. \quad (3.17)$$

As for speech traffic, new download sessions arrive according to the assumed Poisson process. The statistics for the time instant during the snapshot when a new download session arrives is given by (3.5) when replacing λ_{speech} with λ_{dl} .

For each new download session that starts during the snapshot, the file size $S_{\text{f,dl}}$ and the arrival of new packets in the transmitting entity is modelled according to the traffic model as described in section 2.4.

Download traffic sessions end if the whole file is transmitted and no more packets are available in the transmit buffer. The time instant when a download session ends is a result of the transmit conditions during the snapshot.

3.3.4 Web browsing traffic

Web browsing traffic is modelled by a series of packet calls, which are comparable to small file downloads, interrupted by reading time durations T_{RT} , cf. Section 2.4. The packet call size is given by S_{pc} and the number of packet calls is given by N_{pc} so that the average session duration is given by

$$E\{T_{\text{wb}}\} = E\{T_{\text{pc}}\} + (E\{N_{\text{pc}}\} - 1) E\{T_{\text{RT}}\}. \quad (3.18)$$

$E\{T_{pc}\}$ is the expectation value of the packet call durations of the session which is similar to (3.9) given by

$$E\{T_{pc}\} = E\{N_{pc}\} E\{S_{pc}\} \cdot 8 \cdot E\left\{\frac{1}{d_{res}}\right\} \frac{E\{n_{active,wb}\} + 1}{N_{res}} \quad (3.19)$$

with $E\{n_{active,wb}\}$ the average number of active web browsing users, i.e. that are in the packet call period.

Using Little's law, the average number of active sessions, i.e. either being in a packet call or a reading time period, is given by

$$E\{n_{ses,wb}\} = \lambda_{wb} \cdot E\{T_{wb}\} \quad (3.20)$$

with λ_{wb} the average arrival rate of the Poisson process for web browsing users.

Assuming an average user throughput $\bar{r}_{user}^{(i)} \gg 0$ kbit/s, the average packet call duration will become small compared to the average reading time duration. Thus, the average session duration of (3.18) can be approximated by $(E\{N_{pc}\} - 1) E\{T_{RT}\}$. The queueing model indicating how many sessions are active is an $M/G/\infty$ queueing model in Kendall's notation where M indicates a Poisson process as arrival process and G indicates a session duration that is described by an arbitrary distributed random variable. Therefore, the probability that $n_{ses,wb}$ sessions are active at an arbitrary time instant is given by the Poisson distribution as

$$P(n_{ses,wb} = k) = \begin{cases} \frac{E\{n_{ses,wb}\}^k}{k!} \cdot \exp(-E\{n_{ses,wb}\}) & \text{for } k \geq 0 \\ 0 & \text{else.} \end{cases} \quad (3.21)$$

The probability that $n_{pc,wb}$ web browsing users are in a packet call period is given by

$$P(n_{pc,wb} = k) = \begin{cases} \sum_{i=k}^{\infty} \frac{1}{k!(i-k)!} p_{active}^k (1 - p_{active})^{i-k} \cdot \dots \\ \exp(-E\{n_{ses,wb}\}) E\{n_{ses,wb}\}^i & \text{for } 0 \leq k \\ 0 & \text{else} \end{cases} \quad (3.22)$$

and the average activity probability p_{active} is given by

$$p_{active} = \frac{E\{T_{pc}\}}{E\{T_{pc}\} + (E\{N_{pc}\} - 1) E\{T_{RT}\}}. \quad (3.23)$$

Therefore, the average number of active users is given by

$$E\{n_{active,wb}\} = E\{n_{ses,wb}\} \cdot p_{active}. \quad (3.24)$$

Using (3.24), (3.20) and (3.23) results into

$$\mathbb{E}\{n_{\text{active,wb}}\} = \lambda_{\text{wb}} \cdot \mathbb{E}\{N_{\text{pc}}\} \mathbb{E}\{S_{\text{pc}}\} \cdot 8 \cdot \mathbb{E}\left\{\frac{1}{d_{\text{res}}}\right\} \frac{\mathbb{E}\{n_{\text{active,wb}}\} + 1}{N_{\text{res}}}. \quad (3.25)$$

The average number of active users is then given by

$$\mathbb{E}\{n_{\text{active,wb}}\} = \frac{\lambda_{\text{wb}} \cdot \mathbb{E}\{N_{\text{pc}}\} \mathbb{E}\{S_{\text{pc}}\} \cdot 8 \cdot \mathbb{E}\left\{\frac{1}{d_{\text{res}}}\right\} \frac{1}{N_{\text{res}}}}{1 - \lambda_{\text{wb}} \cdot \mathbb{E}\{N_{\text{pc}}\} \mathbb{E}\{S_{\text{pc}}\} \cdot 8 \cdot \mathbb{E}\left\{\frac{1}{d_{\text{res}}}\right\} \frac{1}{N_{\text{res}}}} \quad (3.26)$$

and the probability of $n_{\text{active,wb}}$ active web browsing users at snapshot start is approximated by

$$\mathbb{P}(n_{\text{active,wb}} = k) = \begin{cases} \frac{1}{1 + \mathbb{E}\{n_{\text{active,wb}}\}} \cdot \left(1 + \frac{1}{\mathbb{E}\{n_{\text{active,wb}}\}}\right)^{-k} & \text{for } k \geq 0 \\ 0 & \text{else.} \end{cases} \quad (3.27)$$

The arrival of new web browsing users is again modelled by a Poisson process so that the statistics for the time instant during the snapshot when a new web browsing session starts are given by (3.5) if λ_{speech} is replaced by with λ_{wb} .

For each new web browsing session that starts during the snapshot, the number of packet calls N_{pc} , the packet call size S_{pc} and reading time duration are modelled according to the traffic model as described in section 2.4.

Web browsing sessions end if the last packet of the last packet call is transmitted. The time instant when a download session ends is a result of the transmit conditions during the snapshot.

3.4 Effective resource unit performance

In this section, an effective SIR is described that represents the performance of the resource unit. The effective SIR can be used, e.g., to perform scheduling or link adaptation. A resource unit as defined in Section 2.5 is the smallest unit in time and frequency domain that is allocated for transmission to one user containing N_{sc} subcarriers in frequency domain and N_{sym} OFDMA symbols in time domain that are transmitted with one modulation scheme and one coding rate. Subcarriers spaced within the coherence bandwidth B_{coh} achieve approximately equal small-scale fading so that the complexity can be reduced if only one sample is calculated that represents the SIR of

a group of subcarriers. However, networks like WiMAX utilise frequency diversity by combining subcarriers in one resource unit that are distributed over the whole bandwidth experiencing different SIR values [WiM07]. Thus, different SIR depending on the frequency-selective small-scale fading have to be considered for each subcarrier. In the following, a methodology is described calculating an effective performance using statistical properties of the frequency selective small-scale fading channel and the mutual information leading to lower complexity than the standard approach of calculating the small-scale fading for each subcarrier [WGL⁺05, BAS⁺05].

In the following, it is assumed that the user is connected to BS with index 0 and N_{interf} interfering BSs are present. The large-scale propagation loss between the user and BS with index i is given by $\alpha_{\text{ls},i}$. Using the channel transfer factor $H_i(t, f_k)$ as given by (2.8), the SIR $\gamma(t, f_k)$ at time t and for subcarrier k with centre frequency f_k can be calculated as

$$\gamma(t, f_k) = \frac{\alpha_{\text{ls},0} \cdot |H_0(t, f_k)|^2}{\sum_{i=1}^{N_{\text{interf}}} \alpha_{\text{ls},i} \cdot |H_i(t, f_k)|^2}. \quad (3.28)$$

According to [IM92], the denominator can be approximated using the average value $E\{|H_i(t, f_k)|^2\}$ if the standard deviation of the denominator is smaller than the standard deviation of the numerator which is usually fulfilled if several interfering BSs are considered. Therefore, (3.28) results into

$$\gamma(t, f_k) = \frac{\alpha_{\text{ls},0} \cdot |H_0(t, f_k)|^2}{\sum_{i=1}^{N_{\text{interf}}} \alpha_{\text{ls},i} \cdot E\{|H_i(t, f_k)|^2\}}. \quad (3.29)$$

To determine the effective SIR of the resource unit, the mutual information for each subcarrier is used representing the performance that is achievable with the subcarrier and the modulation scheme, if a perfect adaptation to the channel conditions, e.g., in terms of coding, is possible. The mutual information increases with increasing SIR. Depending on the modulation scheme, a maximum mutual information is achieved for a certain SIR and no further improvement of the mutual information can be achieved with increasing the SIR due to the limited number of bits per channel usage. The mutual information for different modulation schemes is derived in Appendix A.1. In the following, the relationship between the SIR $\gamma(t, f_k)$ and the mutual information $\epsilon(t, f_k)$ is represented by the following equation:

$$\epsilon(t, f_k) = C(\gamma(t, f_k)). \quad (3.30)$$

Assuming that $f_k, t \in \mathcal{RU}$ indicates all subcarriers and OFDMA symbols that belong to the resource unit, the average mutual information of the resource unit is determined

as

$$\bar{\epsilon}_{\text{ru}} = \frac{1}{N_{\text{sym}}N_{\text{sc}}} \sum_{f_k, t \in \mathcal{RU}} \epsilon(t, f_k). \quad (3.31)$$

Based on $\bar{\epsilon}_{\text{ru}}$, the effective SIR of the resource unit is derived using the inverse of $C(\gamma)$ as given by

$$\bar{\gamma}_{\text{ru}} = C^{-1}(\bar{\epsilon}_{\text{ru}}). \quad (3.32)$$

Assuming a distributed subcarrier allocation, resource units that are transmitted at the same time using different subcarriers experience equal performance because of subcarriers that are distributed over the whole bandwidth. Therefore, statistical properties of the channel transfer factors are used to calculate the effective SIR instead of calculating (3.29) for each subcarrier of the resource unit. For the ITU tapped-delay line models described in Section 2.3, the pdf of $|H_0(t, f_k)|^2$ is well approximated by

$$f_{H^2}(H^2) = \begin{cases} \frac{1}{H_{\text{up}} - H_{\text{low}}} & \text{for } H_{\text{low}} \leq H^2 \leq H_{\text{up}} \\ 0 & \text{else} \end{cases}. \quad (3.33)$$

H_{low} and H_{up} are given using the average value

$$\mu_{\text{ctf}}(t) = \frac{1}{N_{\text{sc}}} \sum_{k=1}^{N_{\text{sc}}} |H_0(t, f_k)|^2 \quad (3.34)$$

and the variance

$$\sigma_{\text{ctf}}^2(t) = \frac{1}{N_{\text{sc}}} \sum_{k=1}^{N_{\text{sc}}} |H_0(t, f_k)|^4 - \mu_{\text{ctf}}^2(t), \quad (3.35)$$

as

$$H_{\text{up}} = \mu_{\text{ctf}}(t) + \sqrt{3}\sigma_{\text{ctf}}(t) \quad (3.36)$$

and

$$H_{\text{low}} = \mu_{\text{ctf}}(t) - \sqrt{3}\sigma_{\text{ctf}}(t), \quad (3.37)$$

respectively.

To reduce computational complexity, only a limited number of samples are used for calculating the average mutual information instead of transforming the pdf. [KB83] gives an overview of state-of-the-art approximations of pdfs aiming at approximating the shape of the cumulative distribution function (cdf). For this work, two approximations are proposed that approximate the pdf by three samples with equal probability.

The first approximation assumes that each sample is located in the middle of an interval covering a probability of $\frac{1}{3}$. The three samples $A1$, $A2$ and $A3$ are given as follows:

$$H_0^{(A1)}(t) = \mu_{\text{ctf}}(t) - \frac{2}{\sqrt{3}}\sigma_{\text{ctf}}(t) \quad (3.38a)$$

$$H_0^{(A2)}(t) = \mu_{\text{ctf}}(t) \quad (3.38b)$$

$$H_0^{(A3)}(t) = \mu_{\text{ctf}}(t) + \frac{2}{\sqrt{3}}\sigma_{\text{ctf}}(t). \quad (3.38c)$$

It can be shown that the variance of $|H_0(t, f_k)|^2$ is different from the variance obtained using the three samples given in (3.38). The second proposed approximation also consists of three samples with equal probability but mean value and variance are equal to the values given in (3.34) and (3.35), respectively. The three samples $B1$, $B2$ and $B3$ given by

$$H_0^{(B1)}(t) = \mu_{\text{ctf}}(t) + a_1\sigma_{\text{ctf}}(t), \quad (3.39a)$$

$$H_0^{(B2)}(t) = \mu_{\text{ctf}}(t) + a_2\sigma_{\text{ctf}}(t) \text{ and} \quad (3.39b)$$

$$H_0^{(B3)}(t) = \mu_{\text{ctf}}(t) + a_3\sigma_{\text{ctf}}(t) \quad (3.39c)$$

have to fulfil the following two equations:

$$\mu_{\text{ctf}}(t) = \frac{1}{3}(\mu_{\text{ctf}}(t) + a_1\sigma_{\text{ctf}}(t) + \mu_{\text{ctf}}(t) + a_2\sigma_{\text{ctf}}(t) + \mu_{\text{ctf}}(t) + a_3\sigma_{\text{ctf}}(t)) \quad (3.40)$$

and

$$\sigma_{\text{ctf}}^2(t) = \frac{1}{3}((\mu_{\text{ctf}}(t) + a_1\sigma_{\text{ctf}}(t))^2 + (\mu_{\text{ctf}}(t) + a_2\sigma_{\text{ctf}}(t))^2 + (\mu_{\text{ctf}}(t) + \dots + a_3\sigma_{\text{ctf}}(t))^2) - \mu_{\text{ctf}}^2(t). \quad (3.41)$$

Assuming a symmetric distribution of the samples around the average value leads to $a_2 = 0$ and using (3.40) and (3.41), the samples are given by

$$H_0^{(B1)}(t) = \mu_{\text{ctf}}(t) - \sqrt{\frac{3}{2}}\sigma_{\text{ctf}}(t), \quad (3.42a)$$

$$H_0^{(B2)}(t) = \mu_{\text{ctf}}(t) \text{ and} \quad (3.42b)$$

$$H_0^{(B3)}(t) = \mu_{\text{ctf}}(t) + \sqrt{\frac{3}{2}}\sigma_{\text{ctf}}(t). \quad (3.42c)$$

Assuming a WiMAX network, a resource unit is equivalent to a slot and therefore consists of 48 subcarriers in the downlink [IEE05]. Instead of calculating 48 different SINR values and calculating the mutual information, only three samples using the channel transfer factors in (3.42) have to be calculated and the mutual information is only calculated for these three samples, which reduces complexity.

Further complexity reduction can be obtained in (3.34) and (3.35). If the coherence bandwidth is much larger than the subcarrier spacing, the channel transfer factors of subcarriers within the coherence bandwidth B_{coh} is equal. Therefore, mean and variance will remain the same even if only each K -th subcarrier with $K > 1$ is considered in (3.34) and (3.35). The value of K depends on B_{coh} .

The proposed approximations provide lower complexity compared to scenarios where the mutual information of each subcarrier is taken into account for calculating the effective SIR of the resource unit. Only 3 samples are calculated in each time instant using the mean value and the variance of $|H_0(t, f_k)|^2$. The mutual information is calculated for only these three samples.

3.5 User scheduling

This section describes the procedure of scheduling users and allocating resource units in the proposed system level simulation methodology. Sophisticated and adaptive scheduling algorithms have to be considered when realistic performance results shall be obtained during the evaluation of cellular wireless networks. In conventional dynamic system level simulations, the scheduling decision is performed on resource unit basis by solving an optimisation problem as described in Section 2.6 and deriving which user shall get which resource unit.

Due to the consideration of snapshots in the snapshot based system level simulation methodology, scheduling can also be performed on resource unit basis. It is not the aim of this work to determine new scheduling algorithms. Thus, state-of-the-art scheduling algorithms are considered as depicted in Section 2.6. If scheduling algorithms are used that require, e.g., knowledge of the average user throughput, users are initialised with 0 kbit/s at the beginning of the snapshot no matter if the user was already active before the start of the snapshot. All active users are considered with equal performance during the first scheduling decision. After some scheduling decisions, average user throughput values are achieved so that the scheduling algorithm is able to consider users according to their user throughput performance. Adaptive scheduling strategies using channel knowledge for the user scheduling use the effective performance measure as introduced in Section 3.4. The effective SIR as defined in (3.32) is used for instance in (2.25) indicating which rate can be obtained by user i if the resource unit is allocated to this user.

Although a distributed subcarrier allocation is assumed throughout this work which achieves frequency diversity, scheduling depending on channel state information, e.g.,

proportional fair scheduling, is beneficial. As stated in Section 3.4, the effective SIR of resource units that are transmitted at the same time to one user are equal if a distributed subcarrier allocation is used. However, resource units that are transmitted to one user at time instants that are separated by more than the coherence time have different effective SIR which is utilised by scheduling strategies that consider channel state information.

Compared with dynamic system level simulations, the snapshot based system level simulation methodology is able to apply the same scheduling algorithms. If the snapshot duration is sufficiently large, statistical reliability is achieved for the scheduling results in each snapshot.

3.6 KPI measurements

This section describes how measurements of KPIs are obtained with the proposed simulation methodology. Measurements in the snapshot based system level simulation methodology differ slightly compared to dynamic system level simulations.

Measurements are only possible for the snapshot duration. Results obtained from different snapshots are independent of each other. Therefore, measurements obtained for one user during the snapshot have to be representative for the whole session although the session may last longer than the snapshot. The duration for which a user is active has to be taken into account.

For the snapshot based system level simulation methodology, it is distinguished between measurements that consider a time duration that is shorter than a snapshot and measurements considering a time duration that is longer than a snapshot. The first type of measurements is performed as in conventional dynamic system level simulations, e.g., a block error probability (BLEP) or the usage of different modulation and coding schemes is obtained by evaluating each single resource unit that is used for transmission and counting whether it is decoded correctly and which modulation and coding scheme is used, respectively. Measurements are performed for each snapshot of the simulation. Furthermore, actual user or cell throughput can be determined measuring how much data is transmitted, e.g., during one resource unit duration.

All other measurements have to be limited to the snapshot duration in the snapshot based system level simulation methodology. Therefore, average user throughput as well as average cell throughput are only measured over a time interval of the snapshot

duration. By collecting throughput results of sufficiently many independent snapshots, reliable results are obtained. Based on the user throughput, it is determined whether the user is satisfied or not depending on the required throughput as described in Section 2.7. To determine the number of unsatisfied users, each user is weighted depending on the duration he is active during the snapshot. Thus, users that are active for the whole snapshot duration are counted with higher weight than users that, e.g., arrive shortly before the snapshot ends.

The snapshot based system level simulation methodology is able to obtain the same KPI measurements as in conventional dynamic system level simulations. Resource units can be evaluated, e.g., regarding BLEP and throughput measurements can be obtained both averaged over the snapshot as well as instantaneous. Thus, results regarding the QoS are obtained. Compared with conventional system level simulations, measurements are limited to the snapshot duration. Therefore, it is not possible, e.g., to obtain a measurement of the user throughput development if the user moves from the cell centre to the cell border.

3.7 Performance and complexity evaluation

3.7.1 Introduction

In this section, the developed snapshot based system level simulation methodology is evaluated regarding performance accuracy and complexity using specific test scenarios. Furthermore, parameter settings are proposed in the following so that the snapshot based system level concept can be used achieving accurate results compared to state-of-the-art dynamic system level simulators. The proposed snapshot based system level simulation methodology provides lower complexity compared to state-of-the-art dynamic system level simulations by considering independent and short snapshots, which has impact on the calculation of the large-scale propagation loss as well as on the generation of data traffic, and by using statistical properties of the frequency selective channel transfer factors when calculating the effective SIR of the resource units, cf. Table 3.1.

Table 3.3 summarises the performance and complexity analysis that is elaborated in the following subsections. It is evaluated how many independent snapshot have to be generated to achieve reliable results and how long the snapshot duration has to be. Furthermore, the calculation of the effective SIR for the resource units is evaluated.

Table 3.3. Performance and complexity analysis

Part of the investigation	Parameter under investigation	Optimal Value	Minimum required value	Maximum possible value
Number of Snapshots	Ratio between number of active users per snapshot and the size of the user pool	Infinite size of the user pool	Achieve a sufficient number of independent snapshots	Limited by storage space that can be provided
	Scheduling algorithm and data traffic models	Infinite number of snapshots	Statistical reliability of the results has to be achieved	Minimise complexity and simulation duration
Snapshot duration	User velocity, shadow fading correlation distance	Close to 0 s	Optimal for very short snapshot durations	Depends on error that is accepted due to constant large-scale propagation
	Scheduling algorithm and user velocity	Infinite snapshot duration	Statistics regarding scheduling and small-scale fading have to be fulfilled	Optimal for very long snapshot durations
Effective SIR calculation	Coherence bandwidth of the channel model	Considering all subcarriers in frequency domain and calculate average and variance	Low number of subcarriers considered to reduce the number of the DFT-calculations for the frequency-selective channel transfer factors	High number of subcarriers to keep the error of the calculated average value and the variance of the channel transfer factors low
	3-point approximation methodology	Considering the SIR of each individual subcarrier of the resource unit to calculate the effective SIR	3 appropriate samples describing the SIR of the individual subcarriers accurately	More samples could be used if error in effective SIR is high

The number of snapshots that are necessary to achieve reliable results is elaborated in Section 3.7.2. An analysis is carried out for different ratios between number of active users and sizes of the user pool as well as for different scheduling strategies and data traffic models. To achieve optimal results an infinite user pool size leading to infinite independent snapshots is required. However, the maximum user pool size is limited by memory space that can be provided because of storing the large-scale propagation loss between each user position and each BS in a file. Therefore, a minimum number of snapshots has to be determined that achieves statistical reliable results for a limited user pool size, different scheduling algorithms and data traffic models leading to minimum computational complexity as depicted in Table 3.3.

An evaluation of the duration of one snapshot is given in Section 3.7.3. Parameters that are investigated are the user velocity and the correlation distance of the shadow fading. Assuming a constant user position, the optimal snapshot is close to zero seconds. However, short snapshot durations can be used with small error in the SIR due to large-scale propagation loss of the users. On the other hand, user scheduling and the user velocity are considered. An infinite snapshot duration leads to optimal results. However, statistically reliable results can be achieved for a finite duration of the snapshot if enough scheduling decisions and variations of the effective SIR due to small-scale fading are considered as depicted in Table 3.3.

The calculation of the effective SIR for the resource units is investigated in Section 3.7.4. The average value and the variance of the channel transfer factors are calculated for channel models with different coherence bandwidth. As depicted in Table 3.3, optimal results can be achieved if all subcarriers are considered for calculation of the mean value and the variance of the channel transfer factors. However, the channel transfer factor is constant for subcarriers that are within the coherence bandwidth. Thus, the number of subcarriers considered for calculating the mean value and the variance of the channel transfer factors can be reduced. DFT-calculations in (2.8) can be reduced. Furthermore, the proposed 3-point approximation methodologies for the calculation of the effective SIR of the resource units are evaluated. Optimal effective SIR is achieved if all subcarriers of the resource unit are considered. The proposed 3-point approximation methodologies are compared with state-of-the-art approaches regarding the error in effective SIR compared to the optimal value in Section 3.7.4.

Results showing the impact of user scheduling and data traffic for different number of active users as well as different server data rates are given in Chapter 5.

The χ^2 -test is used to evaluate the reliability of the KPI measurements obtained with the snapshot based system level simulation methodology in Section 3.7.2 and Section

3.7.3. Therefore, a short overview of the χ^2 -test is given in the following. A detailed description of the χ^2 -test can be found, e.g., in [Lan68, GN96]. The χ^2 -test is a well known hypothesis test where samples obtained from an observation are tested against a hypothetical pdf and as a result, the hypothesis is rejected or not rejected. Thus, with a significance level a it can be stated that the samples from the observation are from the distribution with the hypothetical pdf. Applying the χ^2 -test, results obtained from the simulation are summarised in a histogram with N_{sam} intervals. Interval i with $i = 1, \dots, N_{\text{sam}}$ contains all values greater or equal to lb_i and smaller to ub_i . The frequency how often each interval is observed in the results is given by ω_i with $i = 1, \dots, N_{\text{sam}}$ called observed frequencies in the following. The observed frequencies ω_i are tested against a hypothetical pdf $f_x(x)$. Based on $f_x(x)$, expected frequencies ϵ_i with $i = 1, \dots, N_{\text{sam}}$ are derived as

$$\epsilon_i = \int_{lb_i}^{ub_i} f_x(x) dx. \quad (3.43)$$

The size of the intervals is chosen such that expected frequencies are equal, i.e.,

$$\epsilon_i \simeq \frac{1}{N_{\text{sam}}} \text{ for all } i = 1, \dots, N_{\text{sam}}. \quad (3.44)$$

The relative quadratic error between observed and expected frequencies is given by

$$D = \sum_{i=1}^{N_{\text{sam}}} \frac{(\omega_i - \epsilon_i)^2}{\epsilon_i}. \quad (3.45)$$

D has a χ^2 distribution with $N_{\text{sam}} - 1$ degrees of freedom [Jai91]. If $D < \chi_{[1-a; N_{\text{sam}}-1]}^2$, the hypothesis that the observed results come from the hypothetical pdf cannot be rejected with a significance level a . Values of $\chi_{[1-a; k-1]}^2$ are obtained from Tables, cf. [Jai91].

In the following, the significance level a is used to show statistical reliability of the performance measurements. The histogram of a simulation result, e.g., the cell throughput distribution, is compared to a hypothetical cell throughput distribution which might be the outcome of a simulation with optimal results. For a close to one, a good match between observed results and hypothetical distribution is obtained and the results are termed as reliable.

3.7.2 Number of snapshots

In this section, the number of snapshots that are necessary to achieve reliable results is evaluated, cf. Table 3.3. First, the number of snapshots is investigated that is necessary to achieve reliable results depending on the ratio of the number of active users and the user pool size. Afterwards, the number of snapshots that is necessary to obtain reliable results for different data traffic models and scheduling algorithms is examined. As stated in Table 3.3, the size of the user pool has to be big enough to guarantee independent snapshots but a small user pool size is required to save storage capacity. Furthermore, a lower number of snapshots reduces the simulation duration.

The following investigation is performed using a cellular network with equal site-to-site distance. BSs are equipped with omnidirectional antennas and the transmit power is constant for all BSs. The cell radius is chosen so that the network is interference limited and additional noise can be omitted from the investigation. Two tiers of co-channel interfering cells are considered. To avoid border effects, a wrap around technique is applied [ZK01]. The large-scale propagation model consists of distance dependent propagation loss according to (2.4) with $A = -13$ dB and $B = 3.5$ and a random component with pdf given by (2.6). The standard deviation of the shadow fading is 8 dB. The system bandwidth is 1.25 MHz and OFDMA with a 128 FFT is used. The frequency selective fading channel is derived using the Vehicular A test environment as described in Table 2.1. Assuming a user velocity of $v = 1$ km/h, the channel transfer factor does not change significantly over the duration of one snapshot which has a duration of 10 s. Eight resource units are available every 1.4 ms. Eleven different modulation and coding schemes are available. Link adaptation is performed as given in Table 3.4 where $d_{\text{MCS},m}$ for $m = 1, \dots, 11$ indicates the number of bits that can be transmitted with one resource unit and SIR_m for $m = 1, \dots, 11$ indicates the effective SIR that is necessary that the modulation and coding scheme can be received successfully. A download traffic model with an average file size $S_{f,\text{dl}} = 2$ Mbyte as described in Section 2.4 and fair resource scheduling as described in Section 2.6 are assumed. On average, 20 users are active in each cell.

As indicated in Section 3.2, a user pool has to be generated for the snapshot based system level analysis methodology. Active users are selected randomly from the user pool. For each user of the pool, large-scale propagation loss has to be calculated in advance of the investigation and stored in a file. The user pool can be used for many different investigations as long as the assumed scenario, e.g., the location of the BSs and the large-scale propagation model are not changed. However, the size of the file should not be too large. The large-scale propagation loss between the user and each BS is

Table 3.4. Link adaptation parameters

Index m	1	2	3	4	5	6	7	8	9	10	11
$d_{\text{res},m}$ in bit	48	96	144	192	240	288	384	480	576	672	864
SIR_m in dB	-3.4	-0.8	1.5	4.0	5.5	6.7	9.2	12.0	14.1	16.8	20.5

stored as double value which requires 8 bit, the index of the BS the user is allocated to is stored as integer value requiring 4 bit. The storage space increases linearly with the number of users per cell and almost quadratically with the number of BSs. However, the user pool has to be large enough to generate a sufficient number of independent snapshots. It is assumed that reliable results are more important than storage space, the minimum number of snapshots depending on the user pool size and the number of active users per snapshot is determined in the following.

Figure 3.1 shows results obtained for the above described scenario. The significance level a of the χ^2 -test is plotted as function of the number of snapshots for different ratios between the number of active users per snapshot and the user pool size. The χ^2 -test as described in Section 3.7.1 is used to evaluate the statistical reliability. Due to an unknown distribution of expected results, simulation results of a simulation which is expected to achieve optimal results, cf. Table 3.3, are used to determine the expected frequencies in (3.45). The simulation where it is expected to achieve optimal results has an infinite user pool size and 200 independent snapshots are generated. Cell throughput results are collected and histograms with $N_{\text{sam}} = 10$ intervals are calculated. Similar results are achieved if other KPIs are measured, e.g., user throughput results.

To obtain the significance level a in Figure 3.1, histograms of cell throughput results for varying number of snapshots and limited user pool sizes are compared with the histogram obtained for the simulation with 200 snapshots and an infinite user pool size. The significance level a is obtained as result of the χ^2 -test. As shown in Figure 3.1 at least 60 snapshots are necessary for a ratio between the number of active users and the number of users in the pool of 1:20000 to achieve a significance level of one with the χ^2 -test which means that optimal results are achieved. If the size of the user pool is halved, still optimal results can be achieved but the significance level reaches one after nearly 100 snapshots. For even smaller user pool sizes, a significance level of one cannot be achieved so that an error in the distribution of the average cell throughput remains even if many snapshots are considered. It is therefore recommended to generate a user pool in advance of the simulation that is at least 10000 times larger than the number of users that are active per snapshot.

Figure 3.2 shows the significance level a of the χ^2 -test as function of the number of

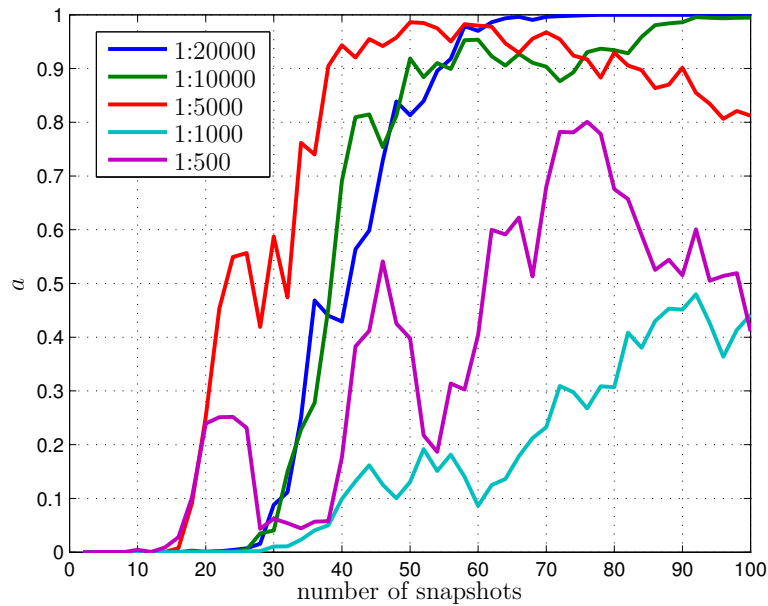


Figure 3.1. Significance level as function of the number of snapshots with the ratio between the number of active users and the size of the user pool as parameter for fair resource scheduling and download traffic

snapshots for different scheduling algorithms and data traffic models. On average, 20 users are considered per cell and the user pool is 20000 times larger than the number of users that are active per snapshot. As for Figure 3.1, results from simulations with 200 snapshots are considered as optimal so that expected frequencies used in the χ^2 -test are calculated from these results. Figure 3.2 shows the results for download traffic with fair resource (FR), proportional fair (PF) and fair throughput (FT) scheduling and additionally fair resource scheduling with web browsing and speech traffic. The other combinations of scheduling algorithm and data traffic models obtain similar results and are omitted for sake of clarity. It can be seen that all combinations reach a significance level of almost one after 80 snapshots which complies with the results shown in Figure 3.1. It can be seen that sophisticated scheduling algorithms like proportional fair or fair throughput scheduling need more snapshots to achieve a high significance level compared to a random scheduling as it is performed with fair resource scheduling. The reason is that, e.g., the throughput of each user also depends on, e.g., channel conditions of other users due to the scheduling decision that considers the average user throughput or actual channel information. Therefore, a large number of snapshots is required for sophisticated scheduling algorithms. The different data traffic models achieve a significance level of almost one after a similar number of snapshots. Only web browsing traffic requires a slightly higher number of snapshot to achieve a significance

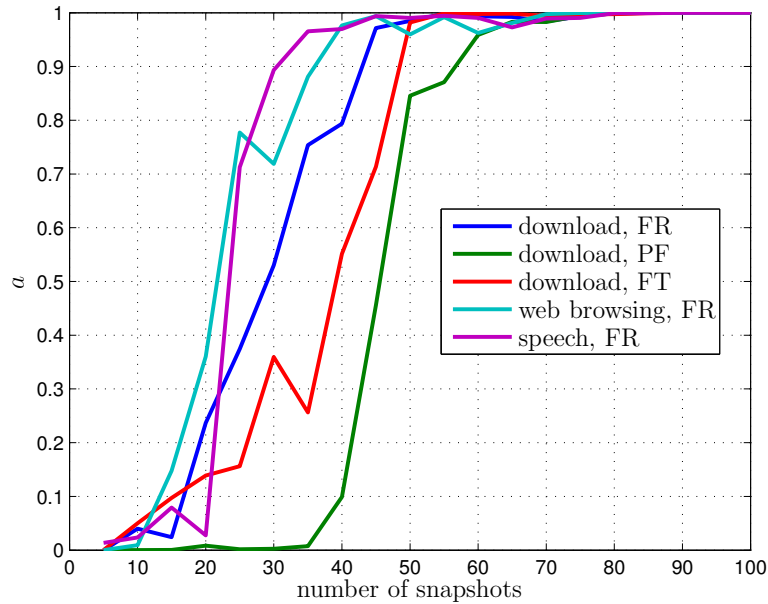


Figure 3.2. Significance level as function of the number of snapshots for different scheduling algorithms and data traffic models with 20 active users per snapshot and cell and a user pool size of 400000 users per cell

level of one due to the burstyness of the model.

Based on the results given in Figure 3.1 and Figure 3.2, it is recommended to use at least 80 snapshots for each simulation run. It can be stated that a larger number of snapshots improves the significance level of the χ^2 -test, but for more than 100 snapshots, no improvement of the significance level can be observed. Regarding the computational complexity of the entire simulation, the simulation duration depends linearly on the number of snapshots, assuming that the user pool is generated offline.

3.7.3 Snapshot duration

This section evaluates the impact of the snapshot duration on accuracy and complexity of the simulation and provides a recommendation for an optimal snapshot duration. As described in Table 3.3 and Section 3.1, the snapshot duration has to be a compromise between two important issues. On the one hand, a snapshot must be short enough so that the assumption of a constant large-scale propagation loss is fulfilled. On the other hand, each snapshot has to be long enough so that scheduling is completely captured.

To determine a maximum snapshot duration, a cellular network with 25 cells is used. Again, Okumura-Hata propagation loss is used and $A = -13$ and $B = 3.5$ in (2.4). The cell radius is set to 5000 m and omnidirectional antennas are used. However, the scenario is still interference limited and additional noise is omitted from the investigation. To avoid border effects, a wrap around technique is applied. The standard deviation of the shadow fading is $\sigma_{\text{SF}} = 8$ dB. For this investigation, it is assumed that users move within the investigation area. Therefore, the random direction mobility model is used [CBD02]. Users that leave the simulation area, e.g., at the right border, reenter at the left border as it is specified by the wrap around model. For the random direction mobility model, a direction is randomly selected between 0 and 2π . The user moves with a constant velocity v in the selected direction. The difference in the SIR due to the large-scale propagation loss is calculated between the position at snapshot start and snapshot end assuming that all BSs transmit with equal power and no fast fading is considered. Figure 3.3 shows the median and 95 %-ile of the absolute value of the SIR difference as function of the snapshot duration for different user velocities. As expected, it can be seen that the difference in SIR between the snapshot start and the snapshot end increases with increasing snapshot duration as the distance a user moves increases. Additionally, a higher difference in SIR can be observed if the user velocity increases for a constant snapshot duration. It can be seen that the user velocity and the snapshot duration have equal impact on the SIR difference so that the snapshot duration has to be reduced by a factor of k if the velocity is increased by a factor of k to obtain the same SIR difference. The absolute difference between the SIR at the snapshot start and the snapshot end is below 4 dB for 95 % of the users with $v = 3$ km/h if the snapshot duration does not exceed 10 s. If $v = 30$ km/h, the snapshot duration has to be shorter than 1 s to achieve an absolute difference between the SIR at snapshot start and at snapshot end below 4 dB. Using the SIR due to large-scale propagation loss in the middle of the snapshot leads to an error that is approximately half the absolute SIR difference as shown in Figure 3.3. The snapshot based methodology cannot be used for scenarios with user velocities $v > 30$ km/h due to an SIR difference between the snapshot start and snapshot end that is too high.

In realistic scenarios, the shadow fading component has a spatial correlation [ZK01, Gud91]. For the results given in Figure 3.3, the spatial correlation was set to 100 m so that for two positions separated by a distance of more than 100 m, the shadow fading component can be assumed to be uncorrelated. Figure 3.4 now shows the median and 95 %-ile of the absolute value of the difference in SIR between the snapshot start and the snapshot end as function of the snapshot duration for different correlation distances of the shadow fading. The user velocity is $v = 3$ km/h in Figure 3.4(a) and $v = 30$ km/h in Figure 3.4(b), respectively. It can be seen that for a correlation distance of 0 m,

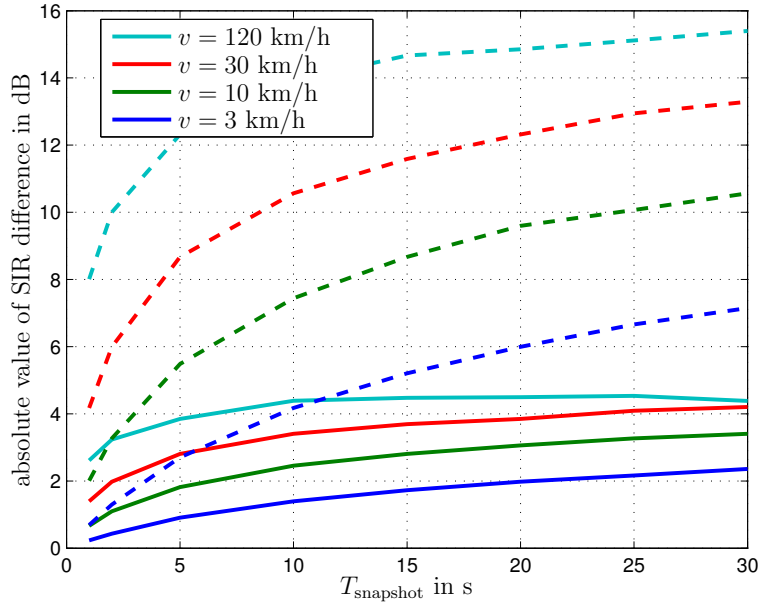


Figure 3.3. Absolute value of SIR difference between snapshot start and end as function of the snapshot duration with the user velocity as parameter; solid lines: median difference, dashed lines: 95 %-ile difference

where shadow fading components of neighboring positions are uncorrelated, a constant SIR difference is observed which is independent of the snapshot duration and the user velocity. The increase for a small snapshot durations with a correlation distance of 0 m in Figure 3.4(a) is due to a shadow fading map resolution which is not small enough. If the correlation distance increases beyond 0 m, the user velocity and the snapshot duration influence the SIR difference. It can be seen that for constant user velocity and constant snapshot duration, the SIR difference decreases if the correlation distance increases. A moving user will experience constant shadow fading over a relatively long distance and the variation in large-scale propagation loss is small compared to the variation introduced by shadow fading. The absolute value of the difference in SIR due to large-scale propagation loss between the snapshot start and the snapshot end is below 4 dB for 95 % of the users with a velocity of 3 km/h in scenarios with a correlation distance of the shadow fading of 200 m if the snapshot duration does not exceed 23 s. If the correlation distance of the shadow fading is reduced to 50 m, the snapshot duration has to be reduced to 5 s that an absolute value of the difference of 4 dB or less is achieved for 95 % the users. If the user velocity is increased from 3 km/h to 30 km/h, the snapshot duration has to be reduced from 23 s to 2 seconds if the absolute value of the SIR difference shall not exceed 4 dB for 95 % of the users. Long snapshot durations can only be used in scenarios with large correlation distance

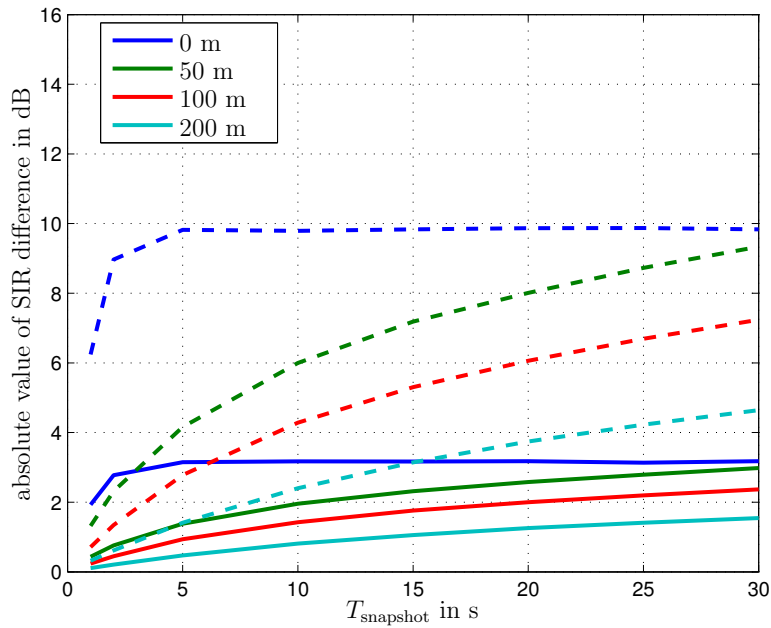
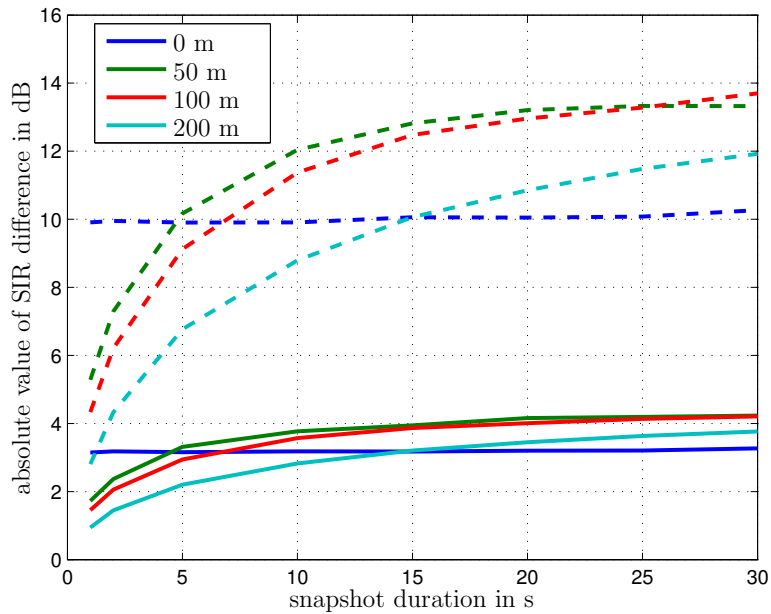
(a) user velocity $v = 3$ km/h(b) user velocity $v = 30$ km/h

Figure 3.4. Absolute value of SIR difference between snapshot start and end as function of the snapshot duration with the shadow fading correlation distance as parameter; solid lines: median difference, dashed lines: 95 %-ile difference

of the shadow fading and slowly moving users.

As already stated in Table 3.3, the minimum snapshot duration is limited due to the scheduling algorithm which needs to schedule users for a certain duration to achieve reliable results. For the second investigation of this section the parameters described in Section 3.7.2 are used. Again, an interference limited cellular network is used with BSs that are equipped with omnidirectional antennas. A download traffic model is used so that each user has always enough data available for transmission. The vehicular A test scenario as described in Table 2.1 is used. It is assumed that the requirement of constant large-scale propagation loss is fulfilled and that optimal results can be obtained for an infinite snapshot duration, where the transient behaviour at the beginning of the snapshot has little impact on the results. The user throughput averaged over one snapshot is measured during the evaluation due to having the highest sensitivity on the scheduling decision. If the user throughput averaged over one snapshot is measured correctly, also the cell throughput averaged over one snapshot will be correct as it is just the sum of the user throughput results. 100 independent snapshots are considered. Results obtained with a snapshot duration of 30 s are assumed to be optimal and the histogram of the users throughput results obtained for a snapshot duration of 30 s are used to calculate the expected frequencies for the χ^2 -test described in Section 3.7.1.

Figure 3.5 shows the significance level α as function of the snapshot duration for fair resource, proportional fair and fair throughput scheduling. Fair resource scheduling, which is equivalent to a random allocation without considering channel state information, reaches a significance level close to one for shorter snapshot durations compared to the other two scheduling algorithms that consider average user throughput or actual throughput conditions during the scheduling decision. Scheduling algorithms considering, e.g., average user throughput conditions require a longer snapshot duration to achieve statistically reliable results. It is assumed that the initial average user throughput conditions are equal for all users so that some scheduling decisions are necessary that the average user throughput reaches a value describing the conditions of each user and scheduling can be performed accurately for the scenario. Furthermore, it can be seen that the user velocity has impact on the accuracy of the results. For users with low velocity, the snapshot duration has to be longer than for users with high velocity. This is due to the time variant fading channel. For low user velocity, the coherence time is high. A long snapshot duration is necessary so that all statistics of the fading channel are collected. For a long coherence time and a short snapshot duration, it might happen that a user is, e.g., in constructive fading conditions during the whole snapshot duration so that the measured average user throughput is too high. It can be seen that, e.g., proportional fair scheduling achieves a significance level close to one after 25 s snapshot duration in a scenario with a user velocity of $v = 1$ km/h while the

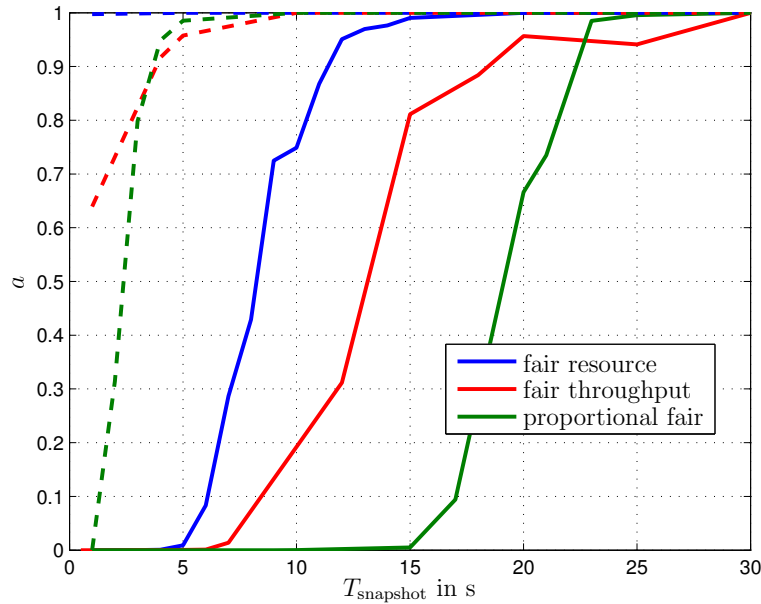


Figure 3.5. Significance level as function of the snapshot duration with different scheduling algorithms as parameter; solid lines: user velocity $v = 1$ km/h, dashed lines $v = 30$ km/h

same significance level is achieved after only 5 s snapshot duration if the user velocity is $v = 30$ km/h.

Considering both results presented in Figure 3.3 and Figure 3.5, it can be concluded that the snapshot duration has to be longer if sophisticated scheduling algorithms like proportional fair or fair throughput scheduling are investigated compared to a random allocation like fair resource scheduling. Scenarios with low user velocity also require a longer snapshot duration compared to scenarios with higher user velocity. However, it can be seen that in a scenario with a user velocity $v = 30$ km/h and a correlation distance of 100 m, the snapshot duration should be around 5 seconds for proportional fair scheduling. This leads to a median SIR difference of roughly 3 dB and 5 % of the users experience an SIR difference that is greater than 8 dB. Assuming that the SIR due to large-scale propagation loss is correct in the middle of the snapshot, the median error is roughly 1.5 dB and for 5 % of the users an error larger than 4 dB is made.

In general, a longer snapshot duration is required for scenarios with low user velocity to fulfil the statistical properties of the small-scale fading channel. A long snapshot duration is possible for low user velocities if the shadow fading correlation distance is in the order of 100 m or higher. The error in SIR due to large-scale propagation loss

is higher than 2 dB only for 5 % of the users. For higher user velocities, the snapshot duration has to be reduced to guarantee similar error in SIR due to large-scale propagation loss. This is possible because, e.g., statistics of the small-scale fading channel can be collected in shorter time than for low user velocity. The proposed snapshot based system level simulation is not suited for scenarios where the user velocity is very high and the correlation distance of the shadow fading is small. Furthermore, it has to be noticed that handovers are not considered in the proposed methodology.

3.7.4 Effective SIR calculation

This section evaluates the accuracy of the proposed approximations to determine the performance measure of the resource unit. In the following, errors are evaluated that occur due to approaches reducing the complexity as described in Section 3.4 and summarised in Table 3.3. The evaluation is made for the measurement accuracy of the average value and variance of the channel transfer factors in frequency domain and of the calculation of the effective SIR $\bar{\gamma}_{\text{ru}}$ of the resource unit which is based on approximating the performance of the individual subcarriers by only three samples that depends on average value and variance of the channel transfer factors in frequency domain.

In the following, channel models as described in Table 2.1 are used. Depending on the channel model, the coherence bandwidth varies from 50 kHz to 2,4 MHz. First, a network with 10 MHz system bandwidth is assumed that uses 1024 subcarriers which is a typical value for a WiMAX network [WiM07]. Second, a network with 1.25 MHz system bandwidth and 128 subcarriers is assumed. The IEEE 802.16 standard permits to operate WiMAX networks with this specification. Broadband wireless access network with a small system bandwidth in the order of 1.25 MHz are currently under consideration for frequency bands with a centre frequencies below 1000 MHz [BMLR04, AW06, ITU06, JKHO06]. For both assumed networks the subcarrier spacing $f_{\text{sc}} = 11.16$ kHz is equal due to the scalability of networks according to, e.g., IEEE 802.16 [IEE05].

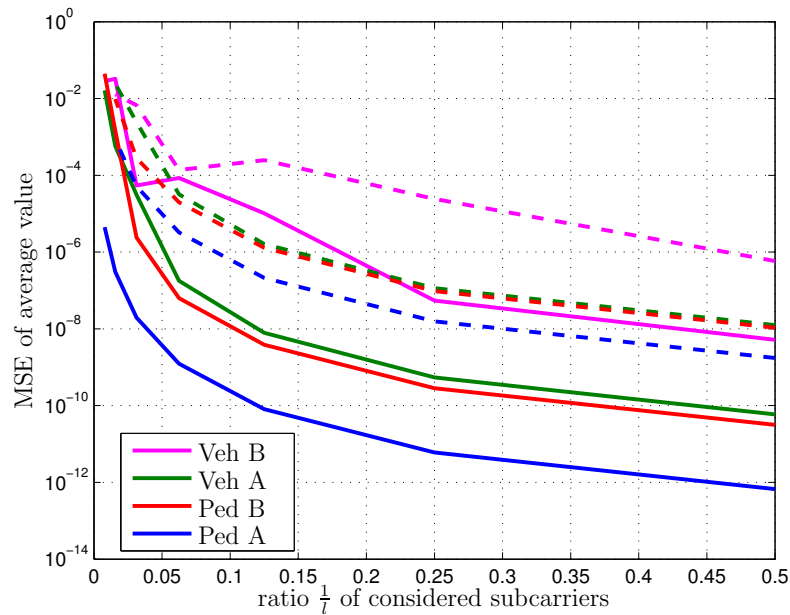
The actual amplification of each tap is an independent and identically distributed (iid) random variable taken from a Rayleigh distribution and the frequency selective channel transfer factors are calculated using (2.7). Average value and variance of the channel transfer factors in frequency domain are calculated as given in (3.34) and (3.35), respectively. To reduce computational complexity, not every subcarrier f_k for $k = 1, \dots, N_{\text{sc}}$ is considered but only each l -th subcarrier f_k with $k = l \cdot \tilde{k} + 1$ for $\tilde{k} = 0, \dots, \frac{N_{\text{sc}}}{l} - 1$. l varies from 2 to 64 or 128, respectively.

Figure 3.6 shows the mean squared error (MSE) of the average value as well as the MSE of the variance of the channel transfer factors as function of the ratio $\frac{1}{l}$ of considered subcarriers with the different channel models as parameter and for both networks with 10 MHz and 1.25 MHz system bandwidth. The MSE of the average value of the channel transfer factors is depicted in Figure 3.6(a) and the MSE of the variance of the channel transfer factors is depicted in Figure 3.6(b). It can be seen that the MSE of the average value as well as of the variance decreases if more subcarriers are considered, e.g., if the Pedestrian A test environment is used in the network with 10 MHz system bandwidth and 50 % instead of 12.5 % of the subcarriers are considered, the MSE of the average value of the channel transfer factors in frequency domain decreases by a factor of 100 and the MSE of the variance of the channel transfer factors in frequency domain decreases by more than a factor of 10. The MSE of the average value of the channel transfer factors in frequency domain roughly increases by a factor of 10 if the coherence bandwidth is reduced from 2.4 MHz to 400 kHz, i.e., Pedestrian A test environment compared with Pedestrian B and Vehicular A test environment, and further increases by a factor of 10 if the coherence bandwidth is further decreased to 50 kHz, i.e., Vehicular B test environment. For a high coherence bandwidth, the channel transfer factor remains constant over a large number of subcarriers so that the average value of the channel transfer factors in frequency domain is not changed significantly if the number of considered subcarriers is reduced. The MSE of the variance of the channel transfer factors remains constant for the different channel models as long as the system bandwidth and therefore N_{sc} is high. If the system bandwidth is reduced from 10 MHz to 1.25 MHz and N_{sc} is reduced from 1024 to 128, the MSE of the average value is increased by a factor of 10 and the MSE of the variance almost by a factor of 20. Due to a smaller number of subcarriers N_{sc} the error increases.

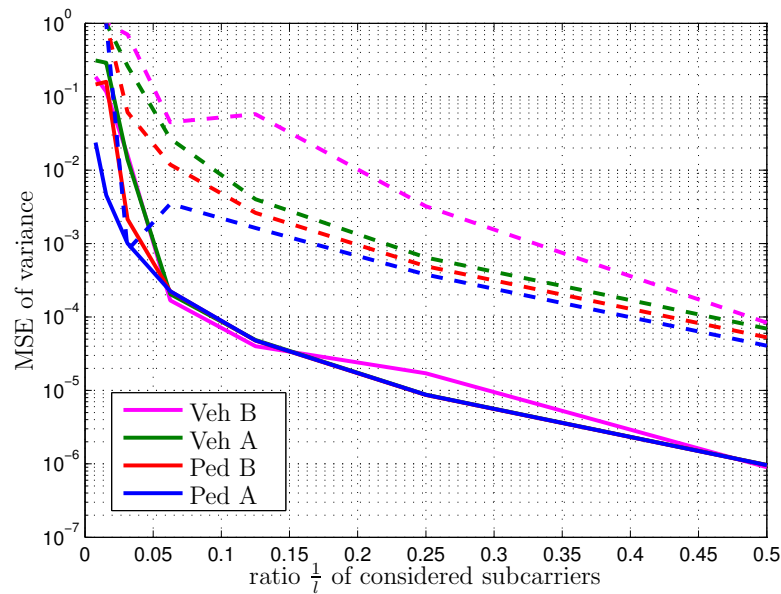
As general conclusion, it can be stated that an acceptable error in calculating the average and the variance of the channel transfer factors in frequency domain can be obtained if each $l = 16$ -th subcarrier is considered when investigating networks with $N_{sc} = 1024$ subcarriers and a system bandwidth of 10 MHz. The MSE of the average value is below 10^{-6} and the MSE of the variance is smaller than 10^{-4} . More subcarriers have to be considered if the coherence bandwidth is small, i.e., as for the vehicular B test environment or the system bandwidth and therefore N_{sc} is small.

The second investigation evaluates the accuracy of the quality measure for the resource units. As the effective SIR mapping methodology is well established for investigations of multicarrier networks [DS04, BSC⁺04, TW05], the following evaluation is focused on the accuracy of the proposed approximations with only three samples.

In the following, the two proposed 3-point approximations as described in Section 3.4



(a) MSE of average value of channel transfer factors in frequency domain



(b) MSE of variance of channel transfer factors in frequency domain

Figure 3.6. MSE of the average value and variance of the channel transfer factors in frequency domain as function of the ratio $\frac{1}{T}$ of considered subcarriers with different channel models as parameter; solid lines: 1024 subcarriers and 10 MHz system bandwidth, dashed lines: 128 subcarriers and 1.25 MHz system bandwidth

are compared with state-of-the-art 3 point approximations. A resource unit with 48 subcarriers is assumed where the subcarriers of the resource unit are distributed over the whole system bandwidth of 1.25 MHz. 128 subcarriers are available in total. The effective SIR $\bar{\gamma}_{\text{ru}}$ is calculated as described in Section 3.4 calculating the mutual information of each subcarrier. The average mutual information of the resource unit leads to the effective SIR. All subcarriers of the resource unit have equal SIR γ_{ls} due to large-scale propagation loss but different channel transfer factors in frequency domain due to frequency selective small-scale fading. To reduce the complexity, the mutual information is not calculated for every subcarrier but three samples depending on average value and standard deviation of the channel transfer factors in frequency domain are used as described in Section 3.4. Besides the proposed approximations, two state-of-the-art 3-point approximations are evaluated as benchmark: The Pearson-Tukey and the Swanson-Megill approximation [KB83]. The Pearson-Tukey approximation replaces the original pdf with the following function:

$$P_{\text{PK}}(x) = \begin{cases} 0.185 & \text{for } x_1 \\ 0.63 & \text{for } x_2 \\ 0.185 & \text{for } x_3 \\ 0 & \text{else} \end{cases} \quad (3.46)$$

The Swanson-Megill approximation replaces the original pdf with the function given by

$$P_{\text{SM}}(x) = \begin{cases} 0.3 & \text{for } x_1 \\ 0.4 & \text{for } x_2 \\ 0.3 & \text{for } x_3 \\ 0 & \text{else} \end{cases} \quad (3.47)$$

The values of x_1 , x_2 and x_3 for the Pearson-Tukey and the Swanson-Megill approximation as well as for the two proposed μ/σ -fitting and 3-Point-Equal-Probability approximation can be found in Table 3.5 as function of the average value μ_{ctf} and the standard deviation σ_{ctf} of the channel transfer factors.

Figure 3.7 shows the MSE of $\bar{\gamma}_{\text{ru}}$ as function of the SIR γ_{ls} due to large-scale propagation loss for different 3-point approximations and modulation schemes. Quadrature Phase

Table 3.5. Samples of the 3 point approximations

Approximation	x_1	x_2	x_3
μ/σ -fitting	$\mu_{\text{ctf}} - \sqrt{\frac{3}{2}}\sigma_{\text{ctf}}$	μ_{ctf}	$\mu_{\text{ctf}} - \sqrt{\frac{3}{2}}\sigma_{\text{ctf}}$
3-Point-Equal-Probability	$\mu_{\text{ctf}} - \frac{2}{\sqrt{3}}\sigma_{\text{ctf}}$	μ_{ctf}	$\mu_{\text{ctf}} - \frac{2}{\sqrt{3}}\sigma_{\text{ctf}}$
Pearson-Tukey	$\mu_{\text{ctf}} - \frac{9}{10}\sqrt{3}\sigma_{\text{ctf}}$	μ_{ctf}	$\mu_{\text{ctf}} - \frac{9}{10}\sqrt{3}\sigma_{\text{ctf}}$
Swanson-Megill	$\mu_{\text{ctf}} - \frac{2}{5}\sqrt{3}\sigma_{\text{ctf}}$	μ_{ctf}	$\mu_{\text{ctf}} - \frac{2}{5}\sqrt{3}\sigma_{\text{ctf}}$

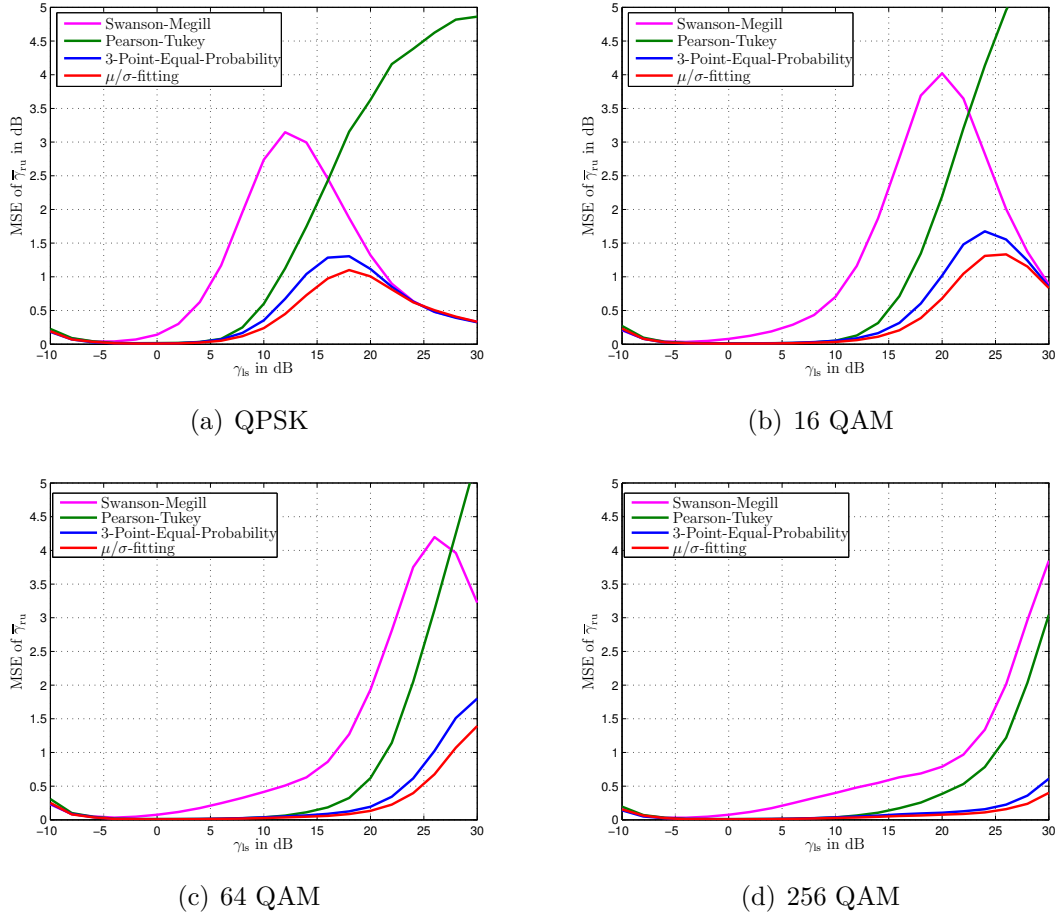


Figure 3.7. MSE of the effective SIR of the resource unit as function of the SIR due to large-scale propagation loss with different 3-point approximations as parameter

Shift Keying (QPSK) is used for the results in Figure 3.7(a), 16 Quadrature Amplitude Modulation (QAM) in Figure 3.7(b), 64 QAM in Figure 3.7(c) and 256 QAM in Figure 3.7(d). It should be noticed that for the assumed link adaptation as depicted in Table 3.4, QPSK is used for modulation and coding schemes with index $1 \leq k < 5$, 16 QAM is used for modulation and coding schemes with index $5 \leq k < 8$, 64 QAM is used for modulation and coding schemes with index $k = 8$ and $k = 9$ and 256 QAM is used for modulation and coding schemes with index $k = 10$ and $k = 11$. It can be seen that both proposed approximations, i.e., 3-Point-Equal-Probability and μ/σ -fitting, approximate the effective SIR $\bar{\gamma}_{\text{ru}}$ of the resource unit with small error and the MSE is below 0.5 dB within the SIR intervals where each modulation scheme is used for transmission. The Pearson-Tukey approximation performs equal as the proposed approximations within the SIR intervals where each modulation scheme is used for transmission except for 256 QAM where the MSE gets higher than 0.5 dB

for $\gamma_{ls} > 22$ dB. The Swanson-Megill approximation performs worse than the other approximations even for the other modulation schemes.

Comparing the two proposed approximations, it can be seen that μ/σ -fitting shows smaller error than the 3-Point-Equal-Probability approximation for high values of γ_{ls} . Therefore, μ/σ -fitting should be used when approximating the effective SIR, because the complexity of the investigated approximations is equal. Compared to the optimal approach where the mutual information is calculated for each subcarrier of the resource unit, the computational complexity is reduced significantly. For the assumed scenario with 48 subcarriers per resource unit, 16 times more calculations of the mutual information are necessary, if the mutual information is calculated for each subcarrier. Instead, average value and variance of the channel transfer factors in frequency domain have to be calculated using μ/σ -fitting. However, the channel transfer factors in frequency domain have to be calculated anyway. The calculation of the average value and variance of the channel transfer factors in frequency domain with reduced complexity was shown in the first part of this subsection.

3.8 Conclusion

This chapter has been about the snapshot based system level simulation methodology developed during this work. The proposed methodology has been implemented as OFDMA Network Performance Simulator (ONe-PS) [FKWD09c] for performance and complexity evaluations. Short and independent snapshots have been considered. During each snapshot it has been assumed that the large-scale propagation loss of each user is constant and values have been taken from a large user pool that has been generated in advance of the simulation. Data traffic models have been considered by statistical properties, e.g., the number of active users at session start, leading to data traffic scenarios that are randomly taken from the busy hour. Furthermore, an approximation has been proposed calculating the effective SIR per resource unit. The effective SIR has been used to perform user scheduling and link adaptation.

Compared with state-of-the-art system level simulations, the proposed snapshot based system level simulation methodology has lower computational complexity while results, e.g., of user or cell throughput can be obtained with equal accuracy. Although, it was not possible to compare the simulation duration of ONe-PS and state-of-the-art dynamic system level simulators directly, it is expected that the duration of dynamic system level simulations is at least three to four times higher than with the snapshot based methodology. Instead of continuously simulating 20 to 30 minutes of the busy

hour with arriving and ending session and including frequently updating the large-scale propagation loss of the moving users, only around 60 to 80 snapshots are necessary where each snapshot lasts 10 s or less. Furthermore, the large-scale propagation loss is calculated in advance of the simulation for the user pool. A user pool can be used for many different investigations as long as the scenario, e.g., location of BSs and channel model do not change.

Calculating the effective SIR of the resource units is also responsible for computational complexity due to the high number of resource units that are considered during each simulation. Instead of calculating the mutual information for each subcarrier, e.g., 48 for WiMAX networks, only 3 samples have been used reducing the computational complexity by a factor of, e.g., 16. Furthermore, complexity has been reduced by calculating the channel transfer factors due to frequency selective small-scale fading for each 4th to 16th subcarrier depending on the bandwidth and total number of available subcarrier of the system and coherence bandwidth of the small-scale fading model.

Although the complexity has be reduced a lot with the proposed snapshot based methodology compared to state-of-the-art dynamic system level simulations, no appreciable loss in terms of accuracy have been observed for the results that have been obtained with the snapshot based methodology.

Chapter 4

Analytical system level evaluation methodology

4.1 Introduction

Throughout this chapter, the developed analytical system level evaluation methodology is described. Aim of the investigation is to develop analytical expressions to obtain estimates of cell and user performance in packet-switched cellular wireless networks. This is achieved by using statistical properties to describe the system level behaviour. Table 4.1 gives an overview of the differences between system level simulations as described in Chapter 3 and the proposed analytical system level evaluation methodology that are described in the following. As depicted in Table 4.1, users are placed in the investigation area and large-scale propagation loss is calculated based on the position of the user and the large-scale propagation loss model. The proposed analytical evaluation methodology derives the pdf of the SIR in the network due to large-scale propagation loss assuming that all BSs transmit with equal transmit power and considering the user distribution within the network. It is also possible to use an approximation of the pdf of the SIR due to large-scale propagation loss if the pdf cannot be derived analytically. Data traffic is considered in system level simulations using a Poisson process for the arrival of new sessions and using data traffic models for the session duration and the arrival of packets in the transmitter. The analytical evaluation methodology describes data traffic only by statistical properties. For instance, expressions are derived indicating how many users are active on average during a specific time duration. While system level simulations model resource units of the network in detail, the analytical evaluation methodology only takes the number of available resource units per second as system parameter into account. User scheduling is also considered in detail using system level simulations by selecting users for transmission and by allocating resource units to the users. Scheduling can be performed, e.g., based on channel state information or QoS requirements of the users. Using the analytical evaluation methodology, statistical expressions are derived describing the impact of user scheduling on the performance. A channel model is derived that describes the statistical properties of the small-scale fading channel if only the small-scale fading of resource units is considered that are allocated to a user. The pdf of the number of resource units allocated to the user is derived taking the statistical properties of, e.g., the number of active users

Table 4.1. Comparison of the simulative and analytical system level analysis methodology

	Simulative	Analytical
User placement / large-scale propagation loss	User positions are determined and large-scale propagation loss model is applied to the user positions	pdf of the SIR due to large-scale propagation loss and the user distribution has to be calculated; pdf can be approximated using empirical investigations or derived using random variable transformation
Data traffic consideration	Session arrival modeled by Poisson process; Data traffic models are considered for the session duration; Packets are generated accordingly	Consideration of the statistical properties of the data traffic, e.g., using queueing theory; Statistical properties of the transient behaviour, e.g., of the number of active users are considered
Resource unit consideration	Frame and resource units are modeled in detail	Abstract modelling of the frame structure by considering the number of available resource units in a given time interval
User scheduling	Select users for transmission and allocate resource units; Scheduling decision based on channel state information, QoS requirements etc.	Derive the impact of the user scheduling by calculating the statistics of a post-scheduling channel model and the statistics of the number of allocated resource units
Performance measurements	Average and instantaneous user, cell and network performance results	Statistics of user, cell and network performance results

into account. System level simulations are able to provide measurements for instantaneous and average user, cell and network performance evaluating each resource unit. The analytical evaluation methodology derives statistics of the user, cell and network performance taking, e.g., all users in the network into account. The analytical methodology is not designed to derive the performance of, e.g., a specific user in the network. By using analytical expressions, results can be obtained very fast with the analytical evaluation methodology and no complex system level simulations are necessary to determine the performance of cellular wireless networks.

Figure 4.1 gives an overview of the analytical system level evaluation methodology. As in Figure 1.1, five different parts are distinguished, i.e., the user placement and the large-scale propagation loss calculation, the data traffic, the resource units, the user scheduling and the performance measurements. Relationships between different parts are indicated by arrows in Figure 4.1 where the property at the beginning of the arrow has impact on the property at the head of the arrow. It should be noted that all relationships are described by analytical expressions and statistical properties in the analytical evaluation methodology. The statistical properties of the user positions and the large-scale propagation loss model are used to derive the pdf of the SIR due to large-scale propagation loss assuming that all BSs transmit with equal transmit power. The transmit power of a BS is reduced if not all resource units are utilised for transmission. Data traffic is also considered by means of statistical properties. The statistics of the session duration depend on the statistics of the traffic model and the statistics of the user throughput. Using the statistics of the session duration and the statistics of the session arrival, the statistical properties of the number of active users can be determined. The statistical properties of the number of active users combined with the server data rate and the number of available resource units is used to obtain statistical properties of the number of utilised resource units, which has impact on the SIR due to large-scale propagation loss as depicted before. Depending on the scheduling algorithm, the statistics of the number of active users and the statistics of the SIR due to large-scale propagation loss have impact on the statistical properties of the number of resource units allocated to the users which is also influenced by the total number of available resource units. Using the channel model of the small-scale fading, statistical properties of the gain in SIR due to the scheduling are calculated depending on the scheduling algorithm and the statistical properties of the number of active users. Combining the statistical properties of the gain in SIR due to the scheduling and the statistical properties of the SIR due to large-scale propagation loss, probabilities are calculated that a certain modulation and coding scheme is used for transmission so that a specific number of bits are transmitted using one resource unit. The probabilities that a specific number of bits are transmitted per resource unit are combined with the pdf of the number of allocated resource units for each user to determine the statistical properties of the user throughput. Based on the statistical properties of the user throughput user, cell and network performance results are obtained. Of course, all pdfs derived in the following are properly normalised.

This chapter is organised as follows. Section 4.2 describes the user placement and the calculation of large-scale propagation loss in the analytical evaluation methodology. Statistical properties of the data traffic, i.e., the pdf of the number of active users depending on the data traffic model and statistics of the resource unit utilisation are

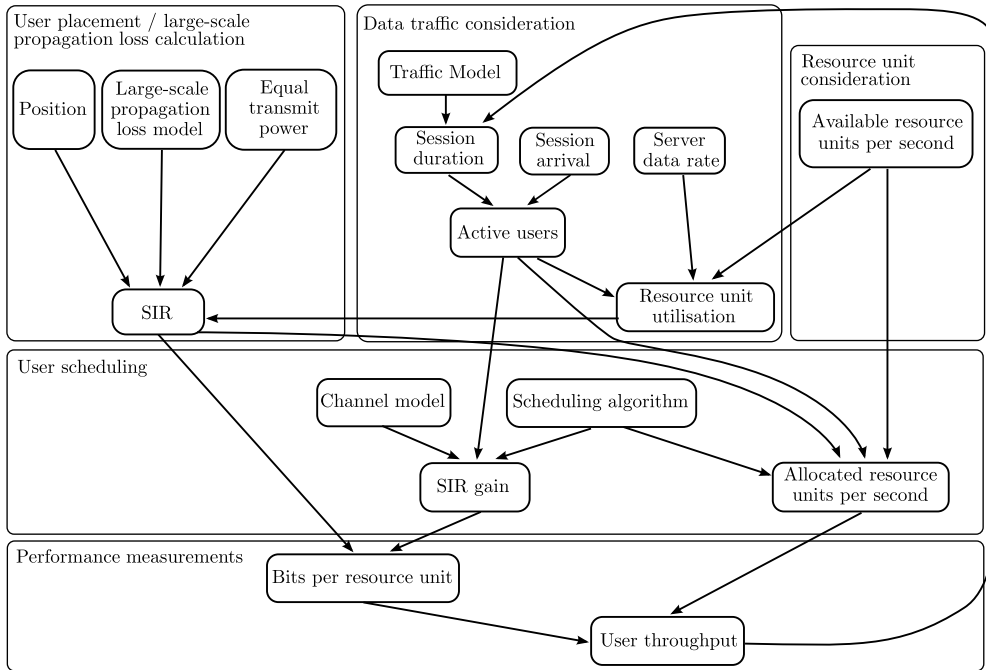


Figure 4.1. Analytical system level evaluation methodology describing interactions in packet-switched cellular wireless network

given in Section 4.3. The number of available resource units as considered for the analytical evaluation methodology is described in Section 4.4. Section 4.5 presents the derivations for statistics of the gain in SIR due to scheduling as well as statistics for the number of resource units that are allocated to each user considering different scheduling algorithms. Section 4.6 describes how results for user, cell and network performance is obtained using the analytical evaluation methodology. Finally, a performance and complexity evaluation of the analytical evaluation methodology is given in Section 4.7.

4.2 User placement and large-scale propagation loss calculation

This section describes the consideration of user locations within the network and the calculation of large-scale propagation loss. As shown in Figure 4.1, the pdf of the SIR γ_{ls} due to large-scale propagation loss has to be calculated considering the user distribution and the large-scale propagation loss model and assuming that all BSs transmit with equal transmit power. With $\alpha_{ls,i}$ the random variable indicating the large-scale propagation loss between the user and BS i and considering N_{interf} interfering

BSs, γ_{ls} is given by the random variable

$$\gamma_{\text{ls}} = \frac{\alpha_{\text{ls},0}}{\sum_{i=1}^{N_{\text{interf}}} \alpha_{\text{ls},i}}. \quad (4.1)$$

The pdf of γ_{ls} can be obtained based on the pdf of the user distribution using random variable transformation and considering the large-scale propagation loss model and (4.1). The logarithmic value of γ_{ls} is given by $\gamma_{\text{ls,dB}}$.

Of course, it is not possible to describe the pdf of γ_{ls} analytically if scenarios with different propagation loss models, arbitrary BS locations and inhomogeneous user distributions are considered. Therefore, the pdf of $\gamma_{\text{ls,dB}}$ can be approximated by a histogram of the relative frequency p_{γ_j} that $\gamma_{\text{ls,dB}}$ is within an interval $[\gamma_{j,\text{dB}}; \gamma_{j+1,\text{dB}}]$ with $j = 0, \dots, \infty$ and $\gamma_{j+1,\text{dB}} - \gamma_{j,\text{dB}} = \Delta_{\gamma_{\text{ls,dB}}}$ for all j . The pdf of $\gamma_{\text{ls,dB}}$ is approximated by

$$f_{\gamma_{\text{ls,dB}}}(\gamma_{\text{ls,dB}}) \approx \sum_{j=0}^{\infty} p_{\gamma_j} \cdot \delta(\gamma_{\text{ls,dB}} - \gamma_{j,\text{dB}}). \quad (4.2)$$

$p_{\gamma_j} \delta(x_j)$ means that the event with the result x_j is achieved with a probability given by p_{γ_j} . The dirac-distribution has the following property:

$$\int_{-\infty}^x \delta(t) dt = u(x) \quad (4.3)$$

with $u(x)$ the unit step function which is defined by

$$u(x) = \begin{cases} 0 & \text{for } x < 0 \\ 1 & \text{for } x \geq 0. \end{cases} \quad (4.4)$$

The relative frequencies p_{γ_j} in (4.2) can be derived using scenarios as described in Section 2.2. Users are randomly located in the investigation scenario so that the assumed user distribution is fulfilled. For each user the SIR $\gamma_{\text{ls,dB}}$ due to large-scale propagation loss in logarithmic scale is calculated and the relative frequencies p_{γ_j} can be derived. It is therefore also possible to use large-scale propagation loss predictions that are obtained from a coverage planning run as input for the developed analytical evaluation methodology.

The pdf of $\gamma_{\text{ls,dB}}$ as given in (4.2) describes the statistics of the SIR considering the distribution of users in the network and the large-scale propagation model and assuming that all BSs transmit with equal transmit power as shown in Figure 4.1.

4.3 Data traffic consideration

4.3.1 General problem statement

This section describes the consideration of data traffic in the analytical evaluation methodology. In contrast to conventional system level simulations, only statistical properties are considered for the analytical evaluation methodology. As depicted in Figure 4.1, the statistical properties of the number of active users and the statistical properties of the resource unit utilisation have to be derived considering the data traffic model, the session arrival process and the server data rate.

As already derived in Section 3.3, data traffic can be separated into data traffic where the session duration is modeled as time interval, i.e., speech traffic, and data traffic where the session duration depends on the user throughput due to the generation of a file size that has to be transmitted and different queueing models that are applied. The latter represents, e.g., download and web browsing traffic. Common to all data traffic models is the Poisson process for the arrival process as already depicted in Section 2.4 which is also assumed for the analytical evaluation methodology. In contrast to the snapshot based system level simulation methodology, the session is not considered in detail for instance with the generation of packets. The analytical evaluation methodology requires analytical expressions, e.g., of the number of active users. The statistical properties of the session arrival time are given by the Poisson process and the statistical properties of the session duration can be derived depending on the traffic model so that the number of active users at a certain time instant can be calculated using results of the queueing theory. Transition probabilities between different states of the queueing model are derived analytically to describe the temporal development, e.g., during a session duration. Finally, the number of active users is combined with a resource unit requirement obtained using the server data rate of the sessions to describe the statistical properties of the utilisation of resource units.

The remainder of the section is organised as follows. Section 4.3.2 deals with speech traffic and Section 4.3.3 describes which statistics have to be applied if data traffic that generates a certain file size is assumed. The goal of this investigation is to derive a statement that can be used to describe how many resource units can be allocated to each user which, among others, will depend on the number of users that are active as indicated in Figure 4.1. Statistical properties of the utilisation of resource units are derived in Section 4.3.4 which are needed to modify the pdf of the SIR due to large-scale propagation loss as calculated in Section 4.2 where equal transmit power per BS is assumed. BSs that do not utilise all resource units may reduce the transmit power.

4.3.2 Speech traffic

In this section, the statistics that are necessary for the consideration of speech traffic are derived. As already depicted in Section 3.3, an $M/M/\infty$ queueing model describes the number of active speech users assuming a Poisson arrival process and an exponentially distributed random variable as session duration. Probabilities are calculated in the following for the number of active users at a certain time instant and the average number of users that are active during the session duration of an investigated user.

With N_{speech} the average number of active user, the probability that n_{active} users are active at an arbitrary time instant with $n_{\text{active}} = 0, 1, \dots, \infty$ is given by (3.3). If a specific user arrives in the network at an arbitrary time instant, he competes with n_{active} other users for resource units. It is assumed that the session starts at $t_{\text{ses}} = 0$ and the total number of active sessions is given by $n_{\text{active}} + 1$ at session start. The development of the number of active users during the session duration of the investigated user can be described by a Markov chain [Kle75] where the states represent the number of active users. The number of active users increases if new users arrive in the network and decreases if sessions terminate.

In the following, λ_{speech} represents the average arrival rate, μ_{speech} the inverse of the average session duration and T_{speech} the session duration of the investigated user. The pdf of the random variable indicating the time instant $t_{\text{arr}}^{(1)}$ when the next user arrives in the network is given by (2.9) as

$$f_{t_{\text{arr}}}(t_{\text{arr}}^{(1)}) = \lambda_{\text{speech}} \cdot \exp(-\lambda_{\text{speech}} t_{\text{arr}}^{(1)}). \quad (4.5)$$

The pdf of the time instant $t_{\text{term}}^{(1)}$ when the first session terminates is given by

$$f_{t_{\text{term}}}(t_{\text{term}}^{(1)}) = n_{\text{active}} \mu_{\text{speech}} \exp(-n_{\text{active}} \mu_{\text{speech}} t_{\text{term}}^{(1)}). \quad (4.6)$$

The pdf of the session duration T_{speech} of the investigated user is given by (2.12).

If T_{speech} is smaller than $t_{\text{term}}^{(1)}$ and smaller than $t_{\text{arr}}^{(1)}$, the number of active users does not change during the session duration of the investigated user and therefore no state transitions occur in the Markov chain model. The probability that no state transition happens is given by

$$\begin{aligned} p_{\text{noStateTrans}}(n_{\text{active}}) &= \text{P} \left(\frac{T_{\text{speech}}}{\min\{t_{\text{arr}}^{(1)}, t_{\text{term}}^{(1)}\}} < 1 \right) \\ &= \int_0^1 \frac{\mu_{\text{speech}} \cdot (\lambda_{\text{speech}} + n_{\text{active}} \mu_{\text{speech}})}{(\mu_{\text{speech}} \beta + (\lambda_{\text{speech}} + n_{\text{active}} \mu_{\text{speech}}))^2} d\beta \\ &= 1 - \frac{\lambda_{\text{speech}} + n_{\text{active}} \mu_{\text{speech}}}{\lambda_{\text{speech}} + (n_{\text{active}} + 1) \mu_{\text{speech}}}. \end{aligned} \quad (4.7)$$

Considering the probability that n_{active} users are active at the beginning of the session, the probability $p_{\text{noStateTrans}}$ that no state transition occurs during the session is calculated as

$$\begin{aligned} p_{\text{noStateTrans}} &= \sum_{n_{\text{active}}=0}^{\infty} p_{\text{noStateTrans}}(n_{\text{active}}) \cdot P(n_{\text{active}}) \\ &= \frac{\text{Exp}(-N_{\text{speech}})}{-N_{\text{speech}}^{N_{\text{speech}}} \cdot \lambda_{\text{speech}}} \cdot \dots \\ &\quad (\lambda_{\text{speech}} \Gamma(N_{\text{speech}}) - \mu_{\text{speech}} \Gamma(1 + N_{\text{speech}}, -N_{\text{speech}})) \end{aligned} \quad (4.8)$$

where

$$\Gamma(z) = \int_0^{\infty} t^{z-1} \exp(-t) dt \quad (4.9)$$

and

$$\Gamma(a, z) = \int_z^{\infty} t^{a-1} \exp(-t) dt. \quad (4.10)$$

With a probability of $1 - p_{\text{noStateTrans}}$, state transitions occur. The number of active sessions for $t_{\text{ses}} > 0$ can be calculated depending on the transition probabilities, i.e., probabilities that new users arrive or sessions of active users terminate. This results into differential-difference equation of the Markov chain model where the derivative of the probability that n_{active} users are active at time t is the function of the probabilities that $n_{\text{active}} - 1$, n_{active} and $n_{\text{active}} + 1$ users are active at time $t - dt$ [GH74, Kle75]. The differential-difference equation can be solved using the coefficients of a Taylor series expansions around zero, the probability that k users are active at time instant t_{ses} is given by [GH74]

$$P_k(t_{\text{ses}}) = \frac{1}{k!} \left. \frac{d^k P(z, t_{\text{ses}})}{dz^k} \right|_{z=0} \quad (4.11)$$

with

$$\begin{aligned} P(z, t_{\text{ses}}) &= \exp(N_{\text{speech}} z) ((z - 1) \exp(-\mu_{\text{speech}} t_{\text{ses}}) + 1)^{k_0} \cdot \dots \\ &\quad \exp(-N_{\text{speech}}(z - 1) (1 - \exp(-\mu_{\text{speech}} t_{\text{ses}}))) \end{aligned}$$

The derivation for (4.11) can be found in Appendix A.2.

Let us define a random process $\{\kappa(t_{\text{ses}}) | \kappa(0) = n_{\text{active}} + 1\}$ indicating the number of active users at time instant t_{ses} with $0 \leq t_{\text{ses}} \leq T_{\text{speech}}$ under the conditions that $n_{\text{active}} + 1$ users are active at $t_{\text{ses}} = 0$. The expectation value of the average number

$\bar{n}_{\text{act,sp}}$ of active users during the session duration of one investigated user is then given by

$$E\{\bar{n}_{\text{act,sp}}\} = \sum_{k=0}^{\infty} \int_0^{\infty} E\{\theta(T_{\text{speech}})|\kappa(0) = k + 1\} \mu_{\text{speech}} \exp(-\mu_{\text{speech}} T_{\text{speech}}) dT_{\text{speech}} \cdot \dots \exp(-N_{\text{speech}}) \frac{N_{\text{speech}}^k}{k!} \quad (4.12)$$

with

$$E\{\theta(T_{\text{speech}})|\kappa(0) = k + 1\} = \frac{1}{T_{\text{speech}}} \int_0^{T_{\text{speech}}} E\{\kappa(t)|\kappa(0) = k + 1\} dt. \quad (4.13)$$

The average number $\bar{n}_{\text{act,sp}}$ of active users during the session duration of one investigated user is one user greater than the average number active users at an arbitrary time instant:

$$E\{\bar{n}_{\text{act,sp}}\} = N_{\text{speech}} + 1. \quad (4.14)$$

The variance of $\bar{n}_{\text{act,sp}}$ can be calculated in a similar way [Pap84] using

$$E\{\bar{n}_{\text{act,sp}}^2\} = \sum_{k=0}^{\infty} \int_0^{\infty} E\{\theta^2(T_{\text{speech}}, k + 1)\} \cdot \mu_{\text{speech}} \exp(-\mu_{\text{speech}} T_{\text{speech}}) dT_{\text{speech}} \cdot \dots \exp(-N_{\text{speech}}) \frac{N_{\text{speech}}^k}{k!} \quad (4.15)$$

where $E\{\theta^2(T_{\text{speech}}, k + 1)\}$ is given using the autocorrelation $R(t_1, t_2, k + 1)$ of the process $\{\kappa(t_{\text{ses}})|\kappa(0) = k + 1\}$ as

$$E\{\theta^2(T_{\text{speech}}, k + 1)\} = \frac{1}{T_{\text{speech}}^2} \int_0^{T_{\text{speech}}} \int_0^{T_{\text{speech}}} R(t_1, t_2, k + 1) dt_1 dt_2. \quad (4.16)$$

The variance of $\bar{n}_{\text{act,sp}}$ is then given by

$$\text{Var}\{\bar{n}_{\text{act,sp}}\} = E\{\bar{n}_{\text{act,sp}}^2\} - (E\{\bar{n}_{\text{act,sp}}\})^2. \quad (4.17)$$

It can be seen that the average number $\bar{n}_{\text{act,sp}}$ of active users during the session duration of one investigated user is obtained by an integration which is similar to the summation of many independent random variables. Therefore, the central limit theorem can be applied and the pdf of $\bar{n}_{\text{act,sp}}$ is approximated by a Gaussian pdf with average value and variance given by (4.13) and (4.17), respectively.

The entire pdf of $\bar{n}_{\text{act,sp}}$ is given by the part approximated by a Gaussian pdf for scenarios with state transitions and the part derived in (4.8) where no state transitions occur. The analytical expression of the pdf is given by

$$f_{\bar{n}_{\text{act,sp}}}(\bar{n}_{\text{act,sp}}) = \begin{cases} \frac{(1-p_{\text{noStateTrans}})}{\sqrt{2\pi\text{Var}\{\bar{n}_{\text{act,sp}}\}}} \cdot \dots & \dots \\ \exp\left(-\frac{(\bar{n}_{\text{act,sp}} - \text{E}\{\bar{n}_{\text{act,sp}}\})^2}{2\cdot\text{Var}\{\bar{n}_{\text{act,sp}}\}}\right) + p_{\text{noStateTrans}} \cdot \dots & \dots \\ \sum_{k=0}^{\infty} p_{\text{noStateTrans}}(k) \cdot \delta(\bar{n}_{\text{act,sp}} - k) & \text{for } \bar{n}_{\text{act,sp}} \geq 1 \\ 0 & \text{else.} \end{cases} \quad (4.18)$$

At least one user, i.e., the investigated user is active during the whole session duration so that $\bar{n}_{\text{act,sp}} \geq 1$.

The probability for k active users are derived for the analytical evaluation methodology as well as the statistical properties for the average number $\bar{n}_{\text{act,sp}}$ of active users during the session duration of one investigated user assuming data traffic where the session duration is modeled by an exponentially distributed random variable, i.e., speech traffic. The probability for k active users is used later on to derive statistical properties for the utilisation of resource units considering also the server data. To derive the number of resource units allocated to each user in one second when investigating the user scheduling, $\bar{n}_{\text{act,sp}}$ is needed.

4.3.3 Download and web browsing traffic

This section gives an overview of the statistics derived in this thesis regarding the number of active users if traffic that models file transmission is assumed. Download and web browsing traffic are treated equally as it can be assumed that one packet call of the web browsing model described in Section 2.4 follows similar statistics as the file download traffic model. As for speech traffic, probabilities are derived that k with $k = 0, 1, 2, \dots$ users are active at an arbitrary time instant and statistical properties are determined for the average number of active users during the session of one investigated user as depicted in Figure 4.1.

As depicted in Section 3.3, a user is active depending on the number n_{alloc} of resource units per second the user gets allocated and the number d_{res} of bits that can be transmitted per resource unit depending on the modulation and coding scheme. An $M/SD/\infty$ queueing system in Kendall's notation is applied.

The average number of active users depending on the average file size, d_{res} and the number N_{res} of available resource units per second is given by (3.11). Again, a random

process $\{\kappa(t_{\text{ses}})|\kappa(0) = n_{\text{active}} + 1\}$ is defined indicating the number of active users at time instant $t_{\text{ses}} \geq 0$ with the conditions that $n_{\text{active}} + 1$ users including the investigated user are active at session start $t_{\text{ses}} = 0$ of the investigated user. The average number $\bar{n}_{\text{act,dl}}$ of active users during the session duration of the investigated user with the condition that $n_{\text{active}} + 1$ users are active at session start is derived by

$$\{\bar{n}_{\text{act,dl}}|\kappa(0) = n_{\text{active}} + 1\} = \int_0^{T_{\text{ses}}} \{\kappa(t_{\text{ses}})|\kappa(0) = n_{\text{active}} + 1\} dt_{\text{ses}}. \quad (4.19)$$

As described in Section 3.3 the session duration of a download user is short if the file size is short and the average user throughput is high. The average user throughput depends on the position of the user within the network, i.e., to users close to the BS more bits per resource unit can be transmitted than to users close to the cell border, and the number of users that are active during the session duration due to the number of resource units that are allocated to each individual user. The effect that the session duration increases with increasing number of active users in the $M/SD/\infty$ queueing model leads to many sessions where only a few users are active on average during the session duration. However, it may also happen that a very high number of active users is observed during the session duration. This behaviour is described by an exponentially distributed random variable and the pdf of $\bar{n}_{\text{act,dl}}$ is given by

$$f_{\bar{n}_{\text{act,dl}}}(\bar{n}_{\text{act,dl}}) = \begin{cases} \frac{1}{\text{E}\{n_{\text{active,dl}}\}} \cdot \exp\left(-\frac{\bar{n}_{\text{act,dl}}-1}{\text{E}\{n_{\text{active,dl}}\}}\right) & \text{for } \bar{n}_{\text{act,dl}} \geq 1 \\ 0 & \text{else.} \end{cases} \quad (4.20)$$

The probability for k active users are derived for the analytical evaluation methodology as well as the statistical properties for the average number $\bar{n}_{\text{act,sp}}$ of active users during the session duration of one investigated user assuming data traffic where the session duration depends on a random file size and a random average user throughput, i.e., download and web browsing traffic. The average user throughput depends, among others, on the number of users that are active. The probability for k active users is used later on to derive statistical properties for the utilisation of resource units considering also the server data rate. To derive the number of resource units allocated to each user in one second when investigating the user scheduling, $\bar{n}_{\text{act,sp}}$ is needed.

4.3.4 Resource unit utilisation

This section investigates the impact of data traffic on the number of allocated resource units per BS. It is assumed that packets due to data traffic of user i arrive with a

rate given by the server data rate $r_{\text{serv}}^{(i)}$ of this user. For low $r_{\text{serv}}^{(i)}$ or small number of active users, it might happen that not all resource units, which are available in the BS, are utilised for transmission as depicted in Figure 4.1. Compared to a network where all resource units are utilised for transmission two consequences are observed in a network that may not utilise all resource units. First, the sum transmit power can be reduced leading to less interference in co-channel cells. Due to the distributed subcarrier allocation that is assumed, every resource unit in the co-channel cell benefits if the transmit power is reduced. The second consequence is a reduction of the cell throughput that is observed compared to a fully loaded network if cells run out of data and resource units are not needed for data transmission. Statistics are derived in the following describing the resource unit utilisation of a cell.

The BS is able to transmit all data arriving at the BS immediately to a user i if the user throughput $r_{\text{user}}^{(i)}$ is equal to $r_{\text{serv}}^{(i)}$. Based on the number of bits $d_{\text{res}}^{(i)}$ that can be transmitted per resource unit, a maximum number $n_{\text{req}}^{(i)}$ of required resource units per second is given by

$$n_{\text{req}}^{(i)} = \frac{r_{\text{serv}}^{(i)}}{d_{\text{res}}^{(i)}}. \quad (4.21)$$

The total number N_{req} of required resource unit per second needed so that all packets can be transmitted immediately is given by the sum of the individual requirements of the n_{active} active users in the cell as

$$N_{\text{req}} = \sum_{i=1}^{n_{\text{active}}} \frac{r_{\text{serv}}^{(i)}}{d_{\text{res}}^{(i)}}. \quad (4.22)$$

It should be noted that N_{req} can be larger than the number N_{res} of available resource units if the network is fully loaded or even overloaded. In the following, it is assumed that $r_{\text{serv}}^{(i)}$ is equal for all users and d_{res} is a random variable obtained from the SIR due to large-scale propagation loss as defined in Section 4.2. Different $r_{\text{serv}}^{(i)}$ per user can be considered straight forward with the developed methodology.

The total number N_{req} of required resource units per second is a sum of the reciprocal of independent random variables indicating the number of bits that can be transmitted per resource unit and the central limit theorem can be applied. Expectation value $E\{\frac{1}{d_{\text{res}}}\} = \mu_{d_{\text{res}}}$ and variance $\text{Var}\{\frac{1}{d_{\text{res}}}\} = \sigma_{d_{\text{res}}}^2$ can be derived, e.g., using the pdf of the SIR due to large-scale propagation loss and a methodology described in [BHIM05]. Due to the central limit theorem, N_{req} can be approximated by a Gaussian distributed random variable if n_{active} is sufficiently large so that the pdf of N_{req} is approximated by

$$f_{N_{\text{req}}}(N_{\text{req}}) = \frac{1}{\sqrt{2\pi n_{\text{active}} r_{\text{serv}} \sigma_{d_{\text{res}}}^2}} \exp\left(-\frac{(N_{\text{req}} - n_{\text{active}} r_{\text{serv}} \mu_{d_{\text{res}}})^2}{2 n_{\text{active}} r_{\text{serv}}^2 \sigma_{d_{\text{res}}}^2}\right). \quad (4.23)$$

Of course, it has to be considered in (4.23) that not less than zero resource units can be allocated so that the final pdf of N_{req} is given by

$$f_{N_{\text{req}}}(N_{\text{req}}) = \begin{cases} \frac{1}{\sqrt{2\pi n_{\text{active}} r_{\text{serv}} \sigma_{\text{dres}}}} \exp\left(-\frac{(N_{\text{req}} - n_{\text{active}} r_{\text{serv}} \mu_{\text{dres}})^2}{2 n_{\text{active}} r_{\text{serv}}^2 \sigma_{\text{dres}}^2}\right) & \text{for } N_{\text{req}} > 0 \\ \frac{1}{2} \text{erf}\left(\frac{n_{\text{active}} r_{\text{serv}} \mu_{\text{dres}}}{\sqrt{2 n_{\text{active}} r_{\text{serv}} \sigma_{\text{dres}}}}\right) \cdot \delta(N_{\text{req}}) & \text{for } N_{\text{req}} = 0 \\ 0 & \text{else} \end{cases} \quad (4.24)$$

with the error function given by

$$\text{erf}(x) = \frac{1}{\sqrt{\pi}} \int_0^x \exp(-t^2) dt. \quad (4.25)$$

The probability p_{fullLoad} that the network is fully loaded and all resource units of the cell are allocated is calculated by

$$\begin{aligned} p_{\text{fullLoad}} &= \int_{N_{\text{res}}}^{\infty} f_{N_{\text{req}}}(N_{\text{req}}) dN_{\text{req}} \\ &= \frac{1}{2} \left(1 - \text{erf}\left(\frac{N_{\text{res}} - n_{\text{active}} r_{\text{serv}} \mu_{\text{dres}}}{\sqrt{2 n_{\text{active}} r_{\text{serv}} \sigma_{\text{dres}}}}\right) \right). \end{aligned} \quad (4.26)$$

Using (4.23) and (4.26), the pdf of the ratio o between the number of resource units that are utilised for transmission per second and the number of available resource units per second is given by

$$f_o(o) = \begin{cases} p_{\text{fullLoad}} \cdot \delta(o) & \text{for } o = 1 \\ \frac{1}{N_{\text{res}}} f_{N_{\text{req}}}(o \cdot N_{\text{res}}) & \text{for } 0 < o < 1 \\ \frac{1}{2} \text{erf}\left(\frac{n_{\text{active}} r_{\text{serv}} \mu_{\text{dres}}}{\sqrt{2 n_{\text{active}} r_{\text{serv}} \sigma_{\text{dres}}}}\right) \cdot \delta(o) & \text{for } o = 0 \\ 0 & \text{else.} \end{cases} \quad (4.27)$$

The average cell throughput $E\{r_{\text{cell,fl}}\}$ that is obtained for a fully loaded network is reduced by the factor o due to resource units that are not used for transmission when considering data traffic. Additionally, the sum transmit power can be reduced due to the resource units that are not utilised. The SIR γ_{ff} including small-scale fading of a user depends on $\alpha_{\text{ls},k}$ the large-scale propagation loss to the connected BS 0 and each of the N_{interf} interfering BSs, the small-scale fading α_{ff} and o_k of interfering BS $k = 1, 2, \dots, N_{\text{interf}}$. γ_{ff} is a random variable given by

$$\gamma_{\text{ff}} = \frac{\alpha_{\text{ff},0} \alpha_{\text{ls},0}}{\sum_{k=1}^{N_{\text{interf}}} \alpha_{\text{ff},k} \alpha_{\text{ls},k} o_k} = \frac{S}{I}. \quad (4.28)$$

The numerator represents the signal power S and the denominator the interference power I . According to [IM92], the pdf of γ_{ff} can be approximated by

$$f_{\gamma_{\text{ff}}}(\gamma_{\text{ff}}) = \text{E}\{I\} f_S(\gamma \cdot \text{E}\{I\}) \quad (4.29)$$

if the variance of the interference I is much smaller than the variance of the signal power S which is fulfilled if the number of interfering BSs is sufficiently large and if there is no dominant interfering BS. This usually holds in cellular wireless networks.

It can be seen in (4.29) that only the expectation value of the interference is required to calculate the pdf of γ_{ff} . Using the denominator of (4.29), the expectation value of the interference is given by

$$\begin{aligned} \text{E}\{I\} &= \text{E} \left\{ \sum_{k=1}^{N_{\text{interf}}} \alpha_{\text{ff},k}^{(i)} \alpha_{\text{ls},k}^{(i)} o(k) \right\} \\ &= \sum_{k=1}^{N_{\text{interf}}} \text{E}\{\alpha_{\text{ff},k}^{(i)}\} \text{E}\{\alpha_{\text{ls},k}^{(i)}\} \text{E}\{o(k)\} \\ &= \text{E}\{\alpha_{\text{ff}}\} \text{E}\{o\} \sum_{k=1}^{N_{\text{interf}}} \text{E}\{\alpha_{\text{ls},k}^{(i)}\}. \end{aligned} \quad (4.30)$$

With the derived statistics for o , the pdf of the SIR due to large-scale propagation loss as depicted in Section 4.2 can be modified so that conditions are considered when BSs do not utilise all resource units for transmission and the transmit power is lower than the maximum transmit power which has been considered in Section 4.2. It has been shown in this section that only the average ratio between utilised resource units and available resource units has to be considered in the developed analytical evaluation methodology.

4.4 Resource unit consideration

In this section, the consideration of resource units in the analytical evaluation methodology is described. It is shown in Figure 4.1 that the number N_{res} of available resource units per second has to be considered when calculating the utilisation of resource units as described in Section 4.3.4 and to derive the number of resource units that are allocated to the users during scheduling.

In contrast to state-of-the-art system level simulations, the analytical evaluation methodology does not consider individual resource units and their position, e.g., in

the frame. The available resource units are taken into account together and statistical properties have to be used in the analytical evaluation methodology to derive effects, e.g., due to the allocation of specific resource units as described in the next section.

Furthermore, a number d_{res} of bits that can be transmitted per resource unit is derived depending on the SIR derived for the resource unit. Different d_{res} can be transmitted depending on the modulation and coding scheme that is used. An overview of the different d_{res} and SIR thresholds has been given in Table 3.4 and is also applied in the analytical evaluation methodology.

The concept of the resource unit considered in the analytical evaluation methodology allows the application of different wireless networks by adapting N_{res} , d_{res} and the SIR thresholds. The remaining parts of the analytical evaluation methodology do not rely on the system design like the definition of a specific resource unit or the design of a frame. N_{res} is used, e.g., to derive the number of resource units allocated to each user considering the number of allocated resource units as derived in Section 4.3 and together with d_{res} the user throughput can be derived.

4.5 User scheduling

4.5.1 General problem formulation

Within this section the consideration of user scheduling in the analytical evaluation methodology is described. User scheduling has impact on two parts of the analytical evaluation methodology as depicted in Figure 4.1. On the one hand, the statistical properties of the number n_{alloc} of resource units per second that are allocated to each user have to be derived considering the total number of resource units that are available per second, the average number of active users as derived in Section 4.3, the scheduling algorithm and the SIR due to large-scale propagation loss if considered during the scheduling decision. On the other hand, the pdf of the gain in SIR considering large-scale propagation loss, small-scale fading and the scheduling decision compared to the SIR due to large-scale propagation loss has to be derived. Three different scheduling algorithms as described in Section 2.6 are considered in the following. While in conventional system level simulations, the scheduling decision is performed for each resource unit, i.e., which user is considered for transmission and allocating each resource unit for transmission to one specific user, statistical properties like the pdf of the number of resource units per second that are allocated to the users and the gain in

SIR considering scheduling compared to the SIR due to large-scale propagation loss is required in the developed analytical evaluation methodology. The statistical properties of the SIR gain are combined with the pdf of the SIR due to large-scale propagation loss to determine probabilities for the usage of the different modulation and coding schemes, i.e., how many bits can be transmitted per resource units. The probabilities for transmitting a certain number of bits per resource unit are used together with the derived pdf of the number of resource units per second that are allocated to each user during the session duration to achieve results for, e.g., the average user throughput. The following investigation is divided into two tasks that can be solved independent of each other.

Task one comprises the determination of the effective transfer factor describing the gain in SIR considering scheduling, small-scale fading and large-scale propagation loss compared to the SIR due to large-scale propagation loss. For each resource unit the statistical properties of the SIR can be given based on random variables for

- the large-scale propagation loss between transmitter and receiver,
- the attenuation due to small-scale fading,
- the transmit power of the transmitter,
- the transmit power of the interferers and
- the large-scale propagation loss and small-scale fading between the interferers and the receiver.

It has been shown in [IM92] that the pdf of the SIR can be approximated using the expectation value of the interference, cf. (4.29). During the scheduling decision, certain resource units are selected for transmission of data to specific users. The actual SIR including small-scale fading of these resource units is considered to calculate the statistics of the post-scheduling SIR $\tilde{\gamma}_{\text{eff}}$.

Task number two contains the statistics of the number of resource units that are allocated to a specific user during the scheduling decision. The analytical evaluation methodology is not designed to evaluate the instantaneous user throughput, thus, as explained in Section 4.4, not each individual resource unit is considered. Statistical properties are derived that describe the number of resource units that are allocated to each user divided by the session duration leading to a number of resource units allocated to each user per second. Again, the three scheduling strategies as described in Section 2.6 are considered.

4.5.2 SIR gain

4.5.2.1 General problem formulation

This section gives an overview of the post-scheduling SIR that is used to describe the impact of the scheduling algorithm. Three different scheduling strategies as described in Section 2.6 are investigated.

It is assumed that all BSs transmit with equal transmit power so that random variable γ_{ls} indicating the SIR due to large-scale propagation loss is given by (4.1). The random variable γ_{ff} of the SIR is obtained using (4.28) and (4.30) as

$$\gamma_{\text{ff}} = \gamma_{\text{ls}} \cdot \alpha_{\text{ff}} \quad (4.31)$$

if the expectation value of the small-scale fading is equal to one.

Using the random variable $\tilde{\alpha}_{\text{eff}}$ describing the gain in SIR due to small-scale fading and the scheduling algorithm, the random variable $\tilde{\gamma}_{\text{eff}}$ of the post scheduling SIR can be displayed by

$$\tilde{\gamma}_{\text{eff}} = \gamma_{\text{ls}} \cdot \tilde{\alpha}_{\text{eff}}. \quad (4.32)$$

In the following sections, the statistical properties of $\tilde{\alpha}_{\text{eff}}$ for the three scheduling algorithms fair resource, proportional fair and fair throughput scheduling are derived.

4.5.2.2 Fair resource scheduling

Fair resource scheduling as described in Section 2.6 does not consider channel state information for the scheduling decision but rather allocates resource units so that each user gets equal number of resource units per second allocated. Therefore, the statistical properties of the random variable α_{ff} describing the channel transfer factor for one resource unit are the same statistical properties as for the random variable $\tilde{\alpha}_{\text{eff,fr}}$ indicating the SIR gain of fair resource scheduling, thus,

$$\tilde{\alpha}_{\text{eff,fr}} = \alpha_{\text{ff}}. \quad (4.33)$$

In this section, the pdf of an effective channel transfer factor is derived used in the analytical evaluation methodology assuming resource units that consist of subcarriers that are distributed over the whole system bandwidth and experience uncorrelated fading as described in Section 2.5.

In case of a distributed subcarrier allocation, it is assumed that subcarriers that are separated by more than the coherence bandwidth experience uncorrelated fading. Based on the effective performance measure introduced in Section 3.4, the mutual information is calculated for each subcarrier and the mutual information averaged over all subcarrier is calculated as performance measure for the resource unit. Based on the average mutual information, α_{ff} is derived using $\bar{\gamma}_{\text{ru}}$ from (3.32) as

$$\alpha_{\text{ff}} = \frac{\bar{\gamma}_{\text{ru}}}{\gamma_{\text{ls}}}. \quad (4.34)$$

Due to the central limit theorem, α_{ff} is approximated by a Gaussian distributed random variable. The expectation value of α_{ff} is given by $\mu_{\text{ff}}(\gamma_{\text{sf}}, \text{modulation})$ and the standard deviation of α_{ff} is given by $\sigma_{\text{ff}}(\gamma_{\text{sf}}, \text{modulation})$ both as function of the SIR due to large-scale propagation loss and the modulation scheme that is used. Values for $\mu_{\text{ff}}(\gamma_{\text{sf}}, \text{modulation})$ and $\sigma_{\text{ff}}(\gamma_{\text{sf}}, \text{modulation})$ are obtained by simulations assuming N_{sc} uncorrelated subcarriers per resource unit. An exponentially distributed random variable models the channel transfer factor for each subcarrier due to small-scale fading. Simulation results for specific scenarios are given later in Section 4.7.4. The pdf of α_{ff} is given by

$$f_{\alpha_{\text{ff}}}(\alpha_{\text{ff}}) = \frac{1}{\sqrt{2\pi}\sigma_{\text{ff}}(\gamma_{\text{sf}}, \text{modulation})} \exp\left(-\frac{(\alpha_{\text{ff}} - \mu_{\text{ff}}(\gamma_{\text{sf}}, \text{modulation}))^2}{2 \cdot \sigma_{\text{ff}}^2(\gamma_{\text{sf}}, \text{modulation})}\right). \quad (4.35)$$

The pdf of α_{ff} in the analytical evaluation methodology represents the small-scale fading model. For fair resource scheduling, (4.35) describes the pdf of $\tilde{\alpha}_{\text{eff,fr}}$ which indicates the random variable of the gain in SIR due to scheduling. The pdf of α_{ff} is used later in this thesis to derive also the statistical properties of the gain in SIR due to the other scheduling algorithms.

4.5.2.3 Proportional fair scheduling

The SIR when using proportional fair scheduling is evaluated in this section. The scheduling decision for proportional fair scheduling is made based on (2.25). In the following (2.25) is approximated by the objective function

$$j(k) \approx \arg \max_i \left\{ \frac{\bar{\gamma}_{\text{ru}}^{(i)}(k)}{\gamma_{\text{ls}}^{(i)}} \right\} \quad (4.36)$$

where $\bar{\gamma}_{\text{ru}}^{(i)}(k)$ is the actual effective SIR of the resource unit k of user i and $\gamma_{\text{ls}}^{(i)}$ the average SIR of user i due to pathloss and shadowing. This approximation holds if

the relationship between achievable user throughput and SIR is linear. However, this is a common approximation when investigating proportional fair scheduling [AML04, CB07].

With this approximation, the proportional fair scheduling algorithm allocates the resource unit always to the user that experiences the best relative SIR. With n_{active} active users, the random variable $\tilde{\alpha}_{\text{eff,pf}}$ describing the gain in SIR due to scheduling compared to the SIR due to large-scale propagation loss is given by

$$\begin{aligned}\tilde{\alpha}_{\text{eff,pf}} &= \max \left\{ \frac{\overline{\gamma}_{\text{ru}}^{(1)}(k)}{\gamma_{\text{ls}}^{(1)}}, \dots, \frac{\overline{\gamma}_{\text{ru}}^{(n_{\text{active}})}(k)}{\gamma_{\text{ls}}^{(n_{\text{active}})}} \right\} \\ &= \max \left\{ \alpha_{\text{ff}}^{(1)}, \dots, \alpha_{\text{ff}}^{(n_{\text{active}})} \right\}\end{aligned}\quad (4.37)$$

The channel transfer factor of user i with $i = 1, \dots, n_{\text{active}}$ given by $\alpha_{\text{ff}}^{(i)}$ is one realization of the random variable α_{ff} derived in Section 4.5.2.2. Assuming that iid realizations are obtained for each user i , the statistical properties of $\tilde{\alpha}_{\text{eff,pf}}$ can be obtained using, e.g., extreme value statistics [Dav81, Pap84]. Assuming that α_{ff} is a Gaussian distributed random variable as derived in Section 4.5.2.2, the pdf of $\tilde{\alpha}_{\text{eff,pf}}$ is given by

$$f_{\tilde{\alpha}_{\text{eff,pf}}}(\tilde{\alpha}_{\text{eff,pf}}) = \frac{n_{\text{active}}}{\sqrt{2\pi}\sigma_{\text{ff}}} \exp\left(-\frac{(\tilde{\alpha}_{\text{eff,pf}} - \mu_{\text{ff}})^2}{2\sigma_{\text{ff}}^2}\right) \cdot \left(\frac{1}{2} \left(1 - \operatorname{erf}\left(\frac{\tilde{\alpha}_{\text{eff,pf}} - \mu_{\text{ff}}}{\sqrt{2}\sigma_{\text{ff}}}\right)\right)\right)^{n_{\text{active}}-1}. \quad (4.38)$$

The pdf of $\tilde{\alpha}_{\text{eff,pf}}$ describes the gain in SIR due to scheduling for proportional fair scheduling that is combined with the SIR due to large-scale propagation loss to derive the number of bits that can be transmitted per resource unit.

4.5.2.4 Fair throughput scheduling

This section describes the gain in SIR that can be achieved with fair throughput scheduling. Throughout this work a fair throughput scheduling approach is used as depicted in Section 2.6 that does not consider channel state information for the scheduling decision. The random variable $\tilde{\alpha}_{\text{eff,ft}}$ indicating the gain in SIR compared to the SIR due to large-scale propagation loss for fair throughput scheduling is equal to $\tilde{\alpha}_{\text{eff,fr}}$ and the pdf is given by

$$f_{\tilde{\alpha}_{\text{eff,ft}}}(\tilde{\alpha}_{\text{eff,ft}}) = \frac{1}{\sqrt{2\pi}\sigma_{\text{ff}}(\gamma_{\text{sf}}, \text{modulation})} \exp\left(-\frac{(\tilde{\alpha}_{\text{eff,ft}} - \mu_{\text{ff}}(\gamma_{\text{sf}}, \text{modulation}))^2}{2 \cdot \sigma_{\text{ft}}^2(\gamma_{\text{sf}}, \text{modulation})}\right). \quad (4.39)$$

4.5.3 Number of allocated resource units

4.5.3.1 General problem formulation

This section describes the number of resource units per second that are allocated to one user during its session duration. The number of resource units per second allocated to each user is the second part of the analytical evaluation methodology that is influenced, among others, by the scheduling algorithm as depicted in Figure 4.1. The impact of the scheduling algorithm on the gain in SIR has already been described in Section 4.5.2. Three different scheduling algorithms are considered as characterised in Section 2.6.

To derive an estimate of the average user throughput, it is necessary to know the number of resource units that are allocated during the session duration. For this investigation, the statistical properties of the number of resource units per second that are allocated to each user during the session duration are derived considering the results obtained in Section 4.3 for the statistical properties of the average number of active users during the session duration of one investigated user and the number N_{res} of available resource units per second as given in Section 4.4. The derived pdf of the number of resource units per second that are allocated to each user are combined with the number of bits that can be transmitted per resource unit to achieve the average throughput of the users.

4.5.3.2 Fair resource scheduling

Fair resource scheduling as defined in Section 2.6 allocates equal number of resource units to all users if the considered time interval is large enough. The number $n_{\text{alloc,fr}}^{(i)}$ of resource units per second allocated to user i is given depending on the average number $\bar{n}_{\text{act}}^{(i)}$ of active users during the session duration by

$$n_{\text{alloc,fr}}^{(i)} = \frac{N_{\text{res}}}{\bar{n}_{\text{act}}^{(i)}}. \quad (4.40)$$

$\bar{n}_{\text{act}}^{(i)}$ is the realization of the random variable \bar{n}_{act} describing the average number of active users during the session duration of an investigated user with the pdf as derived in Section 4.3. Therefore, $n_{\text{alloc,fr}}^{(i)}$ is the realization of the random variable $n_{\text{alloc,fr}}$ which represents the number of resource units per second that are allocated to one user. The pdf of $n_{\text{alloc,fr}}$ is derived using random variable transformation [Pap84] as

$$f_{n_{\text{alloc,fr}}}(n_{\text{alloc,fr}}) = \frac{N_{\text{res}}}{n_{\text{alloc,fr}}^2} f_{\bar{n}_{\text{act}}} \left(\frac{N_{\text{res}}}{n_{\text{alloc,fr}}} \right). \quad (4.41)$$

Assuming speech traffic which is modeled by an $M/M/\infty$ queueing model in Section 4.3.2, the pdf of \bar{n}_{act} is given by (4.18) so that the pdf of the number $n_{\text{alloc,fr,sp}}$ of resource units per second allocated to one user during the session duration is given using (4.41) as

$$f_{n_{\text{alloc,fr,sp}}}(n_{\text{alloc,fr,sp}}) = \begin{cases} \frac{(1-p_{\text{noStatTrans}})N_{\text{res}}}{n_{\text{alloc,fr,sp}}^2 \sqrt{2\pi \text{Var}\{\bar{n}_{\text{act,sp}}\}}} \cdot \dots \\ \exp\left(-\frac{\left(\frac{N_{\text{res}}}{n_{\text{alloc,fr,sp}}} - \text{E}\{\bar{n}_{\text{act,sp}}\}\right)^2}{2\text{Var}\{\bar{n}_{\text{act,sp}}\}}\right) + \dots \\ p_{\text{noStateTrans}} \sum_{k=0}^{\infty} p_{\text{noStateTrans}}(k) \cdot \dots \\ \delta\left(n_{\text{alloc,fr,sp}} - \frac{N_{\text{res}}}{k}\right) & \text{for } 0 < n_{\text{alloc,fr,sp}} \leq N_{\text{res}} \\ 0 & \text{else.} \end{cases} \quad (4.42)$$

If download or web browsing traffic is assumed, the pdf of the number of active users averaged over the session duration is given by (4.20). If again (4.41) is used, the number $n_{\text{alloc,fr,dl}}$ of resource units per second allocated to one user during the session is given by

$$f_{n_{\text{alloc,fr,dl}}}(n_{\text{alloc,fr,dl}}) = \begin{cases} \frac{N_{\text{res}}}{n_{\text{alloc,fr,dl}}^2 \text{E}\{n_{\text{active,dl}}\}} \cdot \dots \\ \exp\left(-\frac{\frac{N_{\text{res}}}{n_{\text{alloc,fr,dl}}} - 1}{\text{E}\{n_{\text{active,dl}}\}}\right) & \text{for } 0 < n_{\text{alloc,fr,dl}} \leq N_{\text{res}} \\ 0 & \text{else.} \end{cases} \quad (4.43)$$

The pdf of the number of resource units per second that are allocated to one user due to fair resource scheduling are described by (4.42) for data traffic where the session duration is modeled by a random variable and by (4.43) for data traffic where the file size of a session is modeled by a random variable. Combining the derived pdfs with the number of bits that can be transmitted per resource unit the user throughput assuming fair resource scheduling is obtained.

4.5.3.3 Proportional fair scheduling

Proportional fair scheduling has the property that equal number of resource units are allocated to all users [Hol01, FKWD07]. Therefore, the same statistics can be used for the number of allocated resource units as derived for fair resource scheduling in Section 4.5.3.2. The property of allocating equal number of resource units is shown exemplarily for two users which is extended to n_{active} users afterwards.

Two users with iid small-scale fading channels are assumed. According to the scheduling criterion in (4.36) each resource unit is allocated to the user with the highest SIR gain. The SIR gain of user one is given by the random variable $\alpha_{\text{ff}}^{(1)}$ and of user two by the random variable $\alpha_{\text{ff}}^{(2)}$ and the pdf $\alpha_{\text{ff}}^{(1)}$ and $\alpha_{\text{ff}}^{(2)}$ is given by

$$f_{\alpha_{\text{ff}}}(\alpha_{\text{ff}}^{(i)}) = \frac{1}{\sqrt{2\pi}\sigma_{\text{ff}}} \exp\left(-\frac{(\alpha_{\text{ff}}^{(i)} - \mu_{\text{ff}})^2}{2\sigma_{\text{ff}}^2}\right) \quad \text{for } i = 1, 2 \quad (4.44)$$

as explained in Section 4.5.2.2. The conditional pdf of $\alpha_{\text{ff}}^{(1)}$ with the condition that $\alpha_{\text{ff}}^{(1)} > \alpha_{\text{ff}}^{(2)}$ is given by

$$f_{\alpha_{\text{ff}}}(\alpha_{\text{ff}}^{(1)} | \alpha_{\text{ff}}^{(1)} > \alpha_{\text{ff}}^{(2)}) = \frac{1}{\sqrt{2\pi}\sigma_{\text{ff}}} \exp\left(-\frac{(\alpha_{\text{ff}}^{(1)} - \mu_{\text{ff}})^2}{2\sigma_{\text{ff}}^2}\right) \cdot \frac{1}{2} \left(1 - \text{erf}\left(-\frac{\alpha_{\text{ff}}^{(1)} - \mu_{\text{ff}}}{\sqrt{2}\sigma_{\text{ff}}}\right)\right). \quad (4.45)$$

This reflects the case that a resource unit is allocated to user one. The probability that a resource unit is allocated to user one is given by

$$\begin{aligned} P\left(\alpha_{\text{ff}}^{(1)} > \alpha_{\text{ff}}^{(2)}\right) &= \int_0^{\infty} f_{\alpha_{\text{ff}}}(\alpha_{\text{ff}}^{(1)} | \alpha_{\text{ff}}^{(1)} > \alpha_{\text{ff}}^{(2)}) \\ &= \frac{1}{2}. \end{aligned} \quad (4.46)$$

Half of the resource units are allocated to user one and the other half to user two. Assuming n_{active} active users, a resource unit is allocated to user i if $\alpha_{\text{ff}}^{(i)}$ is higher than $\alpha_{\text{ff}}^{(j)}$ of user j with $j = 1, 2, \dots, n_{\text{active}}$ and $j \neq i$. Using (4.46) and the assumption that the $\alpha_{\text{ff}}^{(i)}$ are iid, each user gets $\frac{1}{n_{\text{active}}}$ of the available resource units allocated. Therefore, the same statistics regarding n_{alloc} are valid as for fair resource scheduling described in Section 4.5.3.2 and (4.42) and (4.43) describe the pdfs of the number of resource units per second allocated to users with speech and download traffic, respectively, assuming proportional fair scheduling. The user throughput can be calculated as described in Section 4.5.3.2.

4.5.3.4 Fair throughput scheduling

With fair throughput scheduling, a resource unit is allocated to the user with the lowest average user throughput. Therefore in the long term, all user achieve equal user throughput. In contrast to fair resource and proportional fair scheduling as described in the previous sections, the number of resource units allocated to the users depends

on the SIR the users experience in the network [FKWD09a]. As stated previously in Figure 4.1, the average user throughput of user i is given by the product of the number $n_{\text{alloc,ft}}^{(i)}$ of resource units per second allocated to user i and the number $d_{\text{res}}^{(i)}$ of bits that can be transmitted per resource unit as

$$r_{\text{user}}^{(i)} = n_{\text{alloc,ft}}^{(i)} \cdot d_{\text{res}}^{(i)}. \quad (4.47)$$

$n_{\text{alloc,ft}}^{(i)}$ and $d_{\text{res}}^{(i)}$ are both realizations of two random variables. With fair throughput scheduling, equal average user throughput is given to active users, thus

$$r_{\text{user}}^{(i)} = r_{\text{user}} = \text{const} \quad \text{for all } i = 1, \dots, n_{\text{active}} \quad (4.48)$$

where n_{active} is the number of active users in the cell. For simplification it is assumed that n_{active} remains constant during the session duration for the following investigation. If all resource units are allocated, the following expression holds:

$$N_{\text{res}} = \sum_{i=1}^{n_{\text{active}}} n_{\text{alloc,ft}}^{(i)} = \sum_{i=1}^{n_{\text{active}}} \frac{r_{\text{user}}}{d_{\text{res}}^{(i)}} \quad (4.49)$$

which can be rewritten resulting into

$$\frac{N_{\text{res}}}{r_{\text{user}}} = \sum_{i=1}^{n_{\text{active}}} \frac{1}{d_{\text{res}}^{(i)}}. \quad (4.50)$$

The number $d_{\text{res}}^{(i)}$ of bits that can be transmitted per resource unit for user i is the realization of a random variable depending on the distribution of the SIR due to large-scale propagation loss in the cell. The expectation value $E\{\frac{1}{d_{\text{res}}}\} = \mu_{d_{\text{res}}}$ and the variance $\text{Var}\{\frac{1}{d_{\text{res}}}\} = \sigma_{d_{\text{res}}}^2$ of $\frac{1}{d_{\text{res}}}$ can be derived, e.g., using the pdf of the SIR and a methodology described in [BHIM05] or cf. Section 4.3.4. If n_{active} is sufficiently large, the central limit theorem can be applied and

$$\psi = \frac{N_{\text{res}}}{r_{\text{user}}} \quad (4.51)$$

can be approximated by a Gaussian distributed random variable with average value $n_{\text{active}} \cdot \mu_{d_{\text{res}}}$ and variance $n_{\text{active}} \cdot \sigma_{d_{\text{res}}}^2$. The pdf of ψ is given by

$$f_{\psi}(\psi) = \frac{1}{\sqrt{2\pi n_{\text{active}} \sigma_{d_{\text{res}}}^2}} \exp\left(-\frac{(\psi - n_{\text{active}} \mu_{d_{\text{res}}})^2}{2 n_{\text{active}} \sigma_{d_{\text{res}}}^2}\right). \quad (4.52)$$

Using (4.47) and (4.51), the conditional random variable $\{n_{\text{alloc,ft}} | d_{\text{res}} = d_{\text{res}}^{(i)}\}$ indicating the number of resource units per second allocated to one user where $d_{\text{res}}^{(i)}$ bits per resource unit can be transmitted is given as

$$\{n_{\text{alloc,ft}} | d_{\text{res}} = d_{\text{res}}^{(i)}\} = \frac{N_{\text{res}}}{\psi \cdot d_{\text{res}}^{(i)}}. \quad (4.53)$$

Applying random variable transformation to (4.52), the conditional pdf of $\{n_{\text{alloc,ft}}|d_{\text{res}} = d_{\text{res}}^{(i)}\}$ is given by

$$f_{n_{\text{alloc,ft}}}(\{n_{\text{alloc,ft}}|d_{\text{res}} = d_{\text{res}}^{(i)}\}) = \begin{cases} \frac{\rho(d_{\text{res}}^{(i)})N_{\text{res}}}{n_{\text{alloc,ft}}^2 \cdot d_{\text{res}}^{(i)} \sqrt{2\pi n_{\text{active}} \sigma_{d_{\text{res}}}^2}} \cdot \dots \\ \exp\left(-\frac{\left(\frac{N_{\text{res}}}{n_{\text{alloc,ft}} d_{\text{res}}^{(i)}} - n_{\text{active}} \mu_{d_{\text{res}}}\right)^2}{2n_{\text{active}} \sigma_{d_{\text{res}}}^2}\right) & n_{\text{alloc,ft}} > 0 \\ 0 & n_{\text{alloc,ft}} \leq 0 \end{cases} \quad (4.54)$$

where the assumption that $n_{\text{alloc,ft}} > 0$ is considered and the scaling factor

$$\rho(d_{\text{res}}^{(i)}) = \int_{-\infty}^0 \frac{N_{\text{res}}}{n_{\text{alloc,ft}}^2 \cdot d_{\text{res}}^{(i)} \sqrt{2\pi n_{\text{active}} \sigma_{d_{\text{res}}}^2}} \cdot \exp\left(-\frac{\left(\frac{N_{\text{res}}}{n_{\text{alloc,ft}} d_{\text{res}}^{(i)}} - n_{\text{active}} \mu_{d_{\text{res}}}\right)^2}{2n_{\text{active}} \sigma_{d_{\text{res}}}^2}\right) dn_{\text{alloc,ft}} \quad (4.55)$$

is needed so that

$$\int_{-\infty}^{\infty} f_{n_{\text{alloc,ft}}}(n_{\text{alloc,ft}}|d_{\text{res}} = d_{\text{res}}^{(i)}) dn_{\text{alloc,ft}} = 1. \quad (4.56)$$

Comparing the number $n_{\text{alloc,ft}}$ of resource units per second that are allocated to a user when using fair throughput scheduling with the number $n_{\text{alloc,fr}}$ of resource units per second when using fair resource scheduling it can be seen that $n_{\text{alloc,ft}}$ depends on the location of the user while $n_{\text{alloc,fr}}$ is equal for all users and independent of the location within the cell. The conditional random variable

$$\{\Delta_{\text{ru}}|d_{\text{res}} = d_{\text{res}}^{(i)}\} = \frac{\{n_{\text{alloc,ft}}|d_{\text{res}} = d_{\text{res}}^{(i)}\}}{n_{\text{alloc,fr}}} = \frac{\{n_{\text{alloc,ft}}|d_{\text{res}} = d_{\text{res}}^{(i)}\} \cdot n_{\text{active}}}{N_{\text{res}}} \quad (4.57)$$

represents the gain in number of resource units per second allocated to one user that is achieved when $d_{\text{res}}^{(i)}$ bits per resource unit can be transmitted compared to a fair resource scheduling strategy.

In the analytical evaluation methodology, the pdf of $n_{\text{alloc,ft}}$ is combined with d_{res} to achieve the average user throughput of each user and Δ_{ru} is used to derive the throughput gain of a user assuming fair throughput scheduling compared to a user if fair resource scheduling is assumed.

4.6 KPI measurements

This section describes how KPI measurements, i.e., user and cell throughput are obtained using the analytical methodology and considering the derivations for the different parts of the analytical evaluation methodology as described in the previous sections. Of course, it is not possible to measure instantaneous user or cell throughput with the analytical evaluation methodology as with the snapshot based system level simulation approach. However, due to using statistical properties of, e.g, the number of resource units per second that are allocated to one user or the gain in SIR due to scheduling, it is possible to capture the statistics of user and cell throughput. In the following, the performance measurements are derived starting with the pdf of the SIR including the impact of scheduling and data traffic. Afterwards, user and cell throughput is derived.

As stated in Section 4.2, the pdf of the random variable $\gamma_{\text{ls,dB}}$ indicating the SIR due to large-scale propagation loss is given by (4.2). Using the modulation and coding scheme thresholds as defined in Table 3.4, the expectation value $\mu_{\text{d,res}}$ and the variance $\sigma_{\text{d,res}}^2$ of $\frac{1}{d_{\text{res}}}$ can be derived as described in Section 4.3.4 to determine the resource unit utilisation. (4.2) can be evaluated for each BS individually to determine the resource unit utilisation $o^{(k)}$ of BS k with $k = 1, \dots, N_{\text{BS}}$. The pdf in (4.2) is shifted according to the expectation value $E\{o\}$ as explained in Section 4.3.4. To reduce the complexity, the average number n_{active} of active users per BS is assumed constant in the following for deriving $\mu_{\text{d,res}}$ and $\sigma_{\text{d,res}}^2$.

The random variable $\tilde{\alpha}_{\text{eff}}$ indicating the gain in SIR achieved due to scheduling has been derived in linear scale in Section 4.5.2. The random variable $\tilde{\gamma}_{\text{eff,dB}}$ indicating the effective SIR in dB after scheduling in the network is given by

$$\begin{aligned}\tilde{\gamma}_{\text{eff,dB}} &= \tilde{\alpha}_{\text{eff,dB}} + \gamma_{\text{ls,dB}} \\ &= 10 \cdot \log_{10}(\tilde{\alpha}_{\text{eff}}) + \gamma_{\text{ls,dB}}\end{aligned}\quad (4.58)$$

with $\gamma_{\text{ls,dB}}$ the random variable indicating the SIR due to large-scale propagation loss in dB. With the approximation of the pdf of $\gamma_{\text{ls,dB}}$ by (4.2), the pdf of $\tilde{\gamma}_{\text{eff,dB}}$ is obtained as

$$\begin{aligned}f_{\tilde{\gamma}_{\text{eff,dB}}}(\tilde{\gamma}_{\text{eff,dB}}) &= \int_{-\infty}^{\infty} f_{\tilde{\alpha}_{\text{eff,dB}}}(\tilde{\gamma}_{\text{eff,dB}} - \gamma_{\text{ls,dB}}) f_{\gamma_{\text{ls,dB}}}(\gamma_{\text{ls,dB}}) d\gamma_{\text{ls,dB}} \\ &= \int_{-\infty}^{\infty} \frac{10^{\frac{\tilde{\gamma}_{\text{eff,dB}} - \gamma_{\text{ls,dB}}}{10}}}{10 \cdot \log_{10}(\exp(1))} f_{\tilde{\alpha}_{\text{eff}}} \left(10^{\frac{\tilde{\gamma}_{\text{eff,dB}} - \gamma_{\text{ls,dB}}}{10}} \right) f_{\gamma_{\text{ls,dB}}}(\gamma_{\text{ls,dB}}) d\gamma_{\text{ls,dB}} \\ &\approx \sum_{l=0}^{\infty} p_{\gamma_j} \cdot \frac{10^{\frac{\tilde{\gamma}_{\text{eff,dB}} - \gamma_l}{10}}}{10 \cdot \log_{10}(\exp(1))} f_{\tilde{\alpha}_{\text{eff}}} \left(10^{\frac{\tilde{\gamma}_{\text{eff,dB}} - \gamma_l}{10}} \right).\end{aligned}\quad (4.59)$$

The probability $p_{\text{mcs},j}$ that modulation and coding scheme j is used and $d_{\text{res},j}$ bits per resource unit can be transmitted is obtained from (4.59) as described in [BHIM05] so that

$$f_{d_{\text{res}}}(d_{\text{res}}) = \sum_{j=1}^{N_{\text{mcs}}} p_{\text{mcs},j} \cdot \delta(d_{\text{res}} - d_{\text{res},j}). \quad (4.60)$$

The random variable r_{user} indicating the user throughput averaged over the session duration is given by combining the variables n_{alloc} for the number of resource units per second allocated to each user and d_{res} for the bits that can be transmitted per resource unit as

$$r_{\text{user}} = n_{\text{alloc}} \cdot d_{\text{res}}. \quad (4.61)$$

The pdf of n_{alloc} has been derived in Section 4.5.3 for different scheduling algorithms and data traffic models.

As described in [Pap84], the pdf of r_{user} is expressed by

$$f_{r_{\text{user}}}(r_{\text{user}}) = \int_{-\infty}^{\infty} \frac{1}{d_{\text{res}}} f_{n_{\text{alloc}}d_{\text{res}}}\left(\frac{r_{\text{user}}}{d_{\text{res}}}, d_{\text{res}}\right) dd_{\text{res}} \quad (4.62)$$

where $f_{n_{\text{alloc}}d_{\text{res}}}\left(\frac{r}{d_{\text{res}}}, d_{\text{res}}\right)$ is the joint pdf of n_{alloc} and d_{res} . If fair resource or proportional fair scheduling is used, the number of allocated resource units does not depend on the location of the user so that n_{alloc} and d_{res} are independent of each other and (4.62) can be rewritten into

$$\begin{aligned} f_{r_{\text{user}}}(r_{\text{user}}) &= \int_{-\infty}^{\infty} \frac{1}{d_{\text{res}}} f_{n_{\text{alloc}}}\left(\frac{r_{\text{user}}}{d_{\text{res}}}\right) f_{d_{\text{res}}}(d_{\text{res}}) dd_{\text{res}} \\ &= \int_{-\infty}^{\infty} \frac{1}{d_{\text{res}}} f_{n_{\text{alloc}}}\left(\frac{r_{\text{user}}}{d_{\text{res}}}\right) \sum_{j=1}^{N_{\text{mcs}}} p_{\text{mcs},j} \cdot \delta(d_{\text{res}} - d_{\text{res},j}) dd_{\text{res}} \\ &= \sum_{j=1}^{N_{\text{mcs}}} \frac{p_{\text{mcs},j}}{d_{\text{res},j}} f_{n_{\text{alloc}}}\left(\frac{r_{\text{user}}}{d_{\text{res},j}}\right). \end{aligned} \quad (4.63)$$

In case of fair throughput scheduling, it is shown in Section 4.5.3.4 that the number of allocated resource units is not independent of d_{res} . Instead, the conditional pdf for $\{n_{\text{alloc,ft}}|d_{\text{res}} = d_{\text{res},j}\}$ is derived in Section 4.5.3.4. Therefore, the pdf of the user throughput with the condition that $d_{\text{res},j}$ bits are transmitted per resource unit is given by

$$f_{r_{\text{user}}}(\{r_{\text{user}}|d_{\text{res}} = d_{\text{res},j}\}) = \frac{1}{d_{\text{res},j}} f_{n_{\text{alloc,ft}}}\left(\frac{r_{\text{user}}}{d_{\text{res},j}}\right) f_{d_{\text{res},j}}(d_{\text{res}}). \quad (4.64)$$

The pdf of r_{user} for fair throughput scheduling is then given by

$$\begin{aligned}
f_{r_{\text{user}}}(r_{\text{user}}) &= \int_{-\infty}^{\infty} f_{r_{\text{user}}}(\{r_{\text{user}}|d_{\text{res}} = d_{\text{res},j}\}) \cdot f_{d_{\text{res}}}(d_{\text{res}}) dd_{\text{res}} \\
&= \int_{-\infty}^{\infty} f_{r_{\text{user}}}(\{r_{\text{user}}|d_{\text{res}} = d_{\text{res},j}\}) \cdot \sum_{j=1}^{N_{\text{mcs}}} p_{\text{mcs},j} \cdot \delta(d_{\text{res}} - d_{\text{res},j}) dd_{\text{res}} \\
&= \sum_{j=1}^{N_{\text{mcs}}} \frac{p_{\text{mcs},j}}{d_{\text{res},j}} f_{n_{\text{alloc,ft}}}\left(\frac{r_{\text{user}}}{d_{\text{res},j}}\right)
\end{aligned} \tag{4.65}$$

For users experiencing an SIR $\gamma_{\text{ls}} = \gamma_{\text{ls},i}$ due to large-scale propagation loss, the conditional average user throughput is given by the conditional random variable

$$\{r_{\text{user}}|\gamma_{\text{ls}} = \gamma_{\text{ls},i}\} = n_{\text{alloc}} \cdot \{\tilde{d}_{\text{res}}|\gamma_{\text{ls}} = \gamma_{\text{ls},i}\} \tag{4.66}$$

where the pdf of $\{\tilde{d}_{\text{res}}|\gamma_{\text{ls}} = \gamma_{\text{ls},i}\}$ is given by

$$f_{\tilde{d}_{\text{res}}}\left(\{\tilde{d}_{\text{res}}|\gamma_{\text{ls}} = \gamma_{\text{ls},i}\}\right) = \sum_{j=1}^{N_{\text{mcs}}} p_{\text{mcs},j,i} \delta(\tilde{d}_{\text{res}} - \tilde{d}_{\text{res},j}). \tag{4.67}$$

The probability $p_{\text{mcs},j,i}$ that modulation and coding scheme j is utilised is obtained as described in (4.60) considering the conditional random variable

$$\{\gamma_{\text{eff}}|\gamma_{\text{ls}} = \gamma_{\text{ls},i}\} = \tilde{\alpha}_{\text{eff}} \frac{\gamma_{\text{ls},i}}{\text{E}\{o\}} \tag{4.68}$$

with the pdf of $\{\gamma_{\text{eff}}|\gamma_{\text{ls}} = \gamma_{\text{ls},i}\}$ given by

$$f_{\gamma_{\text{eff}}}\left(\{\gamma_{\text{eff}}|\gamma_{\text{ls}} = \gamma_{\text{ls},i}\}\right) = f_{\tilde{\alpha}_{\text{eff}}}\left(\gamma_{\text{eff}} \frac{\text{E}\{o\}}{\gamma_{\text{ls},i}}\right) \tag{4.69}$$

using the pdf of the random variable $\tilde{\alpha}_{\text{eff}}$ indicating the SIR gain as derived for different scheduling strategies in Section 4.5.2. The conditional pdf of the user throughput averaged over the session duration for users with SIR $\gamma_{\text{ls}} = \gamma_{\text{ls},i}$ due to large-scale fading results into

$$f_{r_{\text{user}}}\left(\{r_{\text{user}}|\gamma_{\text{ls}} = \gamma_{\text{ls},i}\}\right) = \sum_{j=1}^{N_{\text{mcs}}} \frac{p_{\text{mcs},j}^{(i)}}{\tilde{d}_{\text{res},j}} f_{n_{\text{alloc}}}\left(\frac{r_{\text{user}}}{\tilde{d}_{\text{res},j}}\right). \tag{4.70}$$

The average user throughput is upper bounded by the service rate r_{serv} so that (4.70) has to be rewritten into

$$f_{r_{\text{user}}}\left(\{r_{\text{user}}|\gamma_{\text{ls}} = \gamma_{\text{ls},i}\}\right) = \begin{cases} \int_{r_{\text{serv}}}^{\infty} \sum_{j=1}^{N_{\text{mcs}}} \frac{p_{\text{mcs},j}^{(i)}}{\tilde{d}_{\text{res},j}} f_{n_{\text{alloc}}}\left(\frac{r_{\text{user}}}{\tilde{d}_{\text{res},j}}\right) & \text{for } r_{\text{user}} = r_{\text{serv}} \\ \sum_{j=1}^{N_{\text{mcs}}} \frac{p_{\text{mcs},j}^{(i)}}{\tilde{d}_{\text{res},j}} f_{n_{\text{alloc}}}\left(\frac{r_{\text{user}}}{\tilde{d}_{\text{res},j}}\right) & \text{for } 0 \leq r_{\text{user}} < r_{\text{serv}} \\ 0 & \text{else.} \end{cases} \tag{4.71}$$

To calculate the cell throughput $E\{r_{\text{cell,fl}}\}$, a methodology proposed in [BHIM05] is adapted in the analytical evaluation methodology [FKWD09b]. In [BHIM05], the average cell throughput is derived based on the SIR due to large-scale propagation loss considering SIR thresholds for different modulation and coding schemes as well as two traffic models with constant download duration and download size. This is different to the analytical evaluation methodology developed in this thesis, which not only considers realistic traffic models, cf. Section 2.4, but also takes user scheduling into account and whether all resource units are utilised for transmission. Thus, obtaining the probability $p_{\text{mcs},j}$ that modulation and coding scheme j is used during transmission in (4.60) using the pdf of the SIR including the gain in SIR due to the scheduling is new compared to the approach in [BHIM05]. The average cell throughput for a fully loaded network and if scheduling is performed so that equal number of resource units are allocated to each user independent of the location within the cell is given by

$$E\{r_{\text{cell,fl}}\} = N_{\text{res}} \cdot \sum_{j=1}^{N_{\text{mcs}}} p_{\text{mcs},j} d_{\text{res},j}. \quad (4.72)$$

As depicted in Section 4.3.4, $E\{r_{\text{cell,fl}}\}$ is reduced by the average resource unit utilisation $E\{o\}$ if data traffic is used and cells are not fully loaded.

If fair throughput scheduling is used, the number of allocated resource units depends on the SIR of the user. The probability $p_{\text{mcs},j}$ that modulation and coding scheme j is used is weighted with the ratio $\{\Delta_{\text{ru}}|d_{\text{res}} = d_{\text{res},j}\}$ given in (4.57) between the number of resource units per second allocated to a user assuming fair throughput scheduling compared to the number of resource units per second allocated to a user assuming fair resource scheduling. This considers that a higher number of resource units are allocated to users with low SIR values than with fair resource scheduling. The average cell throughput assuming fair throughput scheduling is then given by

$$E\{r_{\text{cell,fl}}\} = N_{\text{res}} \cdot \sum_{j=1}^{N_{\text{mcs}}} p_{\text{mcs},j} \{\Delta_{\text{ru}}|d_{\text{res}} = d_{\text{res},j}\} d_{\text{res},j}. \quad (4.73)$$

It can be seen that the analytical evaluation methodology finally gives analytical equations for the KPIs defined in Section 2.7. The average user throughput is given by (4.71), the average cell throughput is given by (4.72) and (4.73), respectively. The outage probability is obtained using the conditional random variable indicating the user throughput if a certain SIR $\gamma_{\text{ls}} = \gamma_{\text{ls},i}$ due to large-scale propagation loss is assumed as given by (4.64). The maximum SIR γ_{max} can be determined where the required user throughput is not achieved. The outage probability of the network is given by the probability that the random variable γ_{ls} is below γ_{max} .

4.7 Performance and complexity evaluation

4.7.1 Introduction

Within this section, investigations regarding the performance and complexity of the developed analytical evaluation methodology are presented. The overall model can be seen in Figure 4.1. As described in the previous sections, the model is based on analytical equations and pdfs of random variables. Therefore, the computational complexity is low compared to the computational complexity of system level simulations and performance results can be obtained within only a few seconds. The accuracy of the proposed analytical evaluation methodology is shown in Chapter 5 where the results obtained with the analytical evaluation methodology are compared with results of a system level simulation. To reduce computational complexity and to derive closed form solutions for the pdfs of certain random variables, parts of the analytical evaluation methodology in Figure 4.1 are solved using approximations, that might lead to a performance degradation. Parts of the analytical evaluation methodology that contain approximations are the calculation of the pdf of the SIR due to large-scale propagation loss where the pdf is approximated by a finite number of probabilities as described in Section 4.2. Furthermore, the random variable indicating the average number of active users during the session duration of an investigated user is approximated by a Gaussian distributed random variable in case of speech traffic and an exponentially distributed random variable in case of download or web browsing traffic as explained in Section 4.3. The channel model used to describe the variations due to small-scale fading as derived in Section 4.5.2.2 requires the average value and the standard deviation of the small-scale fading as function of the SIR due to large-scale propagation loss and the modulation scheme that is used. These parts are evaluated in the following and the remainder of the section is organised as follows.

Section 4.7.2 gives an overview of the approximation that was proposed in Section 4.2 to derive the pdf of the SIR due to large-scale propagation loss. The impact of the approximated pdf of the SIR due to large-scale propagation loss on the performance of the analytical evaluation methodology is also evaluated. The approximated pdf of the average number of active users during the session duration of one investigated user is compared with results obtained by simulations in Section 4.7.3. Results for the average value and the standard deviation of the small-scale fading as function of the the SIR due to large-scale propagation loss and the modulation scheme are depicted in Section 4.7.4.

4.7.2 Approximation of SIR due to large-scale propagation loss

Throughout this section, the approximation of the pdf of the SIR $\gamma_{\text{ls,dB}}$ due to large-scale propagation loss as described in (4.2) is evaluated. The approximation is necessary since it is not possible to derive an analytical expression of the pdf of $\gamma_{\text{ls,dB}}$ if arbitrary cell layouts, inhomogeneous user distributions or different large-scale propagation loss models are considered so that the pdf of $\gamma_{\text{ls,dB}}$ used for the analytical evaluation methodology can be the result of, e.g., a pathloss prediction simulation. Further on, the approximation reduces the complexity because random variable transformation like in (4.59) can be performed easily. In the following, it is evaluated how accurate the pdf of $\gamma_{\text{ls,dB}}$ is approximated depending on the interval size $\Delta_{\text{ls,dB}}$ used in (4.2).

A cellular network with two tiers of co-channel interfering cells is considered as described in Section 3.7.2. The distance between two neighboring BSs is constant and each BS is equipped with omnidirectional antennas. Large-scale propagation loss is modelled according to (2.4) with $A = -13$ dB and $B = 3.5$ and a random component with pdf given by (2.6). The standard deviation σ_{SF} of the random component is varied. The network is assumed to be interference limited so that additional noise can be omitted. It is assumed that all BSs transmit with equal transmit power. 100000 user positions are generated uniformly distributed over the cellular environment. Large-scale propagation loss is calculated between each user position and each BS and $\gamma_{\text{ls,dB}}$ is derived for each user position so that a histogram of $\gamma_{\text{ls,dB}}$ is obtained as approximation for the pdf of $\gamma_{\text{ls,dB}}$. The χ^2 -test as described in Section 3.7.1 is used to measure the error due to the approximation. $N_{\text{sam}} = 20$ intervals are used to determine the expected frequencies e_i with $i = 1, \dots, N_{\text{sam}}$ from the simulated pdf of $\gamma_{\text{ls,dB}}$. The observed frequencies are obtained from (4.2) and (3.45) is applied. Again a significance level of a close to one means that the error due to the approximation is small.

Figure 4.2 shows the significance level a of the approximated pdf of $\gamma_{\text{ls,dB}}$ as function of $\Delta_{\text{ls,dB}}$ for scenarios with different standard deviation of the shadow fading component. It can be seen that all the investigated scenarios have similar behaviour for the significance level. For $\Delta_{\text{ls}} \approx 1$ dB the significance level decreases abruptly. This concludes that Δ_{ls} should be smaller than 1 dB to obtain sufficient accuracy.

Furthermore, the approximation also has impact on the complexity of the analytical evaluation methodology. In (4.59), (4.2) is used to determine the pdf of the SIR including the impact of scheduling. In practical networks, the sum will not contain

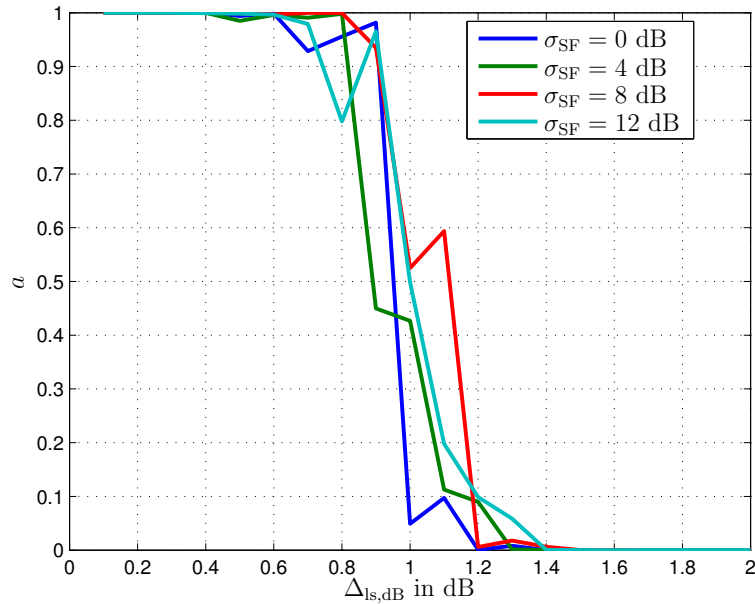


Figure 4.2. Significance level as function of the interval size with different standard deviation for the shadow fading as parameter

infinite summands but the probability is zero that very low and very high SIR due to large-scale propagation loss are observed. Therefore, the approximation in (4.2) is done between a lower and an upper bound SIR value and Δ_{ls} has impact on the number of summands in (4.2) and therefore also in (4.59). Reducing Δ_{ls} by factor 2 leads to a doubled number of summands in (4.59).

Based on the presented results, it is reasonable to use $\Delta_{\text{ls}} = 0.5$ dB which provides a good trade-off between an accurate approximation and justifiable complexity.

4.7.3 Number of active users during the session duration

In Section 4.3, the random variable \bar{n}_{act} is introduced indicating the average number of users that are active during the session duration of one investigated user considering the transient behaviour of the queueing model. The pdf of \bar{n}_{act} is given in Section 4.3.2 for speech traffic assuming that the random variable is approximated by a Gaussian distributed random variable. For download and web browsing traffic, the pdf of \bar{n}_{act} is approximated using an exponentially distributed random variable. Within this section, the accuracy of this approximation is evaluated by comparing the pdf of \bar{n}_{act} obtained

analytically with results from simulations. \bar{n}_{act} is needed among others to derive the number of resource units per second that are allocated to each user as shown in Figure 4.1.

In the first part of this section, speech traffic is analysed as described in Section 4.3.2. It has been shown that speech traffic is modelled by an $M/M/\infty$ queueing system and the pdf of \bar{n}_{act} is given by (4.18). In the following, new users arrive in the network according to a Poisson process with arrival rate λ_{speech} . The session duration is derived from an exponentially distributed random variable with an average session duration of $\frac{1}{\mu_{\text{speech}}} = 120$ s. Simulations are performed where users get active depending on the Poisson process. Each user is active for a random time duration obtained from an exponentially distributed random variable with mean duration given by $\frac{1}{\mu_{\text{speech}}}$. For each user, the average number \bar{n}_{act} of users that are active during the session duration is calculated. 100000 users are considered in total. The histogram of \bar{n}_{act} obtained by simulations is compared with the analytical equation for the pdf of \bar{n}_{act} as derived in Section 4.3.2.

Figure 4.3 shows the relative frequency of \bar{n}_{act} for an average arrival rate of $\lambda_{\text{speech}} = \frac{1}{60} \frac{1}{\text{s}}$. The frequency obtained from the analytical pdf of \bar{n}_{act} fits quite well with the simulation results. It is shown that the relative frequencies obtained for $\bar{n}_{\text{act}} = 1, 2, 3, \dots$ are well captured by (4.7). The remainder of the histogram is approximated by (4.18) very good, especially, in the intervals $1 \leq \bar{n}_{\text{act}} < 2$ and $\bar{n}_{\text{act}} \geq 5$.

In Figure 4.4, the arrival rate is increased to $\lambda_{\text{speech}} = \frac{1}{6} \frac{1}{\text{s}}$ compared to the results shown in Figure 4.3. Again, the analytical pdf matches the results obtained from the simulation very well. The histogram obtained from the simulation results is well captured by (4.18) and (4.7).

In Table 4.2, results for the expectation value and the variance of \bar{n}_{act} are presented as well as the probability $p_{\text{noStateTrans}}$ that no state transition occurs during the session of one investigated user. It can be seen that the simulation results obtained for the two scenarios with $\lambda = \frac{1}{6} \frac{1}{\text{s}}$ and $\lambda = \frac{1}{60} \frac{1}{\text{s}}$ fit the analytical results obtained with the equations given in Section 4.3.2. Results with equal accuracy are also obtained when using other average arrival rates λ_{speech} .

In the second part of this section, different download scenarios are investigated. Again, the pdf of \bar{n}_{act} obtained analytically in (4.20) is compared to results obtained from simulations to show the accuracy of the derived pdf of \bar{n}_{act} . Four different scenarios are considered that represent exemplarily different situations. For the simulation, users come into the network according to the Poisson process with an average arrival rate

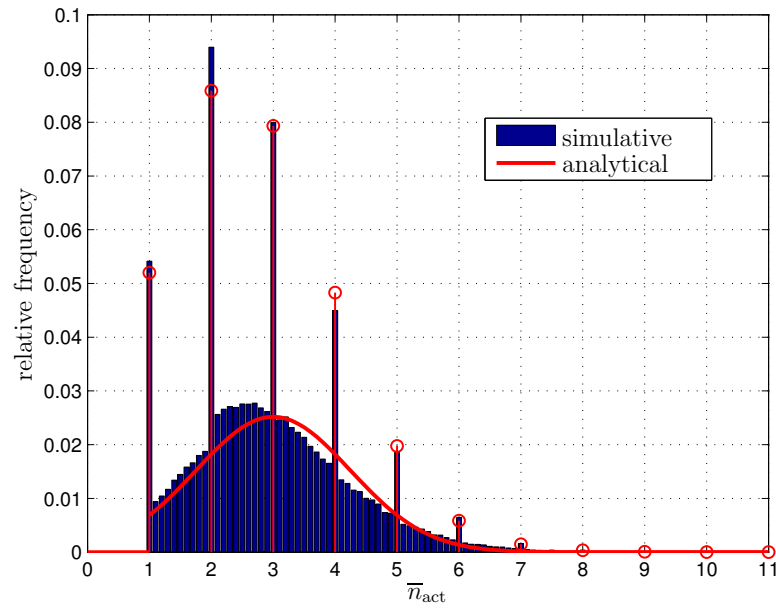


Figure 4.3. Relative frequency of the average number of active users during the session duration of one investigated user for speech traffic with $\lambda = \frac{1}{60} \frac{1}{s}$

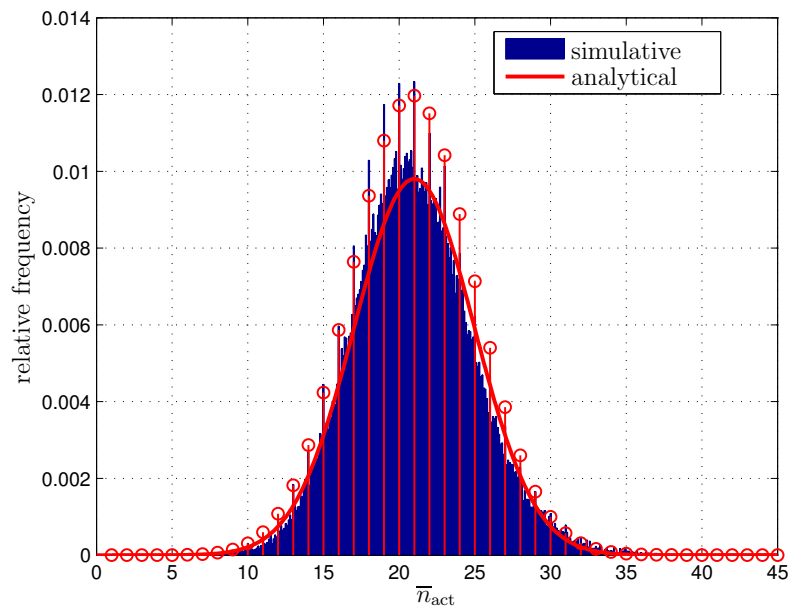


Figure 4.4. Relative frequency of the average number of active users during the session duration of one investigated user for speech traffic with $\lambda = \frac{1}{6} \frac{1}{s}$

Table 4.2. Results of \bar{n}_{act} for speech traffic

λ_{speech} in $\frac{1}{s}$	Parameter	Simulation results	Analytical results
$\frac{1}{60}$	$E\{\bar{n}_{\text{act}}\}$	3.0	3.0
	$\text{Var}\{\bar{n}_{\text{act}}\}$	1.24	1.22
	$p_{\text{noStateTrans}}$	0.217	0.216
$\frac{1}{6}$	$E\{\bar{n}_{\text{act}}\}$	21.0	21.0
	$\text{Var}\{\bar{n}_{\text{act}}\}$	4.0	4.0
	$p_{\text{noStateTrans}}$	0.025	0.025

λ_{dl} . For each active user a file size is generated according to the download traffic model depicted in Section 2.4 with an average file size $S_{\text{dl}} = 2$ Mbyte. The session of a user terminates if the whole file size is transmitted. For transmission, it is assumed that 8 resource units are available each 1.4 ms. For simplicity reason, resource units are shared equally among all users, i.e., fair resource scheduling and d_{res} bits per resource unit can be transmitted. Each 1.4 ms, the file size of the active users is reduced by the product of the number of resource units that are allocated to each user and the number of bits that can be transmitted per resource unit. The pdf of \bar{n}_{act} is calculated analytically using (4.20). Figure 4.5 shows the relative frequency of \bar{n}_{act} as given by the pdf of \bar{n}_{act} in (4.20) and as obtained from the histogram of the simulation results. Scenarios are considered where the average number $E\{n_{\text{active}}\}$ of active users in the network is low, cf. Figure 4.5(a) and Figure 4.5(b), and scenarios where $E\{n_{\text{active}}\}$ is high, cf. Figure 4.5(c) and Figure 4.5(d). In two of the considered scenarios, high d_{res} can be transmitted per resource unit, cf. Figure 4.5(a) and Figure 4.5(d), and in two scenarios, only low d_{res} can be transmitted per resource unit, cf. Figure 4.5(b) and Figure 4.5(c). As expected from the statistical properties of the number of active users in (3.12) and (4.19), it can be seen that a high number of users are alone in one cell or have to share the available resource units with only a small number of other users. While the arrival process for new users is modelled as Poisson process with an average arrival rate, the session duration depends on the throughput achieved by the user. Therefore, a session lasts long if the number of active users is high and each user only gets a small number of resource units allocated. On the other hand, if the user is the only user for a long duration of his session, he is able to utilise all resource units and can transmit the file in a small time duration.

The main results of the download traffic scenario are summarised in Table 4.3. The expectation value of \bar{n}_{act} is depicted for different λ_{dl} and d_{res} . It can be seen that the expectation value that is also used in the approximation of the pdf in (4.19) is calculated with a high accuracy. Similar results are obtained for scenarios with other

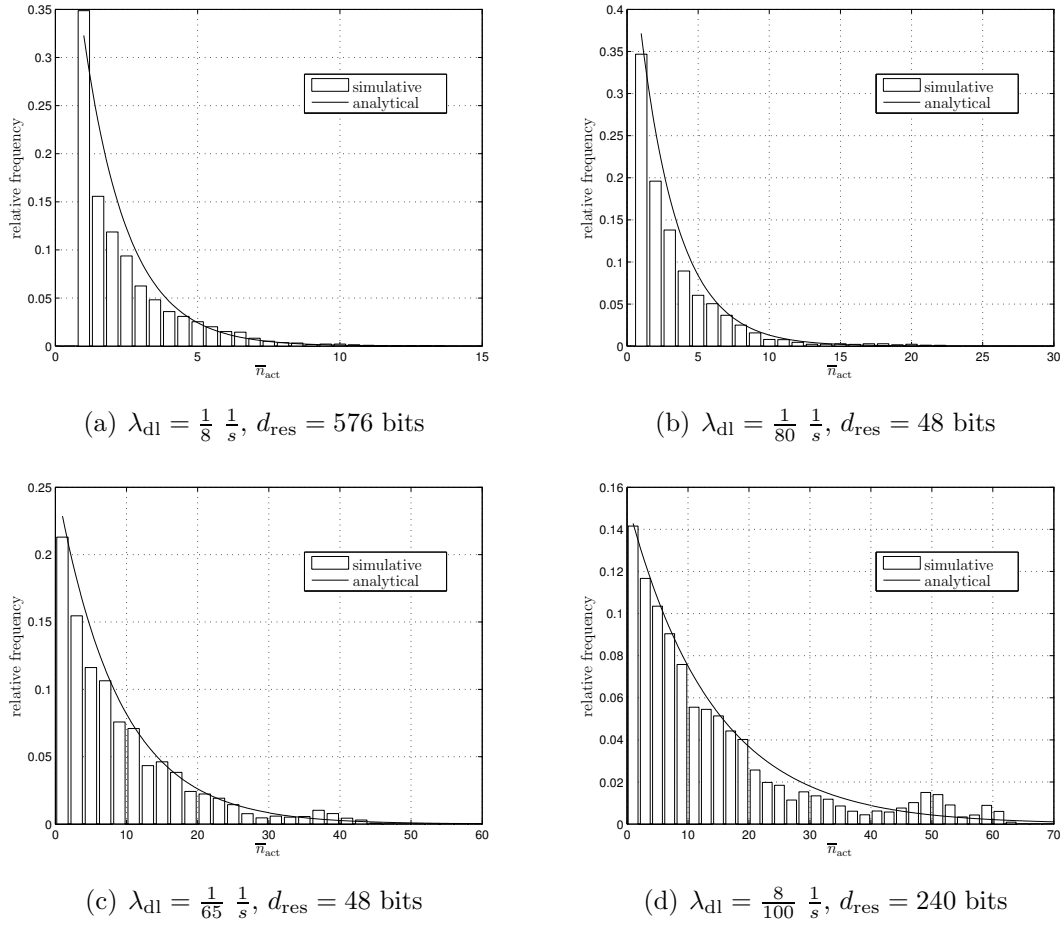


Figure 4.5. Relative frequency of the average number of active users during the session duration of one investigated user for download traffic

Table 4.3. Results of $E\{\bar{n}_{act}\}$ for download traffic

λ_{dl} in $\frac{1}{s}$	d_{res} in bits	$E\{\bar{n}_{act}\}$	
		Simulation result	Analytical results
$\frac{1}{8}$	576	2.55	2.56
$\frac{1}{80}$	48	3.69	3.72
$\frac{1}{65}$	48	9.75	9.95
$\frac{8}{100}$	240	15.0	15.2

d_{res} and λ_{dl} . Therefore, it can be concluded that the pdf of \bar{n}_{act} is calculated in the analytical evaluation methodology with sufficient accuracy.

4.7.4 Effective small-scale fading model

In this section, results for the average value μ_{ff} and the standard deviation σ_{ff} of the effective small-scale fading channel are presented. The effective small-scale fading channel is proposed in Section 4.5.2.2 for networks that use distributed subcarrier allocation like the WiMAX PUSC mode. The pdf of the effective small-scale fading channel is given by (4.35) and can be described by μ_{ff} and σ_{ff} which are both functions of the modulation scheme and the SIR $\gamma_{\text{sf,db}}$ due to large-scale propagation loss. Depending on, e.g., system parameters and the channel model, values for μ_{ff} and σ_{ff} have to be achieved by simulations. The effective small-scale fading model represents an interface mapping the frequency-selective small-scale fading model to the pdf of an effective small-scale fading coefficient. The pdf of the effective small-scale fading coefficient is used in the analytical evaluation methodology, e.g., to derive the statistical properties of the post-scheduling SIR. This section gives values for μ_{ff} and σ_{ff} .

Subcarriers that are separated by more than the coherence bandwidth B_{coh} in frequency or the coherence time t_{coh} in time experience iid Rayleigh fading. In the following, it is assumed that N_{sc} subcarriers of one resource unit experience iid Rayleigh fading. The SIR due to large-scale propagation loss is equal for each subcarrier and all subcarriers of one resource unit are transmitted with the same modulation scheme. Using the expressions described in Section 3.4, the mutual information for each subcarrier is calculated. Using the average mutual information, an effective SIR is calculated. In the following, two different scenarios are considered. In both scenarios, the coherence bandwidth is $B_{\text{coh}} = 400$ kHz and the subcarrier spacing is $f_{\text{sc}} = 11.16$ kHz. For the first scenario, a system bandwidth of 1.25 MHz is assumed and 128 subcarriers are used for transmission. Therefore, four subcarriers of one resource unit are separated by approximately B_{coh} and are assumed to experience iid Rayleigh fading. The second scenario contains a system bandwidth of 10 MHz with 1024 subcarriers in total. For each resource unit, 24 subcarriers are separated by more than B_{coh} experiencing iid Rayleigh fading.

Figure 4.6 shows simulation results for the expectation value μ_{ff} and the standard deviation σ_{ff} of the effective SIR gain for each resource unit as function of the SIR $\gamma_{\text{ls,db}}$ due to large-scale propagation loss for both scenarios and different modulation schemes. The results presented in Figure 4.6 have to be used in (4.35) of the analytical

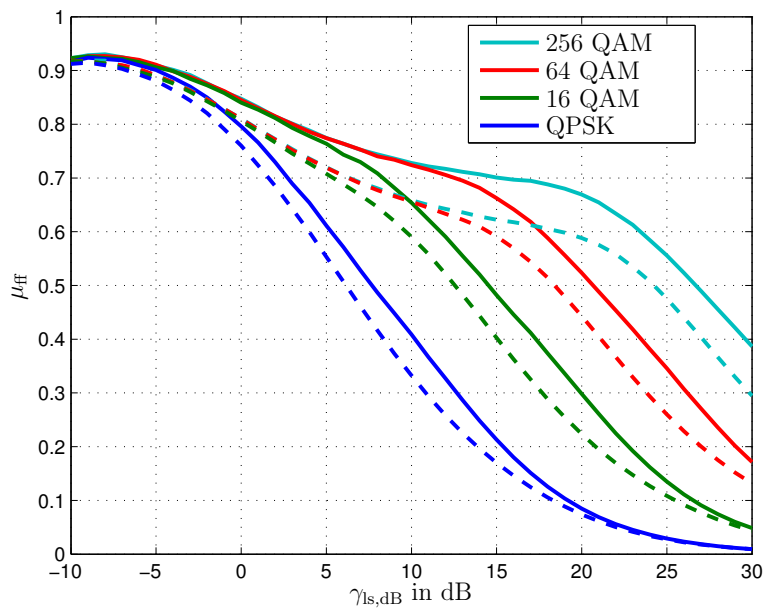
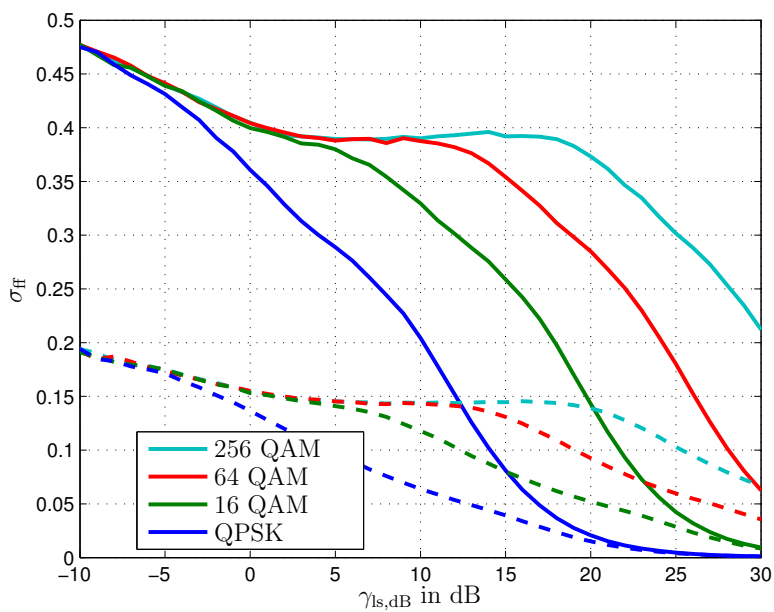
(a) $\mu_{\text{ff}}(\gamma_{\text{ls}}, \text{modulation})$ (b) $\sigma_{\text{ff}}(\gamma_{\text{ls}}, \text{modulation})$

Figure 4.6. Expectation value and standard deviation of small-scale fading as function of the SIR due to large-scale propagation loss for different modulation schemes, solid lines: $N_{\text{sc}} = 4$, dashed lines: $N_{\text{sc}} = 24$

evaluation methodology to model small-scale fading when calculating the gain in SIR due to scheduling. The results presented in Figure 4.6 are obtained for a specific parameter set as described before but some general conclusions can be drawn. It can be seen that both μ_{ff} and σ_{ff} decrease with increasing $\gamma_{\text{ls,dB}}$ due to the shape of the mutual information as function of the SIR. As depicted in Appendix A.1, the mutual information increases with increasing SIR and reaches a maximum value for SIR values that are greater than a threshold SIR. The threshold SIR depends on the modulation scheme. It can be seen that μ_{ff} and σ_{ff} decreases rapidly if $\gamma_{\text{ls,dB}}$ is in the order of the SIR threshold where the mutual information reaches its maximum value for the assumed modulation scheme. Furthermore, an almost constant value is observed for μ_{ff} and σ_{ff} in an interval, e.g., from 4 to 17 dB for 256 QAM. In this interval, the mutual information increases almost linear with the SIR. Comparing the different modulation schemes, it can be seen that μ_{ff} and σ_{ff} are higher if higher order modulation schemes are used due to the higher mutual information that can be achieved with a higher order modulation scheme. Comparing the two scenarios with $N_{\text{sc}} = 4$ and $N_{\text{sc}} = 24$, it is observed that μ_{ff} is slightly reduced with increasing N_{sc} as shown in Figure 4.6(a). A strong decrease in σ_{ff} is observed in Figure 4.6(b) if N_{sc} is increased from 4 to 24. Due to the average value of the mutual information for iid subcarriers that is calculated to achieve μ_{ff} and σ_{ff} , a higher number of subcarriers leads to a smaller standard deviation. The decrease of the average value is due to the nonlinear increase of the mutual information with increasing SIR. Realizations with a low SIR affect the average mutual information calculated for the resource unit more than realizations with higher SIR.

4.8 Conclusion

This chapter has been about the analytical system level evaluation methodology developed during this work. The proposed methodology has been implemented in Matlab for performance and complexity evaluations. The methodology comprises analytical equations and pdfs of random variables describing the behaviour of packet-switched cellular wireless networks. Statistical properties are derived to describe, e.g., the number of active users, the number of allocated resource units or the gain in SIR due to scheduling. Data traffic is considered for traffic services that model a randomly distributed session duration as well as traffic services that model a randomly distributed file size that has to be transmitted. Scheduling algorithms are considered providing fairness among the users as well as improving the performance compared to a random user scheduling by considering channel information. KPIs are measured to identify user, cell and network performance.

Compared with state-of-the-art system level simulations, the proposed analytical evaluation methodology has much lower computational complexity. Due to consideration of analytical equations, results for KPI measurements can be obtained within several seconds so that the proposed methodology is suitable for an application in the network planning process where results on KPIs have to be available fast. The accuracy of the proposed analytical evaluation methodology is expected to be good compared with state-of-the-art system level simulations. A detailed evaluation comparing KPI measurements with the analytical evaluation methodology and the system level simulation methodology described in Chapter 3 is given in the following chapter.

Chapter 5

Impact of scheduling and data traffic on network capacity of packet-switched wireless networks

5.1 Introduction

This chapter presents results for KPIs of cellular wireless networks obtained with the analytical evaluation methodology described in Chapter 4 and the snapshot based system level simulation methodology as depicted in Chapter 3. The calculations of the analytical evaluation methodology are executed using Matlab. The snapshot based system level simulation methodology is implemented in a tool named ONE-PS [FKWD09c]. On the one hand, results obtained with the analytical evaluation methodology are compared with simulation results to evaluate the accuracy of the analytical evaluation methodology. On the other hand, some general rules are derived to describe the impact of data traffic and user scheduling on the network capacity characterised by different KPIs. Comparing the analytical evaluation methodology with the snapshot based system level simulation methodology, it should be noted that it still takes days to achieve results for, e.g., five different average numbers of active users, one traffic model, one server data rate and one scheduling algorithm using the snapshot based system level simulation methodology. The analytical evaluation methodology is able to achieve results for an average number $E\{n_{\text{active}}\}$ of active users for $E\{n_{\text{active}}\} = 1, 2, 3, \dots$ within a duration of less than a minute.

The remainder of the chapter is structured as follows. The system parameters assumed for the investigation are described in Section 5.2. Section 5.3 describes the impact of data traffic on the KPIs. Section 5.4 gives an overview of the influence of user scheduling on the KPIs. In Section 5.5, results are given for a real world scenarios that are provided by the IST MOMENTUM project [MOM03a].

5.2 System parameter assumptions

The following parameters are used for the investigations carried out in this chapter. An overview is given in Table 5.1. An interference limited cellular wireless network

Table 5.1. Parameter settings for the cellular wireless network under consideration

Parameter	Value
Site-to-site distance D_{sts}	So small that the network is interference limited
Number of BSs	25
Antenna pattern of transmitter and receiver	Omnidirectional with 0 dBi antenna gain
Propagation loss coefficients	A = -13 dB, B = 3.5
Shadow fading standard deviation	8 dB
Shadow fading correlation distance	100 m
Small-scale fading model	Vehicular A test environment
User velocity	30 km/h
Speech traffic model [ETS98]	$T_{\text{speech}} = 120$ s
Download traffic model [WiM07]	$E\{S_{\text{f,dl}}\} = 2$ Mbyte
Web browsing traffic model [3GP01]	$E\{S_{\text{pc}}\} = 49.5$ kbyte
	$E\{N_{\text{pc}}\} = 5$
	$E\{T_{\text{RT}}\} = 5$ s
System bandwidth B_{sys}	1.25 MHz
FFT size N_{FFT}	128
Resource unit duration T_{ru}	1.4 ms
Subcarriers per resource unit N_{sc}	12
Available resource units N_{res}	8 per 1.4 ms

with hexagonal cells is assumed. The site-to-site distance is constant and 25 BSs are considered leading to two tiers of interfering BSs. A wrap-around model is applied to avoid border effects [ZK01]. Each BS is equipped with an omnidirectional antenna. Large-scale propagation loss is modeled according to (2.5) with $A = -13$ dB and $B = 3.5$. The standard deviation of the random component is 8 dB with a correlation distance of 100 m. The Vehicular A test environment is used for frequency selective and time variant small-scale fading. Parameters of the assumed tapped-delay line model can be found in Table 2.1. Users move with 30 km/h. Users are distributed uniformly in the investigation area. Each data traffic session arrives in the network according to a Poisson process as described in Section 2.4 and the average arrival rate is given by λ . Speech traffic is modelled with an average session duration $\mu_{\text{speech}} = 120$ s [ETS98]. An average file size of $E\{S_{\text{f,dl}}\} = 2$ Mbyte is assumed for download traffic [WiM07]. An average packet call size $E\{S_{\text{pc}}\} = 49.5$ kbyte is assumed for web browsing sessions. On average, a web browsing session consists of 5 packet calls and the average reading time between two consecutive packet calls is assumed to be $E\{T_{\text{RT}}\} = 5$ s [3GP01]. The bandwidth of the system is 1.25 MHz and OFDMA with 128 subcarriers is used. Each resource unit contains 12 subcarriers in frequency domain and has a time duration of 1.4 ms. Every $T_{\text{ru}} = 1.4$ ms, 8 resource units are available for scheduling. It

is assumed that the channel transfer factor does not change significantly during T_{ru} . Link adaptation is performed using the effective SIR thresholds and the number of bits per resource unit given in Table 3.4. It is assumed that the channel transfer factors are perfectly known for scheduling and link adaptation. Subcarriers combined in one resource unit are distributed over the total system bandwidth so that the effective channel model described in Section 4.7.4 is applied. Three subcarriers per resource unit are separated by less than the coherence bandwidth, respectively, and experience similar channel transfer factors. Therefore, it is assumed that four subcarriers per resource unit experience iid small-scale fading.

The snapshot based system level simulation methodology is used with the following parameters. It has been shown in Chapter 3 that the setting described in the following provides a good trade-off between accurate results and acceptable simulation duration. The user pool size N_{pool} is larger than 130000. 100 snapshots are considered per simulation run. This is a reasonable compromise between an acceptable small user pool size, low simulation duration and high accuracy of the obtained results as it has been shown in Section 3.7.2. The snapshot duration is 5 s which is a reasonable compromise between accurate results for the different scheduling algorithms and the error due to the assumption of a constant SIR due to large-scale propagation loss during the snapshot duration as it has been shown in Section 3.7.3.

5.3 Impact of data traffic on the network capacity

5.3.1 Introduction

This section gives an overview of the impact due to data traffic on the capacity of packet-switched cellular wireless networks. Different traffic models are introduced in Section 2.4 for conversational, download and web browsing services. The server data rate r_{serv} defines the number of bits arriving at each BS in a given time interval for each user with an active session. Therefore, scenarios with equal number of active users and equal server rate lead to the same amount of data in each BS. Parameters for the different data traffic models can be found in Table 5.1.

Figure 5.1 shows the average number of users and sessions that are active as function of the average arrival rate λ of the Poisson process with different data traffic models as parameter. For speech and download traffic, the average number of active sessions is equal to the average number of active users due to each user is active during the

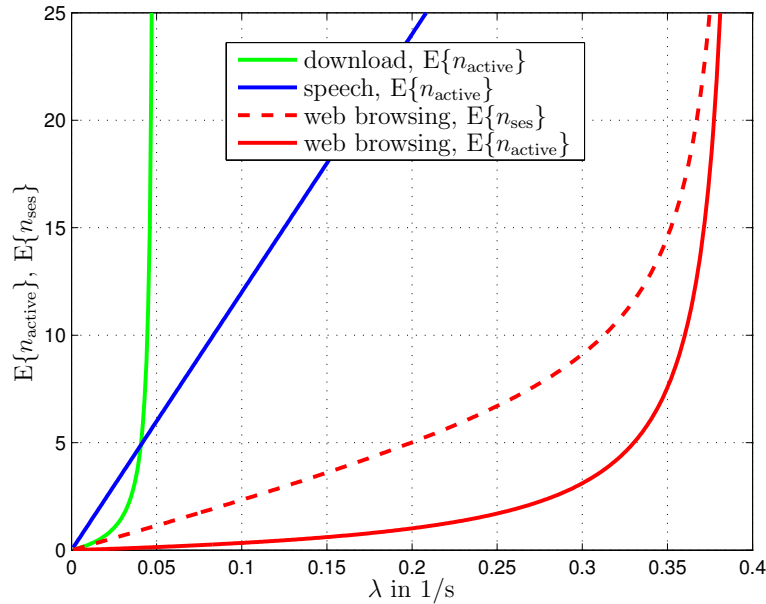


Figure 5.1. Average number of active users and average number of active sessions as function of the average arrival rate for different data traffic models

whole session. In case of web browsing traffic, the average number of active sessions is higher than the average number of active users. A web browsing user is only active during the packet call duration and not active during the reading time duration. It can be seen in Figure 5.1 that the average number of active speech users increases linear with the average arrival rate assuming a constant average session duration. Increasing the average session duration leads to an increasing average number of users assuming a constant average arrival rate. It can be seen that the average number of web browsing and download users increases exponentially with increasing average arrival rate. Due to file size and packet call size, respectively, that is modelled by the traffic model, the session duration also depends on the average user throughput. The average user throughput is higher if only a few users are active simultaneously and each user gets a high portion of resource units allocated than if many users are active simultaneously leading to few resource units that are allocated to each individual user. It can be seen that the average number of active users for download and web browsing traffic suddenly increases fast after a specific average arrival rate, e.g., 0.04 1/s for download traffic. Due to the high number of active users, only few resource units are allocated to each user and low average user throughput is achieved. Thus, the session duration becomes very large.

In the following, the impact of data traffic on the network capacity is investigated.

As mentioned before, scenarios with a constant number of active users, a constant server data rate and the same QoS requirement give equal results, e.g., in cell and user throughput due to an equal amount of data per user that arrives in the BS during a specific time duration. Results for download traffic are presented in the following sections which are also valid for speech and web browsing traffic assuming the same average number of active users. In the following investigation fair resource scheduling is assumed. Results for other scheduling algorithms are presented afterwards in Section 5.4. Section 5.3.2 presents the user performance depending on the average number of active users and the server data rate. Results for the cell performance are given in Section 5.3.3 and the network performance is evaluated in Section 5.3.4. Finally, some common rules for the impact of data traffic on the network capacity are given in Section 5.3.5.

5.3.2 User performance

This section gives an overview of the user performance depending on the service data rate and the average number of active users. Download traffic is considered for the following results and fair resource scheduling is assumed. Results for the average user throughput are presented which are assumed as KPI for the user performance in this work.

Figure 5.2 shows the average user throughput $\bar{r}_{\text{user}}^{(i)}$ of user i as function of the SIR $\gamma_{\text{ls,dB}}^{(i)}$ due to large-scale propagation loss of user i with different average number of active users per BS as parameter. Results are obtained analytically using the methodology proposed in Chapter 4 and using the snapshot based system level simulation methodology as described in Chapter 3. A server data rate $r_{\text{serv}} = 100$ kbit/s and fair resource scheduling are assumed. It can be seen that $\bar{r}_{\text{user}}^{(i)}$ increases with increasing $\gamma_{\text{ls,dB}}^{(i)}$ due to the higher number of bits that can be transmitted with each resource unit depending on the modulation and coding scheme. For a $\gamma_{\text{ls,dB}}^{(i)}$ higher than a certain threshold, $\bar{r}_{\text{user}}^{(i)}$ is upper bounded by r_{serv} and the user is able to transmit all data arriving at the BS immediately. It can be seen from Figure 5.2 that for the assumed scenario the threshold where all data is transmitted immediately increases by 5 - 6 dB if the average number of active users is doubled. Furthermore, it can be stated that $\bar{r}_{\text{user}}^{(i)}$ is reduced by a factor of two if the average number of active users is doubled.

The analytical methodology shows accurate results of $\bar{r}_{\text{user}}^{(i)}$, especially if the average number of active users is greater than 10 users. The analytical results match the simulation results and the error in $\bar{r}_{\text{user}}^{(i)}$ between the analytical and the simulation

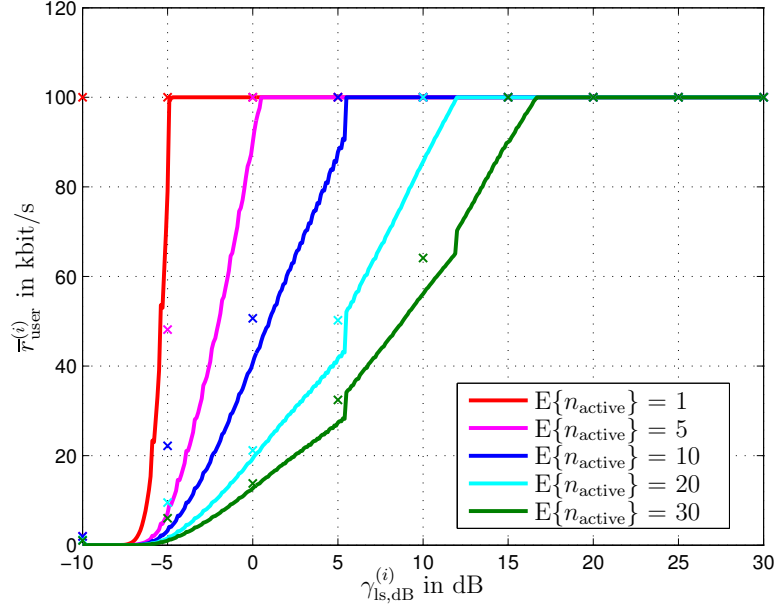


Figure 5.2. Average user throughput as function of the SIR due to large-scale propagation loss of the user with different average number of active users as parameter assuming $r_{\text{serv}} = 100$ kbit/s, download traffic and fair resource scheduling, solid lines: analytical results, markers: simulation results

results is not greater than 15 %. If the average number of users is very small, i.e. below 10 users, the analytical evaluation methodology gives lower results for $\bar{r}_{\text{user}}^{(i)}$ than the simulation. This is due to the fact that users with high $\gamma_{\text{ls,dB}}^{(i)}$ do not need all allocated resource units to achieve $\bar{r}_{\text{user}}^{(i)} = r_{\text{serv}}$. In the simulation, these resource units are allocated to users with low $\gamma_{\text{ls,dB}}^{(i)}$ increasing $\bar{r}_{\text{user}}^{(i)}$ of these users. The analytical evaluation methodology is only able to consider the improvement due to a reduced interference because of resource units that are not utilised and neglects the increase in number of resource units that are allocated to the users with low $\gamma_{\text{ls,dB}}^{(i)}$. In the analytical estimates of $\bar{r}_{\text{user}}^{(i)}$, the thresholds of the different modulation schemes are clearly visible by steps at 5.5 dB and 12 dB.

Figure 5.3 shows the average user throughput $E\{\bar{r}_{\text{user}}^{(i)}\}$ as function of r_{serv} for different number of active users. In contrast to the results shown in Figure 5.2, $E\{\bar{r}_{\text{user}}^{(i)}\}$ is the average user throughput averaged over all users in the cell. It can be seen that if only one user is active per cell, $E\{\bar{r}_{\text{user}}^{(i)}\}$ is almost equal to r_{serv} . The user will get all available resource units allocated. Even users close to the cell border are able to achieve $\bar{r}_{\text{user}}^{(i)} = r_{\text{serv}}$. For $r_{\text{serv}} > 500$ kbit/s, users at the cell border achieve $\bar{r}_{\text{user}}^{(i)} < r_{\text{serv}}$ although all resource units are allocated and the increase of $E\{\bar{r}_{\text{user}}^{(i)}\}$ is no longer linear.

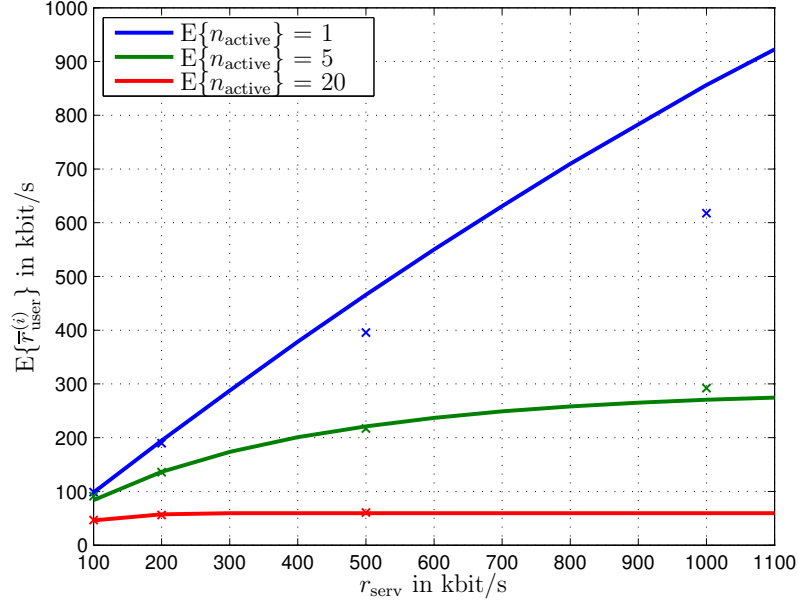


Figure 5.3. Average user throughput as function of the server data rate with different average number of active users as parameter and assuming fair resource scheduling and download traffic, solid lines: analytical results, markers: simulation results

Increasing the average number of active users, a saturation of $E\{\bar{r}_{\text{user}}^{(i)}\}$ is observed. The saturation of $E\{\bar{r}_{\text{user}}^{(i)}\}$ indicates that the network is fully loaded and all resource units are utilised for transmission. The saturation depends on the average number of active users. If the average number of active users is increased by a factor of four, $E\{\bar{r}_{\text{user}}^{(i)}\}$ is reduced by $\frac{1}{4}$.

It can be seen that the results obtained with the analytical evaluation methodology are very accurate compared with the simulation results as long as the average number of active users is higher than 5 users and r_{serv} is smaller than 500 kbit/s. For one active user on average and $r_{\text{serv}} > 500$ kbit/s, results of the analytical evaluation methodology are too optimistic. The reason is that the average number of active users was assumed to be constant for the calculation of the average number of allocated resource units in the analytical methodology which is too optimistic due to not considering that $E\{n_{\text{active}}\}$ is only an average value.

5.3.3 Cell performance

This section gives an overview of the cell performance depending on the average number of active users and the server data rate. Download traffic and fair resource scheduling is assumed for the following results. Results for the average cell throughput averaged over all cells in the investigation area are presented which has been selected as KPI indicating the cell performance.

Figure 5.4 shows $E\{r_{\text{cell}}\}$ as function of the average number of active users per cell with different server data rates as parameter. It can be seen that for the assumed scenario the maximum average cell throughput is given by approximately 1100 kbit/s. With fair resource scheduling a maximum average cell throughput is reached if the network is fully loaded and all resource units are utilised for transmission. Increasing the number of users or increasing the server data rate cannot increase the average cell throughput any further. Reducing the average number of active users or the server data rate results into conditions where not all resource units are utilised any more leading to a reduction in average cell throughput, e.g. for $r_{\text{serv}} = 100$ kbit/s and $E\{n_{\text{active}}\} < 28$. It can be seen from Figure 5.4 that all resource units are utilised for 4 average active users and

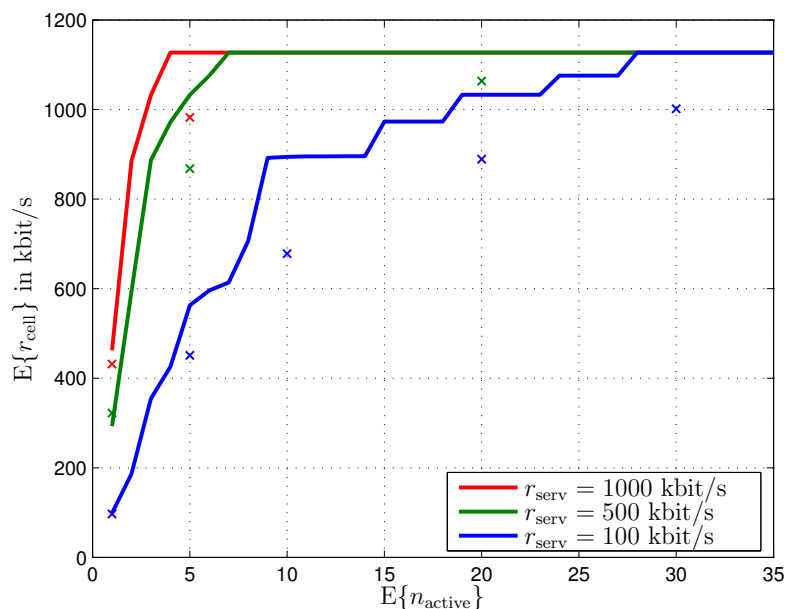


Figure 5.4. Average cell throughput as function of the average number of active users with the server data rate as parameter assuming fair resource scheduling and download traffic, solid lines: analytical results, markers: simulation results

$r_{\text{serv}} = 1000$ kbit/s. The average number of active users has to be increased by nearly a factor of 2 if r_{serv} is halved to 500 kbit/s.

It can be seen that $E\{r_{\text{cell}}\}$ is accurately calculated by the analytical methodology comparing the results with results obtained with ONE-PS. The difference is below 10 % for different average number of active users and server data rates.

5.3.4 Network performance

This section gives an overview of the network performance depending on the average number of active users and the server data rate. Download traffic is considered and fair resource scheduling is assumed. Results for the outage probability p_{out} of the network are shown in the following. The outage probability has been selected as KPI indicating the network performance in Section 2.7. The outage probability indicates the probability that a user becomes unsatisfied. User get unsatisfied if the average user throughput is below a threshold throughput. Due to the assumption of download traffic, a minimum user throughput of 10 % of the server data rate has to be achieved so that the user remains satisfied [ETS98]. For speech traffic services which are not considered in this section the threshold has to be higher as depicted in Section 2.7. It is more likely for users at the cell border to become unsatisfied compared to users in the cell centre. Figure 5.2 indicates that the cell throughput is low for users with low SIR due to large-scale propagation loss. For the network performance, the actual position of the user that is unsatisfied is not important. Usually the outage probability as defined in (2.30) is in the order of 0.01 up to 0.05. Thus, less than 1 - 5 % of the users shall be unsatisfied [Yac93].

Figure 5.5 shows the outage probability p_{out} as function of the server data rate r_{serv} with the average number of active users per cell $E\{n_{\text{active}}\}$ as parameter. An interval $0 \leq p_{\text{out}} \leq 0.2$ is shown in Figure 5.5 which includes outage probabilities that are acceptable for operation of cellular wireless networks. It can be seen that p_{out} increases linearly with r_{serv} , i.e., doubling r_{serv} leads to double p_{out} . It can be seen from the analytical results in Figure 5.5 that $E\{n_{\text{active}}\}$ has to be reduced if r_{serv} is increased and p_{out} should remain constant. In the assumed scenario, $E\{n_{\text{active}}\}$ has to be reduced from 20 to 5 if r_{serv} is increased from 100 kbit/s to 350 kbit/s and $p_{\text{out}} = 0.06$. Or the average number of active users has to be decreased from 5 to 1 if r_{serv} is increased from 200 kbit/s to 900 kbit/s for $p_{\text{out}} \approx 0.02$. It can be stated that an increase of r_{serv} by a factor of k leads to a decrease of roughly a factor of k for the average number of active users if p_{out} should remain constant.

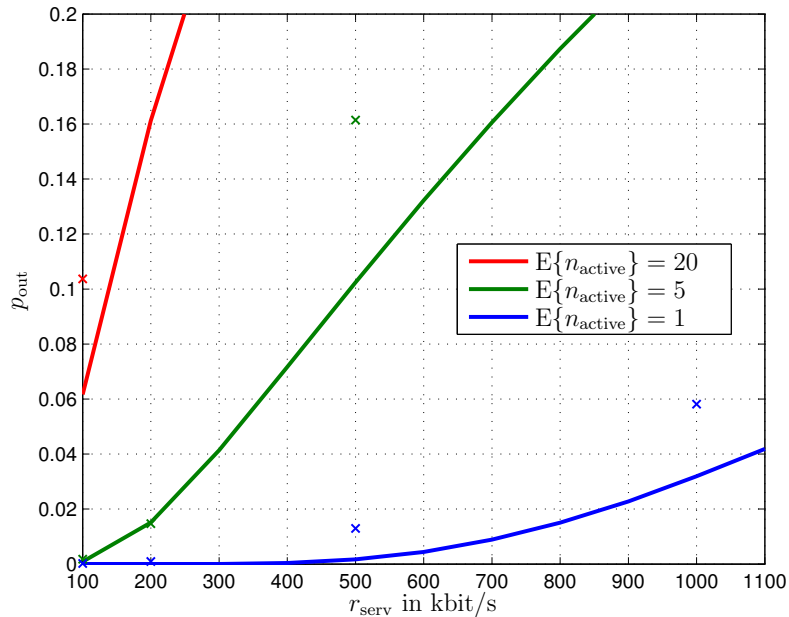


Figure 5.5. Outage probability as function of the server data rate with different average number of active users as parameter assuming fair resource scheduling and download traffic, solid lines: analytical results, markers: simulation results

The analytical results show a good accuracy compared with the simulation results. The difference of the outage probability achieved analytically and using simulations is not greater than 0.05 for different average number of active users and server data rates. Especially, for low outage probabilities the match between analytical and simulation results is good. Low outage probabilities are required when designing cellular wireless networks as stated in Section 2.7.

5.3.5 Rules for the impact of data traffic on the network capacity

This section presents some rules describing KPIs depending on data traffic, server data rate and average number of active users. These rules can be used in the network planning process to derive the capacity of cells. The rules are derived based on the results presented in the previous sections but it should be noted that a specific KPI as function of a specific parameter, e.g., the average user throughput as function of the average number of active users, can be achieved within a few seconds using the proposed analytical evaluation methodology. Thus, results for different scenarios can be

obtained very fast. Fair resource scheduling and download traffic have been assumed for the results used to derive the following rules which are also applicable to other traffic models, e.g., by adapting the average number of active users and by applying another throughput requirement in case of speech traffic. Other scheduling algorithms are considered in Section 5.4.

1. The average user throughput $\bar{r}_{\text{user}}^{(i)}$ of user i is increased if the SIR $\gamma_{\text{ls,dB}}^{(i)}$ due to large-scale propagation loss of user i increases. However, $\bar{r}_{\text{user}}^{(i)}$ cannot exceed the server data rate r_{server} . The increase in $\bar{r}_{\text{user}}^{(i)}$ depending on $\gamma_{\text{ls,dB}}^{(i)}$ depends on the modulation and coding schemes that are used.
2. Increasing the average number $E\{n_{\text{active}}\}$ of active users by a factor of two roughly reduces the average user throughput by a factor of two.
3. The user throughput $E\{\bar{r}_{\text{user}}^{(i)}\}$ averaged over all users in the cell increases if r_{server} is increased. A saturation of $E\{\bar{r}_{\text{user}}^{(i)}\}$ is observed if $E\{n_{\text{active}}\}$ or r_{server} is high, e.g., $E\{n_{\text{active}}\} > 5$ and $r_{\text{server}} > 1000$ kbit/s.
4. The average cell throughput $E\{r_{\text{cell}}\}$ increases with increasing $E\{n_{\text{active}}\}$. More data is available for transmission and more resource units can be utilised if $E\{n_{\text{active}}\}$ is high compared to scenarios with low $E\{n_{\text{active}}\}$. With fair resource scheduling, $E\{r_{\text{cell}}\}$ is limited to a maximum value, which depends on system parameters, e.g., the used modulation and coding schemes or the number of resource units per time interval, as well as on the pdf of $\gamma_{\text{ls,dB}}$ of the users in the network.
5. $E\{r_{\text{cell}}\}$ also increases if r_{server} is increased. More data is available for transmission and more resource units can be utilised if r_{server} is high compared to scenarios with low r_{server} .
6. The outage probability p_{out} of the network increases if r_{server} or $E\{n_{\text{active}}\}$ is increased. To maintain a constant outage probability, $E\{n_{\text{active}}\}$ roughly has to be reduced by the same factor as r_{server} is increased.

5.4 Impact of scheduling on the network capacity

5.4.1 Introduction

This section gives an overview of the impact due to user scheduling and varying average number of active users on the capacity of packet-switched cellular wireless networks.

Three different scheduling algorithms as introduced in Section 2.6 are investigated.

For the following investigation, download traffic with parameters as introduced in Section 5.3 are considered. The server data rate is $r_{\text{server}} = 100$ kbit/s. Section 5.4.2 presents the user performance depending on the scheduling algorithm and the average number of active users. Results for the cell performance depending on the average number of active users and the scheduling algorithm are given in Section 5.4.3. The network performance depending on the scheduling algorithm and the average number of active users is evaluated in Section 5.4.4. Finally, some common rules for the impact of scheduling on the network capacity are given in Section 5.4.5.

5.4.2 User performance

This section gives an overview of the user performance depending on the scheduling algorithm and the average number of active users. Download traffic is considered for the following investigation and $r_{\text{server}} = 100$ kbit/s. Results for the average user throughput are presented which are assumed as KPI for the user performance in this work.

Figure 5.6 shows the average user throughput $\bar{r}_{\text{user}}^{(i)}$ of user i as function of the SIR $\gamma_{\text{ls,dB}}^{(i)}$ due to large-scale propagation loss of user i with different scheduling algorithms as parameter. The average number of active users per cell is $E\{n_{\text{active}}\} = 20$. Results are obtained analytically using the methodology proposed in Chapter 4 and using the snapshot based system level simulation methodology as described in Chapter 3. A server data rate $r_{\text{server}} = 100$ kbit/s is assumed. As depicted in Figure 5.2, $\bar{r}_{\text{user}}^{(i)}$ is upper bounded by r_{serv} and $\bar{r}_{\text{user}}^{(i)}$ increases with increasing $\gamma_{\text{ls,dB}}$ for fair resource and proportional fair scheduling due to the higher number of bits that can be transmitted per resource unit depending on the modulation and coding scheme. Fair resource scheduling achieves the same $\bar{r}_{\text{user}}^{(i)}$ as proportional fair scheduling if $\gamma_{\text{ls,dB}}^{(i)}$ is approximately 5 dB higher. With fair throughput, $\bar{r}_{\text{user}}^{(i)}$ is between 20 and 40 kbit/s if $\gamma_{\text{ls,dB}}^{(i)} > -3$ dB. A higher number of resource units are allocated to users with low $\gamma_{\text{ls,dB}}^{(i)}$ compared to users with high $\gamma_{\text{ls,dB}}^{(i)}$. Thus, $\bar{r}_{\text{user}}^{(i)}$ achieved with fair throughput scheduling is increased for users with low $\gamma_{\text{ls,dB}}^{(i)}$ compared to fair resource scheduling where all users get equal number of resource units allocated. The increase in $\bar{r}_{\text{user}}^{(i)}$ compared to fair resource scheduling for users with low $\gamma_{\text{ls,dB}}^{(i)}$ due to the allocation of a high portion of resource units, leads to a decrease in $\bar{r}_{\text{user}}^{(i)}$ compared to fair resource scheduling for users with high $\gamma_{\text{ls,dB}}^{(i)}$. The assumption of a constant number of allocated resource units within a $\gamma_{\text{ls,dB}}^{(i)}$ interval as derived in Section 4.5.3 leads to the varying $\bar{r}_{\text{user}}^{(i)}$ as shown in Figure

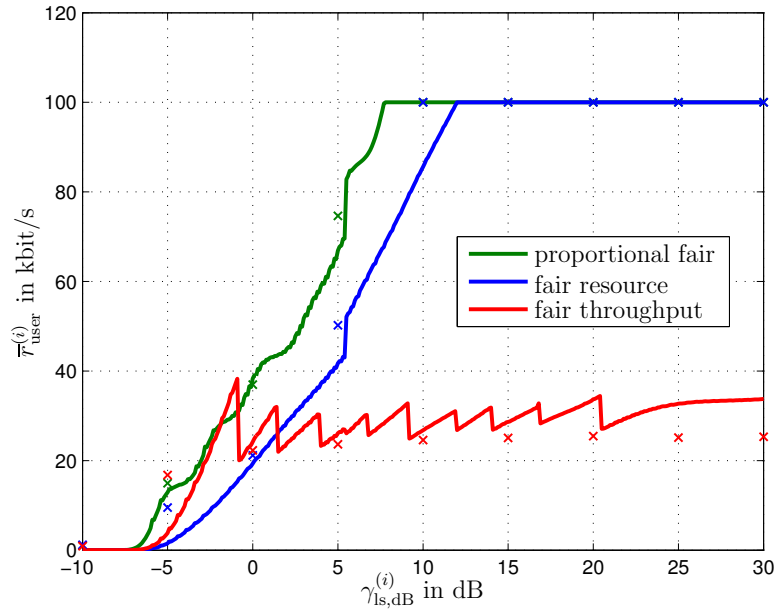


Figure 5.6. Average user throughput as function of the SIR due to large-scale propagation loss with different scheduling algorithms as parameter for $r_{\text{serv}} = 100$ kbit/s, $E\{n_{\text{active}}\} = 20$ and download traffic, solid lines: analytical results, markers: simulation results

5.6 because users with a $\gamma_{\text{ls,dB}}^{(i)}$ close to the next interval are able to transmit more bits per resource units compared with users with a $\gamma_{\text{ls,dB}}^{(i)}$ close to the previous interval.

Again, the analytical results fit well with the simulation results obtained with ONE-PS. The difference of $\bar{r}_{\text{user}}^{(i)}$ obtained analytically and by simulations for fair resource and proportional fair scheduling is small. If fair throughput scheduling is used, $\bar{r}_{\text{user}}^{(i)}$ obtained analytically is slightly higher than $\bar{r}_{\text{user}}^{(i)}$ obtained by simulations. The error is in the order of 10 - 30 % over the whole range of $\gamma_{\text{ls,dB}}$, e.g., due to the assumption of the average number of active users when calculating the number of resource units that are allocated to each of the users. In case of fair throughput scheduling, the number of allocated resource units which is calculated based on $\gamma_{\text{ls,dB}}$ so that each user gets equal $\bar{r}_{\text{user}}^{(i)}$ leads to too optimistic values due to not considering that the number of bits that can be transmitted per resource unit varies due to small-scale fading.

Figure 5.7 shows the average user throughput $E\{\bar{r}_{\text{user}}^{(i)}\}$ as function of the average number of active users for different average number of active users $E\{n_{\text{active}}\}$ per cell. The service rate is $r_{\text{serv}} = 100$ kbit/s and download traffic is considered. As already observed in Section 5.3.2, it can be seen that $E\{\bar{r}_{\text{user}}^{(i)}\}$ decreases with increasing $E\{n_{\text{active}}\}$ for all

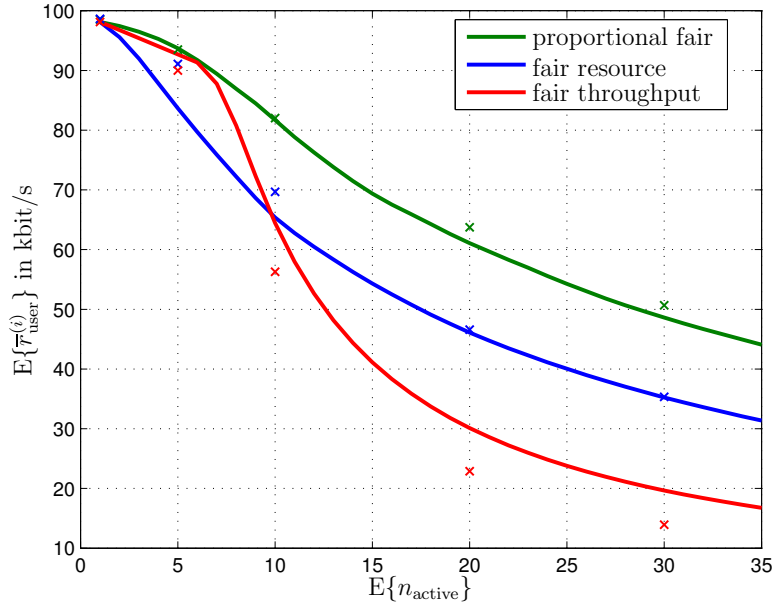


Figure 5.7. User throughput average over all users in the cell as function of the average number of active users per cell with different scheduling algorithms as parameter for $r_{\text{serv}} = 100$ kbit/s and download traffic, solid lines: analytical results, markers: simulation results

considered scheduling algorithms. Using fair throughput or proportional fair scheduling, the gradient of the curve is similar and proportional fair scheduling has always a gain in $E\{\bar{r}_{\text{user}}^{(i)}\}$ compared to fair resource scheduling. If $E\{n_{\text{active}}\}$ is doubled, e.g., from 5 to 10 users, $E\{\bar{r}_{\text{user}}^{(i)}\}$ is reduced by a factor that is smaller than 2. The network is not fully loaded and the available resource units are not fully utilised. This has two effects that are beneficial for $E\{\bar{r}_{\text{user}}^{(i)}\}$. On the one hand, the interference is smaller than in a fully loaded network due to interference averaging effects and a higher number of bits can be transmitted with each resource unit compared to a fully loaded network. On the other hand, when increasing $E\{n_{\text{active}}\}$, resource units will be used for transmission that are not utilised in a scenario with lower $E\{n_{\text{active}}\}$ and $\bar{r}_{\text{user}}^{(i)}$ of each user is only reduced by a small amount. In case of fair throughput scheduling, a steeper decrease can be observed with increasing $E\{n_{\text{active}}\}$ than for fair resource and proportional fair scheduling. Due to all users getting equal $\bar{r}_{\text{user}}^{(i)}$, active users at the cell border have more impact on $E\{\bar{r}_{\text{user}}^{(i)}\}$ if fair throughput scheduling is assumed than assuming the other scheduling algorithms.

The accuracy of the analytical evaluation methodology is good if fair resource or proportional fair scheduling is assumed and the analytical results match the simulation

results with an error of less than 10 %. However, using fair throughput scheduling, $E\{\bar{r}_{\text{user}}^{(i)}\}$ obtained with the analytical evaluation methodology is higher than obtained with ONe-PS due to the reasons shown in Section 5.3.2. The error is in the order of 15 %.

5.4.3 Cell performance

This section gives an overview of the cell performance depending on the scheduling algorithm and the average number of active users. Download traffic is assumed and the server data rate is $r_{\text{server}} = 100$ kbit/s. Results for the average cell throughput average over all cells in the investigation area are presented which has been selected as KPI for the cell performance.

Figure 5.8 shows the average cell throughput $E\{r_{\text{cell}}\}$ as function of the average number of active users $E\{n_{\text{active}}\}$ for different scheduling algorithms. Download traffic with $r_{\text{serv}} = 100$ kbit/s is assumed. As already described in Section 5.3.3, $E\{r_{\text{cell}}\}$ increases with increasing $E\{n_{\text{active}}\}$ since more data is provided to each BS and the number of resource units that are not utilised is reduced. However, differences are observed comparing the three scheduling algorithms. For fair resource scheduling an increasing $E\{r_{\text{cell}}\}$ is obtained that saturates at approximately 1100 kbit/s as already shown in Figure 5.4. Proportional fair scheduling shows similar performance like fair resource scheduling up to $E\{n_{\text{active}}\} \approx 10$. For $E\{n_{\text{active}}\} < 10$, the network is not fully loaded and the impact of the adaptive proportional fair scheduling is not visible. For $E\{n_{\text{active}}\} > 10$, nearly all resource units are utilised and proportional fair scheduling is able to gain from multiuser diversity due to allocating resource units to the user with the best ratio between actual achievable and average user throughput. Therefore, higher $E\{r_{\text{cell}}\}$ is obtained with proportional fair scheduling than with fair resource scheduling. Fair throughput scheduling also shows similar performance as proportional fair and fair resource scheduling up to $E\{n_{\text{active}}\} \approx 5$. In contrast to the other two scheduling algorithms, no further improvement is observed if the average number of active users is further increased. As shown in Section 5.4.2, fair throughput scheduling gives equal throughput to all users, thus, the user with the lowest SIR due to large-scale propagation loss limits also $E\{r_{\text{cell}}\}$. With $E\{n_{\text{active}}\} > 5$, it is very likely that at least one user is only able to utilise the most robust modulation and coding scheme so that $E\{r_{\text{cell}}\}$ is limited by approximately 35 % of the value that can be achieved if fair resource scheduling is used and the network is fully loaded.

The analytical results match the simulation results obtained with ONe-PS. The error in $E\{r_{\text{cell}}\}$ is not higher than 10 %. Only if the average number of active users is around

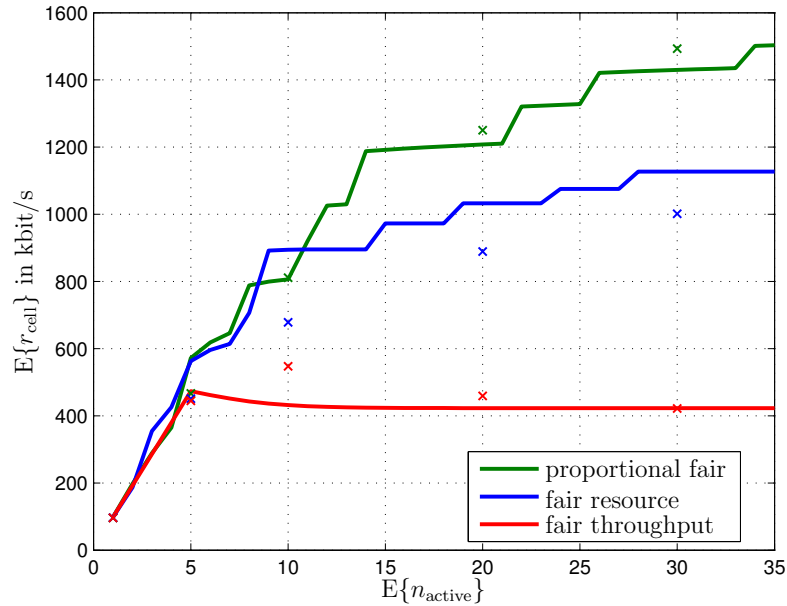


Figure 5.8. Average cell throughput as function of the average number of active users with different scheduling algorithms as parameter for $r_{\text{serv}} = 100$ kbit/s and download traffic, solid lines: analytical results, markers: simulation results

10 users and fair throughput scheduling is used, a larger difference between analytical and simulation results can be observed. The analytical calculation assumes that the central limit theorem can be applied which is not fulfilled for the number of active users. If the average number of active users is higher, the central limit theorem can be applied and the results fit well. If the average number of active users is lower, the network is only partially loaded and scheduling hardly has an impact on the results of $E\{r_{\text{cell}}\}$ so that also a good match is observed.

5.4.4 Network performance

This section gives an overview of the network performance depending on the scheduling algorithm and the average number of active users. Download traffic is assumed with a server data rate $r_{\text{serv}} = 100$ kbit/s. Results for the outage probability of the network are shown in the following. The outage probability has been selected as KPI indicating the network performance in Section 2.7. A user becomes unsatisfied if the average user throughput of this user is below 10 % of r_{serv} as described in Section 5.3.4. The outage probability describes the ratio between the number of unsatisfied users and the total number of active users.

Figure 5.9 shows the outage probability p_{out} as function of the average number of active users $E\{n_{\text{active}}\}$ for three different scheduling algorithms. An interval $0 \leq p_{\text{out}} \leq 0.2$ is shown in Figure 5.5 which includes outage probabilities that are acceptable for the operation of cellular wireless networks. As already observed in Figure 5.5, p_{out} increases almost linearly with $E\{n_{\text{active}}\}$ if fair resource scheduling is assumed. With fair throughput and proportional fair scheduling, p_{out} is smaller than with fair resource scheduling and increases slower with increasing $E\{n_{\text{active}}\}$ than if fair resource scheduling is assumed. Proportional fair scheduling achieves lower p_{out} than fair resource scheduling by allocating only resource units where a high modulation and coding scheme can be used. This improves the average user throughput of all users in the network as shown in Figure 5.6 where the average user throughput of a user with a specific SIR due to large-scale propagation loss is always higher with proportional fair than with fair resource scheduling. Fair throughput scheduling increases the throughput of users at the cell border compared to fair resource scheduling by allocating more resource units to users at the cell border than to users in the cell centre. Therefore, a lower p_{out} is observed with fair throughput scheduling compared to fair resource scheduling. With fair throughput scheduling, all users get similar average user throughput as shown in Figure 5.6. If $E\{n_{\text{active}}\}$ is too high, the average user throughput of many users in the network will drop below the required throughput and p_{out} increases fast. Using proportional fair scheduling, the average user throughput of users with an SIR due to large-scale propagation loss below a certain threshold SIR drops below the required throughput first. Therefore, the increase in p_{out} with increasing $E\{n_{\text{active}}\}$ is smaller with proportional fair scheduling than with fair throughput scheduling.

Comparing the results obtained analytically with simulation results of ONe-PS, it can be seen that the outage probability calculated analytically and obtained by ONe-PS fit well for fair resource scheduling. Using proportional fair scheduling the analytical methodology gives a lower outage probability for $E\{n_{\text{active}}\} > 5$. The analytical methodology derives the average user throughput $\bar{r}_{\text{user}}^{(i)}$ of user i depending on the SIR $\gamma_{\text{ls,dB}}^{(i)}$ due to large-scale propagation loss of the user as depicted in Figure 5.6 and determines which $\gamma_{\text{ls,dB}}^{(i)}$ is required to achieve $\bar{r}_{\text{user}}^{(i)}$ greater than the required throughput. The outage probability is given by the ratio of the area with $\gamma_{\text{ls,dB}}^{(i)}$ below the value that is necessary to achieve $\bar{r}_{\text{user}}^{(i)}$ greater than the required throughput and the total investigated area. This seems to lead to too optimistic values due to not considering that the average throughput achieved during the session of a specific user can also be lower than $\bar{r}_{\text{user}}^{(i)}$ which is an average value of all users with $\gamma_{\text{ls,dB}}^{(i)}$. The analytical results obtained for fair throughput scheduling match the simulation results closely up to 20 average active users. For a higher number of active users the increase in unsatisfied users is smaller for the analytical results as for the simulation results. Results in

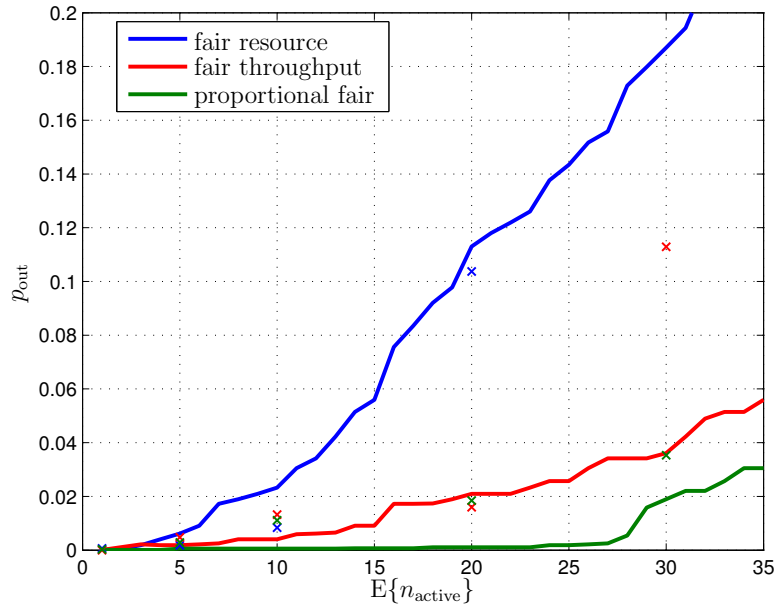


Figure 5.9. Outage probability as function of the average number of active users with different scheduling algorithms as parameter for $r_{\text{serv}} = 100$ kbit/s and download traffic, solid lines: analytical results, markers: simulation results

Section 5.4.2 have already shown that $\bar{r}_{\text{user}}^{(i)}$ achieved with the analytical methodology is too optimistic compared with simulation results. Thus, the number of unsatisfied users obtained with the analytical methodology is lower than obtained with simulations leading to too optimistic results in terms of outage probability for the analytical methodology.

5.4.5 Rules for the impact of user scheduling on the network capacity

This section presents some rules describing KPIs depending on scheduling and the average number of active users. These rules can be used in the network planning process to derive the capacity of cells. The rules are derived based on the results presented in the previous sections but it should be noted that a specific KPI as function of a specific parameter, e.g., the average cell throughput depending on the scheduling algorithm, can be achieved within a few seconds using the proposed analytical evaluation methodology. Thus, results for different scenarios can be obtained very fast. Download traffic and a server data rate of $r_{\text{server}} = 100$ kbit/s have been assumed for the results that are used

to derive the following rules. The impact due to other traffic models or server data rates has been shown in Section 5.3.

1. The average user throughput $\bar{r}_{\text{user}}^{(i)}$ of user i achieved with proportional fair scheduling is higher than achieved with fair resource scheduling. $\bar{r}_{\text{user}}^{(i)}$ achieved with fair throughput scheduling is higher compared to fair resource scheduling for user i with low SIR $\gamma_{\text{ls,dB}}^{(i)}$ due to large-scale propagation loss. $\bar{r}_{\text{user}}^{(i)}$ achieved with fair throughput scheduling is lower compared to fair resource scheduling for user i with medium and high SIR $\gamma_{\text{ls,dB}}^{(i)}$ due to large-scale propagation loss.
2. All users with $\gamma_{\text{ls,dB}}^{(i)}$ higher than a threshold SIR achieve similar $\bar{r}_{\text{user}}^{(i)}$ if fair throughput scheduling is used. The threshold SIR describes the minimum SIR that is required to establish a reliable transmission with the most robust modulation and coding scheme.
3. The user throughput $E\{\bar{r}_{\text{user}}^{(i)}\}$ averaged over all users in the cell is higher if proportional fair scheduling is assumed than if fair resource scheduling is assumed. The difference in $E\{\bar{r}_{\text{user}}^{(i)}\}$ achieved with proportional fair scheduling and fair resource scheduling is constant for all average numbers of active users $E\{n_{\text{active}}\} > 10$.
4. If $E\{n_{\text{active}}\}$ is increased, $E\{\bar{r}_{\text{user}}^{(i)}\}$ decreases much faster if fair throughput scheduling is assumed than if fair resource scheduling is assumed.
5. Different scheduling algorithms lead to similar average cell throughput $E\{r_{\text{cell}}\}$ results as long as $E\{n_{\text{active}}\}$ is low and the available resource units are not fully utilised.
6. Proportional fair scheduling leads to higher $E\{r_{\text{cell}}\}$ than fair resource scheduling if all available resource units are allocated.
7. $E\{r_{\text{cell}}\}$ saturates for $E\{n_{\text{active}}\} > 10$ if fair throughput scheduling is used. The cell performance is limited by users located at the cell border and $E\{r_{\text{cell}}\}$ achieved with fair throughput scheduling is much lower than achieved with fair resource scheduling.
8. The outage probability p_{out} of the network increases almost linearly with $E\{n_{\text{active}}\}$ assuming fair resource scheduling. p_{out} is smaller for equal $E\{n_{\text{active}}\}$ if fair throughput or proportional fair scheduling is assumed than if fair resource scheduling is assumed.

9. Fair throughput and proportional fair scheduling achieve similar p_{out} for $E\{n_{\text{active}}\} < 20$. However, p_{out} is higher if fair throughput scheduling is assumed than if proportional fair scheduling is assumed if $E\{n_{\text{active}}\}$ increases to more than 20 users.

5.5 Real world scenarios

This section is intended to show how the analytical system level evaluation methodology can be applied in the network planning process by providing results of KPIs of the cellular wireless network within only a few seconds needed to execute the calculations. Scenarios that have to be considered in the network planning process reflect real world scenarios where BS locations are given due to the environmental conditions and the user distribution. Users are distributed inhomogeneous in the network. Areas with high user density, e.g., city or shopping centres, as well as low user density, e.g., forests can be observed. Different large-scale propagation loss models have to be used, e.g., for areas with many buildings or parks. A map can be created indicating the large-scale propagation loss at each point in the investigated area, e.g., based on measurements that are performed. Together with a map indicating the probability that a user arrives in the network at a specific location, the large-scale propagation loss map is used to determine KPIs of the network.

In the following, real world scenarios provided by the IST MOMENTUM project are used, which provide BS locations, large-scale propagation loss and user location maps for different European cities, i.e., Berlin, Den Hague and Lisbon [MOM03a]. For the following investigations, download traffic is assumed for all users as described in the previous sections and the server data rate is $r_{\text{server}} = 100$ kbit/s. The average number of active users $E\{n_{\text{active}}\}$ per BS depends on the city that is considered. The Berlin scenario consists of 193 BSs and $E\{n_{\text{active}}\} = 12.0$, the Hague scenario consists of 36 BSs with $E\{n_{\text{active}}\} = 18.7$ and the Lisbon scenario consists of 164 BSs with $E\{n_{\text{active}}\} = 17.3$. Assuming an interference limited network so that additional noise can be omitted, the SIR $\gamma_{\text{ls,dB}}$ due to large-scale propagation loss is calculated using the propagation loss model provided by the scenario data. It is assumed that all BSs can utilise the whole frequency bandwidth leading to a frequency reuse of one.

Figure 5.10 shows $\gamma_{\text{ls,dB}}$ of the users plotted over the investigation area assuming that all BSs transmit with equal transmit power for the Berlin scenario. BS locations are marked with black circles. Every user position obtained from the user distribution data is marked with a coloured dot in Figure 5.10. The colour of the dot represents $\gamma_{\text{ls,dB}}$

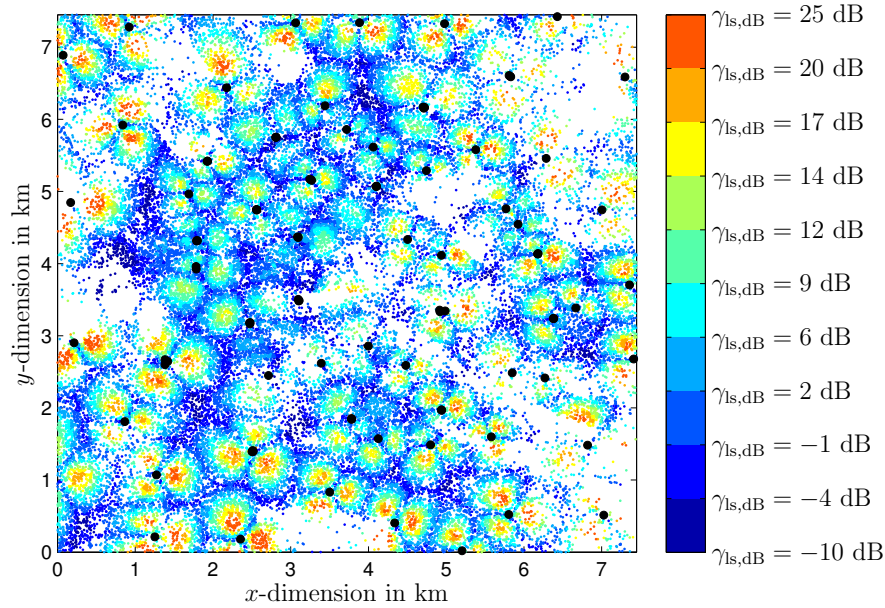


Figure 5.10. SIR due to large-scale propagation loss as colour code for the IST MOMENTUM Berlin scenario

of the user at this position where dark-blue dots represent $\gamma_{ls,dB} < -4$ dB and orange dots represent $\gamma_{ls,dB} > 17$ dB. White areas do not contain any users due to the scenario data. It can be seen that BSs contain transmit antennas with directional radio pattern so that each BS only serves users in a sector and $\gamma_{ls,dB}$ depends, e.g., on tilt values of the antennas provided by the scenario data. The map is used to calculate the pdf of $\gamma_{ls,dB}$ as explained in Chapter 4. Similar maps are obtained also for the Hague and Lisbon scenario. The same system as described in Section 5.1 is used and a parameter overview is given in Table 5.1 the hexagonal cells are replaced by the scenario data described by the IST MOMENTUM project. The large-scale propagation loss including gain due to a directional antenna pattern is described in the scenario data and one large-scale propagation loss value to each BS is obtained for each location in the network using the scenario data.

In the following, user, cell and network performance results are presented. Figure 5.11 shows the user throughput $\bar{r}_{user}^{(i)}$ of user i averaged over the session duration that can be achieved if user i is located at a certain position within the network for the Berlin scenario. Results are given for three different scheduling strategies using the analytical system level evaluation methodology. Again each user position is represented by a coloured dot and the colour of the dot represents $\bar{r}_{user}^{(i)}$ that can be achieved user i at that location. It can be seen that it is expected that user i will achieve $\bar{r}_{user}^{(i)} \geq r_{serv}$

when using fair resource scheduling in large areas. However, there are also areas where users will achieve $\bar{r}_{\text{user}}^{(i)}$ in the order or even below 10 % of r_{serv} , i.e. 10 kbit/s, e.g., around coordinates at 2 km in x- and y-direction. Using proportional fair scheduling instead of fair resource scheduling increases $\bar{r}_{\text{user}}^{(i)}$ over the whole area. Larger areas are expected to achieve $\bar{r}_{\text{user}}^{(i)} \geq r_{\text{serv}}$. Furthermore, areas with expected $\bar{r}_{\text{user}}^{(i)}$ around 50 kbit/s for fair resource will increase $\bar{r}_{\text{user}}^{(i)}$ to more than 70 kbit/s as seen for coordinates at 1.5 km in x-direction and 4 km in y-direction.

Finally, results for fair throughput scheduling are shown in Figure 5.11(c). It can be seen that almost every user is expected to achieve $\bar{r}_{\text{user}}^{(i)}$ in the interval between 40 and 60 kbit/s. Compared with fair resource scheduling and proportional fair scheduling, it is observed that $\bar{r}_{\text{user}}^{(i)} = r_{\text{serv}}$ is no longer achieved but the fairness between the users is higher and only small areas will achieve low $\bar{r}_{\text{user}}^{(i)}$ in the order of 10 kbit/s compared to fair resource scheduling.

Results for the cell and network performance are presented in Table 5.2. Table 5.2 shows the average cell throughput $E\{r_{\text{cell}}\}$ and the outage probability p_{out} for the IST MOMENTUM scenarios with different scheduling algorithms as parameter. It can be seen that different $E\{r_{\text{cell}}\}$ and p_{out} are achieved for the different scenarios due to different average number of active users per BS and different pdfs of $\gamma_{\text{ls,dB}}$. Comparing the results obtained for the different scheduling algorithms, it can be seen that proportional fair scheduling improves $E\{r_{\text{cell}}\}$ compared to fair resource scheduling by 20 to 40 %. The relative increase assuming the Berlin scenario is smaller than the increase assuming the Hague scenario due to a smaller average number of active users in the Berlin scenario than in the Hague scenario. $E\{r_{\text{cell}}\}$ achieved with fair throughput scheduling is approximately 50 % of $E\{r_{\text{cell}}\}$ achieved with fair resource scheduling.

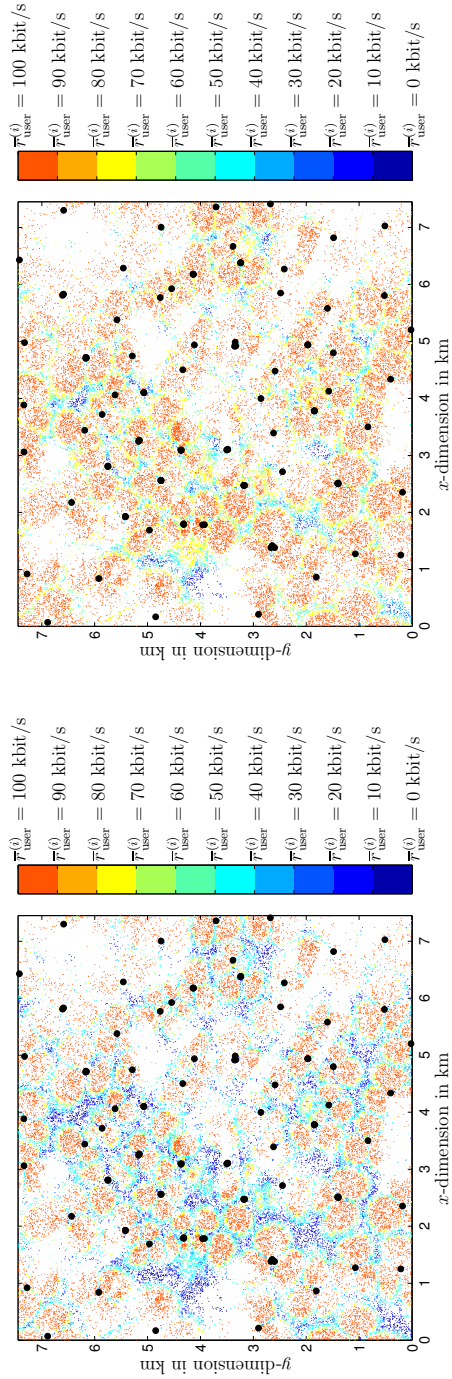
The outage probability p_{out} indicating the network performance is also depicted in Table 5.2 for the IST MOMENTUM scenarios with different scheduling algorithms as parameter. It can be seen that p_{out} is between 0.03 and 0.1. A low p_{out} in the Berlin

Table 5.2. Cell and network performance for the IST MOMENTUM scenarios with different scheduling algorithms as parameter

Scenario	Fair resource		Proportional fair		Fair throughput	
	$E\{r_{\text{cell}}\}$ in kbit/s	p_{out}	$E\{r_{\text{cell}}\}$ in kbit/s	p_{out}	$E\{r_{\text{cell}}\}$ in kbit/s	p_{out}
Berlin scenario	861.1	0.036	1038.7	0.004	435.8	0.013
Hague scenario	761.9	0.098	1081.0	0.001	377.2	0.019
Lisbon scenario	1024.0	0.031	1314.3	0.001	509.0	0.005

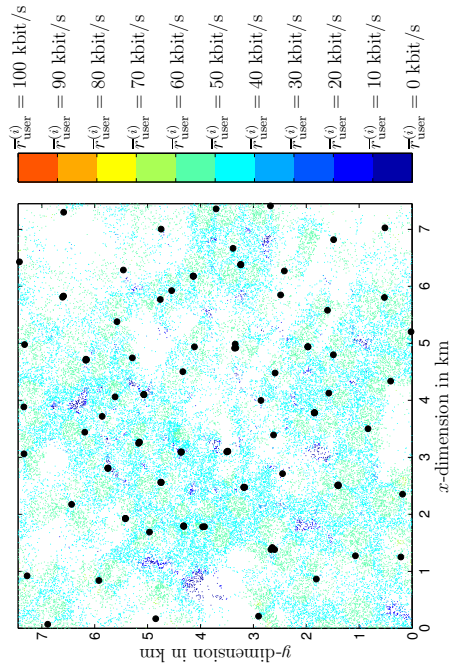
scenario due to a small average number of active users per cell and in the Lisbon scenario where $\gamma_{\text{ls,dB}}$ is higher than in the other two scenarios. Similar to the results achieved in Section 5.4, p_{out} can be improved compared to fair resource scheduling using fair throughput or proportional fair scheduling.

The scenarios provided in the IST MOMENTUM project can also be investigated using in the snapshot based system level simulation methodology described in Chapter 3. The large-scale propagation loss map is used to determine the large-scale propagation loss when generating the user pool. However, simulations for the IST MOMENTUM scenarios are not performed due to the long simulation duration and the memory demand to simulate scenarios with almost 200 BSs. The performance of the analytical evaluation methodology compared to simulation results has been shown in Section 5.3 and Section 5.4. The analytical evaluation methodology provides user, cell and network performance results within only a few seconds calculation time. The results presented in this section for the IST MOMENTUM scenarios take less than 10 s using a conventional personal computer. Using the analytical evaluation methodology during the network planning process, areas can easily identified where user throughput requirements are not fulfilled as shown in Figure 5.11 within only a few seconds calculation duration even if scenarios with hundreds of BSs are considered.



(a) Fair resource scheduling

(b) Proportional fair scheduling



(c) Fair throughput scheduling

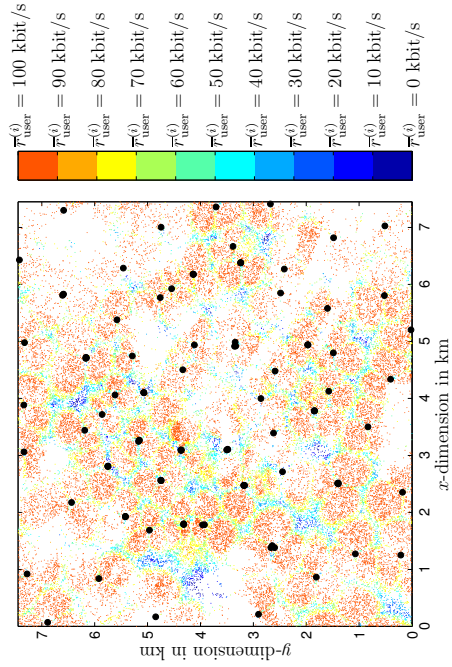


Figure 5.11. Average user throughput as colour code for the IST MOMENTUM Berlin reference scenario

Chapter 6

Conclusions

This thesis deals with the performance evaluation of OFDMA based packet-switched wireless networks. Accurate results of KPIs are required for planning of packet-switched wireless networks that are usually obtained using system level simulations. Two novel methodologies have been derived in this thesis to determine KPIs in OFDMA based packet-switched wireless networks like WiMAX or LTE whose deployment currently started. The first proposed methodology is a system level simulation methodology that provides results with similar accuracy as state-of-the-art dynamic system level simulations. The developed system level simulation methodology has lower computational complexity than state-of-the-art system level simulations so that results are achieved faster. Another system level evaluation methodology has been proposed that achieves KPI results even faster than the first methodology due to using analytical derivations to determine KPIs. The analytical system level evaluation methodology considers all issues of packet-switched wireless networks including, e.g., data traffic and user scheduling to be applicable in the network planning process.

A framework has been developed in Chapter 1 that summarises aspects that have to be considered for performance evaluation of OFDMA based packet-switched wireless networks. The framework has been designed in a very general way considering the user placement including large-scale propagation loss, the generation of data traffic and the frame setup including small-scale propagation loss. All three aspects have impact on the scheduling decision, which finally results into measurements for KPIs.

Based on the derived framework and limitations or disadvantages of state-of-the-art system level simulators, a novel system level simulation methodology has been developed in Chapter 3. State-of-the-art system level simulators either achieve inaccurate KPI measurements due to limiting assumptions that are made during simulation like no user movement, averaging the influence of small-scale fading or a full buffer traffic model where always data is available for transmission as in static system level simulations or they suffer from high computational complexity due to, e.g., the modelling of data traffic, small-scale fading and the user scheduling in detail as in dynamic system level simulations. The developed system level simulation methodology provides results of KPIs showing similar accuracy as with state-of-the-art dynamic system level simulations but decreases the computational complexity by a factor of three to four. The improvement in computational complexity is achieved by considering short snapshots

of the busy hour that are independent of each other. Due to the short duration of one snapshot, the user location does not vary during one snapshot although mobile users are assumed. The location of each user and the large-scale propagation loss can be derived in advance of the simulation. During each snapshot, aspects like data traffic, the frame setup, small-scale propagation loss and the user scheduling have been considered in detail. To generate snapshots that are randomly taken from the busy hour, random variables have been defined for constraints, e.g., the number of active users or the buffer occupancy at the beginning of the snapshot. Furthermore, a novel calculation of the effective SIR that represents the performance, e.g., in terms of BLEP of a resource unit containing several subcarriers and consecutive OFDM symbols has been described. The effective SIR has been derived by calculating the pdf of the channel transfer factors in frequency domain and deriving the average mutual information using three samples of the pdf of the channel transfer factors. For the calculation of the pdf of the channel transfer factors only a fraction of the available subcarriers has been used.

An analytical derivation of KPIs like the blocking probability in circuit-switched networks using the Erlang B formula has not been available for packet-switched wireless networks considering all effects including, e.g. data traffic and user scheduling. Based on the developed framework for KPI measurements, an analytical system level evaluation methodology has been derived that describes relationships in OFDMA based packet-switched networks analytically so that results are available very fast. Derivations have been given for pdfs of the random variables indicating for instance the number of active users at a random time instant, the interference power at a randomly chosen receiver, the average number of resource units that are allocated to one user or the gain in SIR that is achieved due to user scheduling considering, e.g., channel state information compared to a random user scheduling. With the derived pdfs of the random variables, KPIs like user throughput, cell throughput and the probability that a user does not achieve the QoS requirement during the transmission have been calculated analytically and results can be achieved within seconds even for large networks with many BSs and users.

The snapshot based system level simulation methodology has been evaluated using an exemplary packet-switched wireless network. The methodology has been designed so that a short simulation duration is obtained while still KPI results are achieved with comparable accuracy as with state-of-the-art dynamic system level simulations. The simulation duration has been reduced by a factor of three to four comparing the novel system level simulation methodology with state-of-the-art dynamic system level simulations, i.e., simulations last several hours up to one day instead of days using a state-of-the-art personal computer.

The analytical evaluation methodology has been evaluated using an exemplary packet-switched wireless network. Due to the usage of analytical derivations, results for KPIs can be achieved within seconds even for large wireless networks. A comparison with results achieved with the snapshot based system level simulation methodology has been shown that results for KPIs can be achieved with the analytical evaluation methodology with an error less than 10 % for several different scenarios.

The novel snapshot based system level simulation methodology and the analytical evaluation methodology are used to evaluate the impact of data traffic and user scheduling on KPIs indicating user, cell and network performance. It has been shown how the average number of active users and the server data rate have impact on the user and cell throughput as well as on the outage probability. For instance, it has been shown, that the ratio between the average number of active users and the server data rate roughly is constant for a specific outage probability. Furthermore, the impact of user scheduling has been evaluated using three widely used scheduling algorithms. It has been shown that a proportional fair user scheduling leads to a gain of roughly 15 kbits/s compared to a random user scheduling for different average number of active users for the assumed network. Furthermore, it has been shown for a special network scenario that fair throughput user scheduling leads to a constant average cell throughput for more than 15 average active users while with a random user scheduling the average cell throughput increases until 30 average active users and proportional fair scheduling has not reached the maximum average cell throughput for even 35 average active users. Furthermore, the methodologies can be applied in the network planning process where real world scenarios have to be considered. Results for a public real world scenario from the IST MOMENTUM project have been obtained using the analytical evaluation methodology.

In summary, a snapshot based system level simulation methodology has been proposed that achieves KPI results as accurate as state-of-the-art system level simulations and reduce the computational complexity by a factor of three to four, i.e., achieves results within several hours to one day using a standard personal computer. Furthermore, an analytical evaluation methodology is derived for OFDMA based packet-switched wireless networks that is able to obtain KPI results within seconds. The error of the calculated KPIs is below 15 % for many different scenarios. Hence, both methodologies are able to improve the planning of OFDMA based packet-switched wireless networks by providing accurate and fast KPIs.

Appendix

A.1 Numerical solution of the mutual information formula

In the following, a numerical solution for the mutual information formula given by (3.30) is presented. The mutual information has been used in Section 3.4 to calculate the effective SIR for a resource unit. In general, the mutual information between the channel input X in terms of equally distributed constellation points and the corresponding channel output $Y = X + N$ is calculated assuming an Additive White Gaussian Noise (AWGN) channel [CT91]. N is a Gaussian noise process with variance σ_n^2 . This assumption is justified as long as the interference for one frequency sample can be assumed Gaussian distributed. Therefore, the fading channel is approximated as piece-wise AWGN channel [ADSK03]. It is shown in [tBKA04] that the mutual information between channel input and channel output can be calculated analytically if Binary Phase Shift Keying (BPSK) or QPSK is assumed. For higher order modulation schemes as well as other constellations like QAM, the calculation of the mutual information becomes intractable. Thus, the application of a Monte Carlo method for obtaining the mutual information [HtB03] is well suited. In the following, the mutual information as function of the SIR is derived for different modulation schemes.

With $H(\cdot) = -E\{\log_2(P(\cdot))\}$ the entropy function, the mutual information may be expressed in the form

$$I(X; Y) = H(Y) - H(Y|X). \quad (\text{A.1})$$

Assuming a complex AWGN channel [Pro01], $H(Y|X) = H(Z)$, which corresponds to the entropy of a Gaussian variable $Z \sim N(0, \sigma_n^2)$. The entropy then results in:

$$\begin{aligned} H(Z) &= -E \left\{ \log_2 \left(\frac{1}{\sqrt{\pi\sigma_n^2}} \exp \left(\frac{-Z^2}{\sigma_n^2} \right) \right) \right\} \\ &= -E \left\{ -\frac{Z^2}{\sigma_n^2} \log_2(\exp(1)) - \log_2(\sqrt{\pi\sigma_n^2}) \right\} \\ &= \frac{E\{Z^2\}}{\sigma_n^2} \log_2(\exp(1)) + \log_2(\sqrt{\pi\sigma_n^2}) \\ &= \log_2(\exp(1)\sqrt{\pi\sigma_n^2}) \end{aligned} \quad (\text{A.2})$$

which is valid for any symbol constellation.

In order to calculate $H(Y)$, it is necessary to know the probability density of the output signal. Assuming signalling where constellations occur with equal probability, and recalling that the difference between the output and input signals results in a Gaussian distributed random variable, the probability density of the output signal may be expressed as

$$P(Y) = \sum_{i=1}^M P(Y|X_i) P(X_i) = \frac{1}{M} \sum_{i=1}^M \frac{1}{\sqrt{\pi\sigma_n^2}} \exp\left(-\frac{|Y - X_i|^2}{\sigma_n^2}\right) \quad (\text{A.3})$$

where X_i corresponds to each symbol of the M -sized constellation.

The expectation contained within the entropy $H(Y) = -E\{\log_2(P(Y))\}$ may be approximated by generating a reasonably large number of iid samples of the output Y_1, Y_2, \dots, Y_N , and then calculating the average value as

$$\begin{aligned} \hat{H}(Y) &= -\frac{1}{N} \sum_{j=1}^N \log_2(P(Y_j)) \\ &= -\frac{1}{N} \sum_{j=1}^N \log_2\left(\frac{1}{M} \sum_{i=1}^M \frac{1}{\sqrt{\pi\sigma_n^2}} \exp\left(-\frac{|Y_j - X_i|^2}{\sigma_n^2}\right)\right). \end{aligned} \quad (\text{A.4})$$

The mutual information expression is finally given as

$$\begin{aligned} I(X; Y) &\approx \hat{H}(Y) - H(Z) \\ &= -\frac{1}{N} \sum_{j=1}^N \log_2\left(\frac{1}{M} \sum_{i=1}^M \frac{1}{\sqrt{\pi\sigma_n^2}} \exp\left(-\frac{|Y_j - X_i|^2}{\sigma_n^2}\right)\right) - \dots \\ &\quad \log_2(\exp(1)\sqrt{\pi\sigma_n^2}). \end{aligned} \quad (\text{A.5})$$

It should be noted that for QAM, since differently from Phase Shift Keying (PSK) the symbols do not have the same energy, the spacing among the constellation elements for each simulated SIR has to be determined based on the average energy per symbol, i.e., $E_{\text{avg}} = \frac{1}{M} \sum_{i=1}^M d_i^2$, where d_i corresponds to the distance of each symbol to the origin.

Figure A.1 shows the mutual information as function of the effective SIR $\bar{\gamma}_{\text{ru}}$ for the resource unit for QPSK and QAM constellations in an AWGN channel. The results are obtained by employing the Monte Carlo methodology, assuming 100.000 iid output samples. It can be seen that the mutual information increases with increasing $\bar{\gamma}_{\text{ru}}$ for all modulation schemes. At a certain SIR threshold, e.g., approximately 10 dB for QPSK modulation, the maximum mutual information is achieved, i.e., 2 bits per channel usage for QPSK modulation and no further increase of the mutual information is possible. The results of Figure A.1 are used in this work via lookup tables to derive the effective SIR of the resource unit as depicted in Section 3.4 and the the small-scale fading model of the analytical evaluation methodology as depicted in Section 4.5.2.2.

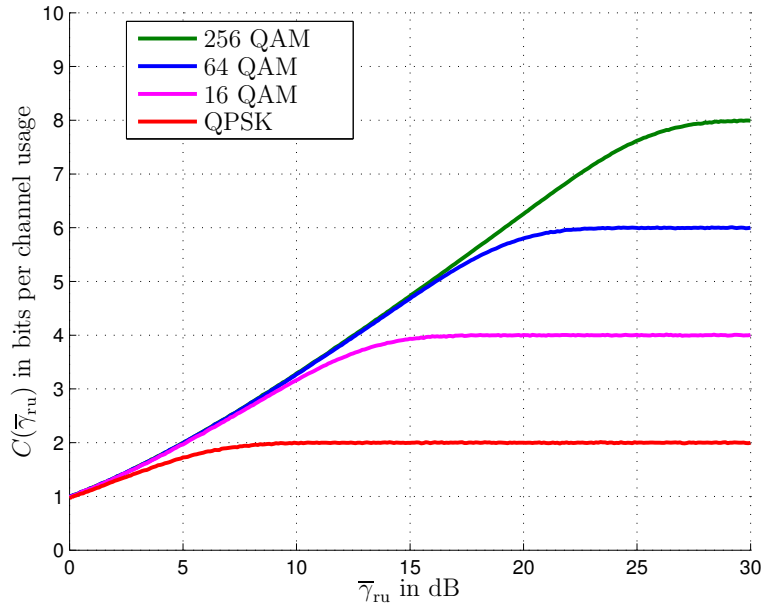


Figure A.1. Mutual information as function of the effective SIR with different modulation schemes as parameter

A.2 Derivation of state transition probabilities in an $M/M/\infty$ queueing system

In the following, the transient behaviour of an $M/M/\infty$ queueing system as it is assumed for data traffic with exponentially distributed session duration is analysed and the probabilities of state transitions given by (4.11) are derived. As described in Section 3.3, the queueing system is in state k if k users are active. With an average arrival rate of $\lambda_k = \lambda$ the system changes from state k to $k + 1$ and with the average session ending rate $\mu_k = k \cdot \mu$ the system changes from state k to $k - 1$. λ and μ have been defined in Section 3.3 as λ_{speech} and μ_{speech} , respectively. The arrival rate λ is independent of the state of the system due to the Poisson process which is a memoryless process. The session ending rate μ_k depends on the state k of the system. If a high number of sessions are active, the probability that one of the sessions ends is higher than if a low number of sessions are active. The following derivations are based on an approach proposed in [Kle75]. The derivation is an extension to the transient analysis presented in [GH74].

The two differential-difference equations of the assumed system considering that $P_k(t)$

is the probability that the system is in state k at time instant t are given by

$$\frac{dP_k(t)}{dt} = -(\lambda + k \cdot \mu)P_k(t) + \lambda P_{k-1}(t) + (k+1) \cdot \mu P_{k+1}(t) \quad \text{for } k \geq 1 \quad (\text{A.6})$$

$$\frac{dP_0(t)}{dt} = -\lambda P_0(t) + \mu P_1(t) \quad \text{for } k = 0, \quad (\text{A.7})$$

[GH74, Kle75].

These equations describe that the system is in state k at time instant t if it already was in state k at time instant $t - dt$ and no state transition occurred or it was in state $k - 1$ and an arrival happened or it was in state $k + 1$ and a session end happened. If dt is small enough, maximal one state transition occurs during the time interval dt .

It is assumed that the system is in state K at time instant $t = 0$ so that the initial condition of the system is described by

$$P_k(0) = \begin{cases} 1 & \text{for } k = K \\ 0 & \text{else.} \end{cases} \quad (\text{A.8})$$

As described in [GH74, Kle75], the generating function of the transient probabilities is defined by

$$P(z, t) \triangleq \sum_{k=0}^{\infty} P_k(t) \cdot z^k \quad (\text{A.9})$$

as the Z-Transform of $P_k(t)$.

Multiplying each k th summand in (A.6) with z^k and summing up all equations with $k > 0$ [Kle75] leads to

$$\sum_{k=1}^{\infty} \frac{dP_k(t)}{dt} z^k = \sum_{k=1}^{\infty} -(\lambda + k\mu)P_k(t)z^k + \sum_{k=1}^{\infty} \lambda P_{k-1}(t)z^k + \sum_{k=1}^{\infty} (k+1)\mu P_{k+1}(t)z^k. \quad (\text{A.10})$$

On the left hand side of (A.10), the derivation and the sum can be swapped as

$$\begin{aligned} \sum_{k=1}^{\infty} \frac{dP_k(t)}{dt} z^k &= \frac{d \sum_{k=1}^{\infty} P_k(t) z^k}{dt} \\ &= \frac{d}{dt} [P(z, t) - P_0(t)]. \end{aligned} \quad (\text{A.11})$$

Using (A.11) and (A.9), (A.10) can be written as

$$\begin{aligned} \frac{d}{dt} [P(z, t) - P_0(t)] &= -\lambda (P(z, t) - P_0(t)) - \mu \sum_{k=1}^{\infty} k P_k(t) z^k + \dots \\ &\quad \lambda z P(z, t) + \frac{\mu}{z} \sum_{k=2}^{\infty} k P_k(t) z^k. \end{aligned} \quad (\text{A.12})$$

The equation can be further transformed using (A.7) and (A.9):

$$\begin{aligned} \frac{dP(z, t)}{dt} + \lambda P_0(t) - \mu P_1(t) &= -\lambda (P(z, t) - P_0(t)) + \lambda z P(z, t) + \dots \\ &\quad \left(-\mu + \frac{\mu}{z}\right) \sum_{k=0}^{\infty} k P_k(t) z^k - \mu z P_1(t) \end{aligned} \quad (\text{A.13})$$

leading to

$$\frac{dP(z, t)}{dt} = -\lambda P(z, t) + \lambda z P(z, t) + (-\mu z + \mu) \frac{dP(z, t)}{dz}. \quad (\text{A.14})$$

This represents a planar differential equation [BBE64] given by

$$\frac{dP(z, t)}{dt} + \mu(z - 1) \frac{dP(z, t)}{dz} = \lambda(z - 1)P(z, t). \quad (\text{A.15})$$

which can be solved using the following expression:

$$\frac{dt}{1} = \frac{dz}{\mu(z - 1)} = \frac{dP(z, t)}{\lambda(z - 1)P(z, t)}. \quad (\text{A.16})$$

As shown in [GH74] the solution for $P(z, t)$ using (A.15) is given by

$$P(z, t) = \exp\left(\frac{\lambda}{\mu}z\right) \cdot g((1 - z)\exp(-\mu t)). \quad (\text{A.17})$$

To determine $g((z - 1)\exp(-\mu t))$, the initial condition given by (A.8) is used. Applying (A.8) to (A.7) leads to

$$P(z, 0) = \sum_{k=0}^{\infty} P_k(0)z^k = z^K \quad (\text{A.18})$$

so that

$$g(1 - \tilde{z}) = \tilde{z}^K \exp\left(-\frac{\lambda}{\mu}\tilde{z}\right) \quad (\text{A.19})$$

and

$$\begin{aligned} g((z - 1)\exp(-\mu t)) &= (1 - ((z - 1)\exp(-\mu t)))^K \dots \\ &\quad \exp\left(-\frac{\lambda}{\mu}((1 - z)\exp(-\mu t) + 1)\right). \end{aligned} \quad (\text{A.20})$$

Finally, $P(z, t)$ is then given by

$$P(z, t) = (1 + ((z - 1)\exp(-\mu t)))^K \cdot \exp\left(\frac{\lambda}{\mu}(z - 1)(1 - \exp(-\mu t))\right) \quad (\text{A.21})$$

and $P_k(t)$ is obtained by expanding (A.21) in a power series $\sum_{k=0}^{\infty} a_k z^k$. The coefficients a_k represents the probability $P_k(t)$ that the system is in state k at time instant t . This can be achieved by a Taylor series expansion for $z = 0$ as

$$P_k(t) = \frac{1}{k!} \left. \frac{d^k P(z, t)}{dz^k} \right|_{z=0}, \quad (\text{A.22})$$

[GH74].

For arbitrary initial conditions, $P_k(t)$ results into

$$P_k(t) = \sum_{j=0}^{\min\{K, k\}} j (\exp(-\mu t))^{\min\{k, j\}} \max \left\{ \binom{K}{j}, 1 \right\} (1 - \exp(-\mu t))^{\min\{K-j, 0\}} \dots$$

$$\left(\frac{\lambda}{\mu} \right)^{k-j} (1 - \exp(-\mu t))^{k-j} \exp \left(\frac{\lambda}{\mu} (1 - \exp(-\mu t)) \right). \quad (\text{A.23})$$

List of Acronyms

3GPP	3 rd Generation Partnership Project
AWGN	Additive White Gaussian Noise
BLEP	block error probability
BPSK	Binary Phase Shift Keying
BS	base station
cdf	cumulative distribution function
CDMA	Code Division Multiple Access
COST	European Cooperation in the Field of Scientific and Technical Research
dB	decibel
DFT	Discrete Fourier Transform
EDGE	Enhanced Data rates in GSM Evolution
FFT	Fast Fourier Transform
FUSC	Full Usage of Subchannels
FTP	File Transfer Protocol
GPRS	General Packet Radio Service
GSM	Global System for Mobile Communications
http	Hypertext Transfer Protocol
IEEE	Institute of Electrical and Electronic Engineers
iid	independent and identically distributed
IP	Internet Protocol
ISO	International Organization for Standardization
IST	Information Society Technology
ITU	International Telecommunication Union

KPI	key performance indicator
LTE	Long Term Evolution
MOMENTUM	Models and Simulation for Networkplanning and Control of UMTS
MSE	mean squared error
NLOS	non-line of sight
OFDM	Orthogonal Frequency Division Multiplexing
OFDMA	Orthogonal Frequency Division Multiple Access
ONe-PS	OFDMA Network Performance Simulator
OSI	Open Systems Interconnection
pdf	probability density function
PSK	Phase Shift Keying
PUSC	Partial Usage of Subchannels
QAM	Quadrature Amplitude Modulation
QoS	Quality of Service
QPSK	Quadrature Phase Shift Keying
RTP	Real-time Transport Protocol
SNR	signal to noise ratio
SIG	Special Interest Group
SINR	signal to interference plus noise ratio
SIR	signal to interference ratio
SMS	Short Message Service
TCP	Transmission Control Protocol
TDMA	Time Division Multiple Access
UDP	User Datagram Protocol
UMTS	Universal Mobile Telecommunications System

VoIP	Voice over IP
WiMAX	Worldwide Interoperability for Microwave Access
WINNER	Wireless World Initiative New Radio
WLAN	Wireless Local Area Network

List of Symbols

a	Significance level of the χ^2 -test
$\tilde{\alpha}_{\text{eff}}$	Gain in SIR due to scheduling
$\alpha_{\text{ls,dB}}$	Large-scale propagation loss in dB
$\alpha_{\text{ls},i,k}$	Large-scale propagation loss between BS k and user i
$\arg \max_i \{f_i\}$	Returns the value i that maximizes f_i
D_{sts}	Site-to-site distance
d_{res}	Random variable for the number of bits transmitted per resource unit
$d_{\text{user}}^{(i)}$	Number of bits transmitted to user i
$\delta(x)$	Dirac distribution of x
$E\{r_{\text{cell}}\}$	Average cell throughput average over all cells
$E\{\bar{r}_{\text{user}}^{(i)}\}$	Average user throughput averaged over all users
$E\{x\}$	Expectation value of x
$\epsilon(t, f_k)$	Mutual information at time t for subcarrier k with center frequency f_k
$\text{erf}(x)$	Error function of x
$\text{erfc}(x)$	Complementary error function of x
$\exp(x)$	Exponential function of x
$f_x(x)$	pdf of x
f_{ru}	Separation in frequency domain of two resource units
f_{sc}	Subcarrier frequency spacing
$\gamma(t, f_k)$	SIR at time t for subcarrier k with center frequency f_k
$\tilde{\gamma}_{\text{eff}}$	Random variable for the post scheduling SIR including large-scale propagation loss, small-scale fading and scheduling
γ_{ff}	Random variable for the SIR including large-scale propagation loss and small-scale fading
$\gamma_{\text{ls,dB}}$	Random variable for the SIR due to large-scale propagation loss assuming that all BSs transmit with equal transmit power
$\bar{\gamma}_{\text{ru}}$	Effective SIR of the resource unit
λ_{dl}	Average arrival rate of download users
λ_{speech}	Average arrival rate of speech users
λ_{wb}	Average arrival rate of web browsing users
$\log_a(x)$	Logarithm of x to the basis a
$\max\{a, b\}$	Maximum value of a and b
$\min\{a, b\}$	Minimum value of a and b

\bar{n}_{act}	Random variable for the average number of active users during the session duration of one investigated user
n_{active}	Random variable for the number of active users at an arbitrary time instant
n_{alloc}	Random variable for the number of resource units per second allocated to one user
N_{BS}	Number of BSs
N_{PC}	Random variable for the number of packet calls for web browsing traffic
N_{sc}	Number of subcarriers in one resource unit
$n_{\text{ses,wb}}$	Random variable for the number of active web browsing sessions
N_{sym}	number of OFDMA symbols in one resource unit
$P(x y)$	Probability for x under the condition y
p_{out}	Outage probability
$r_{\text{cell}}^{(k)}$	Average cell throughput of cell k
r_{req}	Required user throughput
r_{serv}	Server data rate
$\bar{r}_{\text{user}}^{(i)}$	Average user throughput of user i
$S_{\text{buffer}}^{(i)}$	Random variable for the buffer level of user i at the beginning of the snapshot
$S_{\text{f,dl}}$	Random variable for the file size of download traffic
S_{pc}	Random variable for the file size of one packet call for web browsing traffic
T_{RT}	Random variable for the reading time duration for web browsing traffic
T_{ru}	Time duration of one resource unit
T_{snapshot}	Time duration of one snapshot
T_{speech}	Random variable for the session duration of speech traffic
T_{sym}	Symbol duration
$\{x y = y_i\}$	Conditional random variable x under the condition that the realization of y has been y_i

Bibliography

- [3GP01] 3GPP, “Improvement of RRM across RNS and RNS/BSS,” TR 25.881, V5.0.0, Dec. 2001.
- [3GP06] —, “Physical layer aspects for evolved Universal Terrestrial Radio Access (UTRA),” TR 25.814, V7.1.0, Sep. 2006.
- [3GP08a] —, “Services and service capabilities,” TS 22.105, V9.0.0, Dec. 2008.
- [3GP08b] —, “UTRAN overall description,” TS 25.401, V8.2.0, Dec. 2008.
- [AB73] J. Aitchison and J. A. C. Brown, *The lognormal distribution: with special reference to its uses in economics*. Cambridge University Press, 1973.
- [ADSK03] G. Auer, A. Dammann, S. Sand, and S. Kaiser, “On modelling cellular interference for multi-carrier based communication systems including a synchronization offset,” in *Proc. of International Symposium on Wireless Personal Multimedia Communications*, Yokosuka, Japan, Oct. 2003.
- [AE99] D. Ayyagari and A. Ephremides, “Cellular multicode CDMA capacity for integrated (voice and data) services,” *IEEE J. Select. Areas Commun.*, vol. 17, no. 5, pp. 928 – 938, May 1999.
- [AML04] D. Avidor, S. Mukherjee, J. Ling, and C. Papadias, “On some properties of the proportional fair scheduling policy,” in *Proc. of International Symposium on Personal, Indoor and Mobile Radio Communications*, Barcelona, Spain, Sep. 2004.
- [Ang01] I. Angus, “An introduction to Erlang B and Erlang C,” *Telemangement*, no. 187, pp. 6 – 8, 2001.
- [APS99] M. Allman, V. Paxson, and W. R. Stevens, “TCP congestion control,” RFC 2581, Apr. 1999.
- [AW06] S. Aarnikoivu and J. Winter, “Mobile broadband wireless access,” in *Proc. of Research Seminar on Telecommunications Business*, Espoo, Finland, Jan. 2006.
- [BAS⁺05] K. Brueninghaus, D. Astély, T. Sälzer, S. Visuri, A. Alexiou, S. Karger, and G.-A. Seraji, “Link performance models for system level simulations of broadband radio access systems,” in *Proc. of International Symposium on Personal, Indoor and Mobile Radio Communications*, Berlin, Germany, Sep. 2005.
- [BBE64] H. Betz, P. B. Burcham, and G. M. Ewing, *Differential Equations with Applications*. Harper & Row, 1964.
- [Ber87] R. C. Bernhardt, “Macroscopic diversity in frequency reuse radio systems,” *IEEE J. Select. Areas Commun.*, vol. 5, no. 5, pp. 862 – 870, Jun. 1987.

- [BFM⁺97] K. Buchanan, R. Fudge, D. McFarlane, T. Phillips, A. Sasaki, and H. Xia, "IMT-2000: Service provider's perspective," *IEEE Personal Commun. Mag.*, vol. 4, no. 4, pp. 8 – 13, Aug. 1997.
- [BHIM05] C. F. Ball, E. Humburg, K. Ivanov, and R. Müllner, "Rapid estimation method for data capacity and spectrum efficiency in cellular networks," in *Proc. of IST Mobile and Wireless Communications Summit*, Dresden, Germany, Jun. 2005.
- [BHIT05a] C. F. Ball, E. Humburg, K. Ivanov, and F. Treml, "Comparison of IEEE802.16 WiMax scenarios with fixed and mobile subscribers in tight reuse," in *Proc. of IST Mobile and Wireless Communications Summit*, Dresden, Germany, Jun. 2005.
- [BHIT05b] —, "Performance analysis of IEEE802.16 based cellular MAN with OFDM-256 in mobile scenarios," in *Proc. of IEEE Vehicular Technology Conference*, Stockholm, Sweden, May 2005.
- [Bin90] J. A. C. Bingham, "Multicarrier modulation for data transmission: an idea whose time has come," *IEEE Commun. Mag.*, vol. 28, no. 5, pp. 5 – 14, May 1990.
- [BMLR04] J. Burns, P. Marks, F. LeBrogne, and R. Rudd, "Implications of digital switchover for spectrum management," Jun. 2004, study on Spectrum Management in the field of Broadcasting, Final Report, prepared for the European Commission.
- [BSC⁺04] Y. W. Blankenship, P. J. Sartori, B. K. Classon, V. Desai, and K. L. Baum, "Link error prediction methods for multicarrier systems," in *Proc. of Vehicular Technology Conference*, Los Angeles, USA, Sep. 2004.
- [BSS⁺97] A. Benyassine, E. Shlomot, H.-Y. Su, D. Massaloux, C. Lamblin, and J.-P. Petit, "ITU-T Recommendation G.729 Annex B: a silence compression scheme for use with G.729 optimized for V.70 digital simultaneous voice and data applications," *IEEE Commun. Mag.*, vol. 35, no. 9, pp. 64 – 73, Sep. 1997.
- [BXG07] W. Bolton, Y. Xiao, and M. Guizani, "IEEE 802.20: Mobile broadband wireless access," *IEEE Wireless Commun. Mag.*, vol. 14, no. 1, pp. 84 – 95, Feb. 2007.
- [CB07] J.-G. Choi and S. Bahk, "Cell-throughput analysis of the proportional fair scheduler in the single-cell environment," *IEEE Trans. Veh. Technol.*, vol. 56, no. 2, pp. 766 – 778, Mar. 2007.
- [CBD02] T. Camp, J. Boleng, and V. Davies, "A survey of mobility models for ad hoc network research," *Wireless Communications and Mobile Computing: Special issue on Mobile Ad Hoc Networking: Research, Trends and Applications*, vol. 2, no. 5, pp. 483 – 502, 2002.

- [CL99] H.-K. Choi and J. O. Limb, "A behavioral model of web traffic," in *Proc. of International Conference on Network Protocols*, Toronto, Canada, Nov. 1999.
- [CL01] Y. Cao and V. O. K. Li, "Scheduling algorithms in broad-band wireless networks," *Proc. IEEE*, vol. 89, no. 1, pp. 76–87, Jan. 2001.
- [CLC04] T. K. Chee, C.-C. Lim, and J. Choi, "Adaptive power allocation with user prioritization for downlink orthogonal frequency division multiple access systems," in *Proc. of International Conference on Communications Systems*, Singapore, Singapore, Sep. 2004.
- [CMN84] D. C. Cox, R. Murray, and A. Norris, "800 MHz attenuation measured in and around suburban houses," *AT&T Bell Laboratory Technical Journal*, vol. 673, no. 6, Jul. - Aug. 1984.
- [COS91] COST 231, "Urban transmission loss models for mobile radio in the 900 and 1800 MHz bands," TD(90)119 Rev. 2, Sep. 1991.
- [CT91] T. M. Cover and J. A. Thomas, *Elements of Information Theory*. John Wiley & Sons Inc., 1991.
- [Dav81] H. A. David, *Order Statistics*. John Wiley & Sons Inc., 1981.
- [DS04] A. Das and A. Sampath, "Link error prediction for wireless system simulations," in *Proc. of Wireless Communications and Networking Conference*, Atlanta, USA, Mar. 2004.
- [EFK⁺06] H. Ekström, A. Furuskär, J. Karlsson, M. Meyer, S. Parkvall, J. Torsner, and M. Wahlqvist, "Technical solutions for the 3G Long-Term Evolution," *IEEE Commun. Mag.*, vol. 44, no. 3, pp. 38–45, Mar. 2006.
- [EKL05] M. Einhaus, O. Klein, and M. Lott, "Interference averaging and avoidance in the downlink of an OFDMA system," in *Proc. of International Symposium on Personal, Indoor and Mobile Radio Communications*, Berlin, Germany, Sep. 2005.
- [Erl17] A. K. Erlang, "Solutions of some problems in the theory of probabilities of significance in automatic telephone exchanges," *Electroteknikeren*, vol. 13, pp. 5–13, 1917.
- [ETS98] ETSI European Telecommunications Standards Institute, "Universal mobile telecommunications system (UMTS); selection procedure for the choice of radio transmission technologies of the UMTS," TR 101 112 v3.2.0, Apr. 1998.
- [FB08] M. Feher and H. Bühler, "The vienna reference scenario," COST 2100 TD(08) 534, Jun. 2008. [Online]. Available: <http://www.cost2100.org>
- [FKCS05] T. Frank, A. Klein, E. Costa, and E. Schulz, "IFDMA - a promising multiple access scheme for future mobile radio systems," in *Proc. of International Symposium on Personal, Indoor and Mobile Radio Communications*, Berlin, Germany, Sep. 2005.

- [FKW⁺07] A. Fernekeß, A. Klein, B. Wegmann, K. Dietrich, and E. Humburg, "Performance of IEEE 802.16e OFDMA in tight reuse scenarios," in *Proc. of International Symposium on Personal, Indoor and Mobile Radio Communications*, Athens, Greece, Sep. 2007.
- [FKW⁺08] A. Fernekeß, A. Klein, B. Wegmann, K. Dietrich, and M. Litzka, "Load dependent interference margin for link budget calculations of OFDMA networks," *IEEE Commun. Lett.*, vol. 12, no. 5, pp. 398 – 400, May 2008.
- [FKWD06] A. Fernekeß, A. Klein, B. Wegmann, and K. Dietrich, "Influence of traffic models and scheduling on the system capacity of packet-switched mobile radio networks," in *Proc. of IST Mobile and Communications Summit*, Mykonos, Greece, Jun. 2006.
- [FKWD07] ———, "Influence of high priority users on the system capacity of mobile networks," in *Proc. of IEEE Wireless Communications and Networking Conference*, Hong Kong, China, Mar. 2007.
- [FKWD09a] ———, "Analysis of cellular mobile networks using fair throughput scheduling," in *Proc. of International Symposium on Personal, Indoor and Mobile Radio Communications*, Tokyo, Japan, Sep. 2009.
- [FKWD09b] ———, "Estimating cell throughput of OFDMA systems with scheduling," in *Proc. of International Wireless Communications and Mobile Computing Conference*, Leipzig, Germany, Jun. 2009.
- [FKWD09c] ———, "Modular system-level simulator concept for OFDMA systems," *IEEE Commun. Mag.*, vol. 47, no. 3, pp. 150 – 156, Mar. 2009.
- [Flo97] J. Flood, *Telecommunication networks*. IEE London, 1997.
- [FN00] R. Fantacci and S. Nannicini, "Multiple access protocols for integration of variable bit rate multimedia traffic in UMTS/IMT-2000 based on wideband CDMA," *IEEE J. Select. Areas Commun.*, vol. 18, no. 8, pp. 1441 – 1454, Aug. 2000.
- [GH74] D. Gross and C. M. Harris, *Fundamentals of Queueing Theory*. John Wiley & Sons Inc., 1974.
- [GKT⁺08] A. Greenspan, M. Klerer, J. Tomcik, R. Canchi, and J. Wilson, "IEEE 802.20: Mobile broadband wireless access for the twenty-first century," *IEEE Commun. Mag.*, vol. 46, no. 7, pp. 56 – 63, Jul. 2008.
- [GLMS09] R. Giuliano, P. Loreti, F. Mazzenga, and G. Santella, "Planning and performance evaluation of OFDM/OFDMA multi-carrier cellular systems with femto cells," in *Proc. of International Wireless Communications and Mobile Computing Conference*, Leipzig, Germany, Jun. 2009.
- [GM09] R. Giuliano and F. Mazzenga, "Dimensioning of OFDM/OFDMA-based cellular networks using exponential effective SINR," *IEEE Trans. Veh. Technol.*, vol. 58, no. 8, pp. 4204 – 4213, Oct. 2009.

- [GN96] P. E. Greenwood and M. S. Nikulin, *A guide to chi-squared testing*. John Wiley & Sons Ltd, 1996.
- [Goo02] B. Goode, “Voice over internet protocol (VoIP),” *Proc. IEEE*, vol. 90, no. 9, pp. 1495 – 1517, Sep. 2002.
- [GP99] R. A. Guérin and V. G. Peris, “Quality-of-service in packet networks: basic mechanisms and directions,” *The International Journal of Computer and Telecommunications Networking*, vol. 31, no. 3, pp. 169 – 189, Feb. 1999.
- [Gud91] M. Gudmundson, “Correlation model for shadow fading in mobile radio systems,” *Electronics Letters*, vol. 27, no. 23, pp. 2145 – 2146, Nov. 1991.
- [Hah91] E. L. Hahne, “Round-robin scheduling for max-min fairness in data networks,” *IEEE J. Select. Areas Commun.*, vol. 9, no. 7, pp. 1024 – 1039, Sep. 1991.
- [Hat80] M. Hata, “Empirical formula for propagation loss in land mobile radio services,” *IEEE Trans. Veh. Technol.*, vol. 29, no. 3, pp. 317 – 325, Aug. 1980.
- [HB02] K. Hiltunen and N. Binucci, “WCDMA downlink coverage: Interference margin for users located at the cell coverage border,” in *Proc. of IEEE Vehicular Technology Conference*, Birmingham, USA, May 2002.
- [HDP⁺04] M. Hildebrand, K. David, G. Piao, R. Sigle, D. Zeller, and I. Karla, “Performance investigation on multi standard radio resource management for circuit switched services,” in *Proc. of IST Mobile and Wireless Communications Summit*, Jun. 2004.
- [HHS99] S. Hämmäläinen, H. Holma, and K. Sipilä, “Advanced WCDMA radio network simulator,” in *Proc. of International Symposium on Personal, Indoor and Mobile Radio Communications*, Osaka, Japan, Sep. 1999.
- [HNA00] M. Hassan, A. Nayandoro, and M. Atiqussaman, “Internet telephony: Services, technical challenges, and products,” *IEEE Commun. Mag.*, vol. 38, no. 4, pp. 96 – 103, Apr. 2000.
- [Hol01] J. M. Holtzman, “Asymptotic analysis of proportional fair algorithm,” in *Proc. of International Symposium on Personal, Indoor and Mobile Radio Communications*, San Diego, USA, Oct. 2001.
- [HP03] S. Hara and R. Prasad, *Multicarrier techniques for 4G mobile communications*. Artech House, 2003.
- [HPD⁺04] M. Hildebrand, G. Piao, K. David, R. Sigle, D. Zeller, and I. Karla, “Performance investigation of multi standard radio resource management for packet switched services,” in *Proc. of IEEE Vehicular Technology Conference*, Los Angeles, USA, Sep. 2004.

- [HS04] T. Hoßfeld and D. Staehle, “A semi-analytic model of the UMTS downlink capacity with WWW traffic on dedicated channels,” Research Report No. 340, University of Würzburg, Sep. 2004.
- [HSH⁺97] S. Hämmäläinen, P. Slanina, M. Hartman, A. Lappeteläinen, H. Holma, and O. Salonaho, “A novel interface between link and system level simulations,” in *Proc. of ACTS Summit*, Aalborg, Denmark, Oct. 1997.
- [HSVC03] C. Y. Huang, H. Y. Su, S. Vitebsky, and P.-C. Chen, “Schedulers for 1xEV-DO: third generation wireless high-speed data systems,” in *Proc. of IEEE Vehicular Technology Conference*, Seoul, Korea, Apr. 2003.
- [HT02] H. Holma and A. Toskala, *WCDMA for UMTS*. John Wiley & Sons, Ltd, 2002.
- [HT06] ———, *HSDPA/HSUPA for UMTS: High Speed Radio Access for Mobile Communications*. John Wiley & Sons Ltd, 2006.
- [HtB03] B. M. Hochwald and S. ten Brink, “Achieving near-capacity on a multiple-antenna channel,” *IEEE Trans. Commun.*, vol. 51, no. 3, pp. 389 – 399, Mar. 2003.
- [IEE05] IEEE Std.802.16e-2005, “IEEE Standard for Local and metropolitan area networks, Part 16: Air Interface for Fixed Broadband Wireless Access Systems, Amendment 2: Physical and Medium Access Control Layers for Combined Fixed and Mobile Operation in Licensed Bands,” Dec. 2005.
- [II94] International Organization for Standardization and International Electrical Commission, “Information technology - open systems interconnection - basic reference model: The basic model,” ISO/IEC 7498-1, Nov. 1994.
- [IM92] G. Immovilli and M. L. Merani, “A new methodology for the evaluation of outage probability in cellular systems,” in *Proc. of International Conference on Communications*, Chicago, USA, Jun. 1992.
- [Inf81a] Information Sciences Institute, “Internet protocol,” RFC 791, Sep. 1981.
- [Inf81b] ———, “Transmission control protocol,” RFC 793, Sep. 1981.
- [ITU97] ITU-R Recommendation M.1255, “Guidelines for evaluation of radio transmission technologies for IMT-2000,” 1997.
- [ITU00] ITU-R Report M.2023, “Spectrum requirements for international mobile telecommunications-2000 IMT-2000,” 2000.
- [ITU03] ITU-T Recommendation G.114, “One-way transmission time,” May 2003.
- [ITU06] ITU-R Working Party 8F, “Summary of spectrum usage survey results for WRC-07 Agenda item 1.4,” Feb. 2006.
- [Jai91] R. Jain, *The Art of Computer Systems Performance Analysis*. John Wiley & Sons Inc., 1991.

- [JK77] N. L. Johnson and S. Kotz, *Urn models and their application: an approach to modern discrete probability theory*. John Wiley & Sons Ltd, 1977.
- [JKHO06] T. Javornik, G. Kandus, A. Hrovat, and I. Ozimek, "Comparison of WiMAX coverage at 450MHz and 3.5GHz," in *Proc. of International Conference on Software in Telecommunications and Computer Networks*, Split - Dubrovnik, Croatia, Sep. 2006.
- [JL03] J. Jang and K. B. Lee, "Transmit power adaptation for multiuser OFDM systems," *IEEE J. Select. Areas Commun.*, vol. 21, no. 2, pp. 171 – 178, Feb. 2003.
- [JPP00] A. Jalali, R. Padovani, and R. Pankaj, "Data throughput of CDMA-HDR a high efficiency-high data rate personal communication wireless system," in *Proc. of Vehicular Technology Conference*, Tokyo, Japan, May 2000.
- [JZY⁺07] H. Jia, Z. Zhang, G. Yu, P. Cheng, and S. Li, "On the performance of IEEE 802.16 OFDMA system under different frequency reuse and subcarrier permutation patterns," in *Proc. of International Conference on Communications*, Glasgow, UK, Jun. 2007.
- [KB83] D. L. Keefer and S. E. Bodily, "Three-point approximations for continuous random variables," *Management Science*, vol. 29, no. 5, pp. 595 – 609, May 1983.
- [Ken51] D. G. Kendall, "Some problems in the theory of queues," *Journal of Royal Statistical Society*, vol. 13, no. 2, pp. 151 – 173, Mar. 1951.
- [KFM02] T. E. Kolding, F. Frederiksen, and P. E. Mogensen, "Performance aspects of WCDMA systems with high speed downlink packet access (HSDPA)," in *Proc. of Vehicular Technology Conference*, Vancouver, Canada, Sep. 2002.
- [KH95] R. Knopp and P. A. Humblet, "Information capacity and power control in single-cell multiuser communications," in *Proc. of International Conference on Communications*, Seattle, USA, Jun. 1995.
- [KKHY04] H. Kim, K. Kim, Y. Han, and S. Yun, "A proportional fair scheduling for multicarrier transmission systems," in *Proc. of Vehicular Technology Conference*, Los Angeles, USA, Sep. 2004.
- [Kle75] L. Kleinrock, *Queueing Systems, Volume I: Theory*. John Wiley & Sons Ltd, 1975.
- [Kol03] T. E. Kolding, "Link and system performance aspects of proportional fair scheduling in WCDMA/HSDPA," in *Proc. of Vehicular Technology Conference*, Vancouver, Canada, Oct. 2003.
- [Kür98] T. Kürner, "Radio network aspects and planning issues for evolving mobile radio systems," in *Proc. of COST252/259 Joint Workshop: Communications for the Millenium*, Bradford, UK, Apr. 1998.

- [Kür01] ———, “Advanced propagation models for GSM1800 and UMTS,” in *Proc. of Asia-Pacific Radio Science Conference*, Tokyo, Japan, Aug. 2001.
- [Kür05] ———, “The role of propagation models for the development and deployment of future wireless communication systems,” in *Proc. of International Conference on Electromagnetics in Advanced Applications*, Torino, Italy, Sep. 2005.
- [Lan68] F. W. Lancaster, *Information Retrieval Systems: Characteristics, Testing, and Evaluation*. John Wiley & Sons Inc., 1968.
- [LBS99] S. Lu, V. Bharghavan, and R. Srikant, “Fair scheduling in wireless packet networks,” *IEEE/ACM Trans. Networking*, vol. 7, no. 4, pp. 473 – 489, Aug. 1999.
- [Lit61] J. D. C. Little, “A proof for the queuing formula: $L=\lambda w$,” *Operations Research*, vol. 9, no. 3, pp. 383 – 387, May 1961.
- [LJZ09] D. López-Pérez, A. Jüttner, and J. Zhang, “Dynamic system-level simulation of dynamic frequency planing for real time services in WiMAX networks,” in *Proc. of International Wireless Communications and Mobile Computing Conference*, Jun. 2009.
- [LW01] J. Laiho and A. Wacker, “Radio network planning process and methods for WCDMA,” *Annals of Telecommunications*, vol. 56, no. 5-6, pp. 317 – 331, May 2001.
- [LWN02] J. Laiho, A. Wacker, and T. Novosad, *Radio Network Planning and Optimisation for UMTS*. John Wiley & Sons, Ltd, 2002.
- [LWNH01] J. Laiho, A. Wacker, T. Novosad, and A. Hämäläinen, “Verification of WCDMA radio network planning prediction methods with fully dynamic network simulator,” in *Proc. of IEEE Vehicular Technology Conference*, Atlantic City, USA, Oct. 2001.
- [LWS00] J. Laiho-Steffens, A. Wacker, and K. Sipilä, “Verification of 3G radio network dimensioning rules with static network simulations,” in *Proc. of IEEE Vehicular Technology Conference*, Tokyo, Japan, May 2000.
- [LZ06] K. B. Letaief and Y. J. Zhang, “Dynamic multiuser resource allocation and adaptation for wireless systems,” *IEEE Wireless Commun. Mag.*, vol. 13, no. 4, pp. 38 – 47, Aug. 2006.
- [Mah97] B. A. Mah, “An empirical model of HTTP network traffic,” in *Proc. of IEEE INFOCOM*, Kobe, Japan, Apr. 1997.
- [MFK⁺06] S. N. Moiseev, S. A. Filin, M. S. Kondakov, A. V. Garmonov, D. H. Yim, J. Lee, S. Chang, and Y. S. Park, “Analysis of the statistical properties of the interference in the IEEE 802.16 OFDMA network,” in *Proc. of Wireless Communications and Networking Conference*, Las Vegas, USA, Apr. 2006.

- [Mis04] A. R. Mishra, *Fundamentals of Cellular Network Planning and Optimisation*. John Wiley & Sons Ltd, 2004.
- [MLTS97] J. G. Markoulidakis, G. L. Lyberopoulos, D. F. Tsirkas, and E. D. Sykas, "Mobility modeling in third generation mobile telecommunication systems," *IEEE Personal Commun. Mag.*, vol. 4, no. 4, pp. 41 – 56, Apr. 1997.
- [Mol05] A. F. Molisch, *Wireless Communications*. John Wiley & Sons Ltd, 2005.
- [MOM03a] MOMENTUM Project, "Deliverable D5.2: Reference scenarios," Nov. 2003.
- [MOM03b] —, "Final report on automatic planning and optimisation," Oct. 2003.
- [NBL05] J. Niemelä, J. Borkowski, and J. Lempiäinen, "Performance of static WCDMA simulator," in *Proc. of International Symposium on Wireless Personal Multimedia Communications*, Aalborg, Denmark, Sep. 2005.
- [New08] Newport networks, "VoIP bandwidth calculation," 2008. [Online]. Available: www.newport-networks.com
- [NGM08] NGMN Alliance, "Next generation mobile networks radio access performance evaluation methodology," White Paper, Jan. 2008. [Online]. Available: www.ngmn.org
- [OOKF68] Y. Okumura, E. Ohmori, T. Kawano, and K. Fukuda, "Field strength and its variability in the VHF and UHF land mobile service," *Review Electronic Communication Lab.*, vol. 16, no. 9 - 10, pp. 825 – 873, Sep. - Oct. 1968.
- [Ort07] S. Ortiz, "4G wireless begins to takeshapes," *IEEE Computer*, vol. 40, no. 11, pp. 18 – 21, Nov. 2007.
- [Pap84] A. Papoulis, *Probability, Random Variables, and Stochastic Processes*, 2nd ed. McGraw Hill, 1984.
- [Par01] J. D. Parsons, *The Mobile Radio Propagation Channel*. John Wiley & Sons Ltd, 2001.
- [Pät02] M. Pätzold, *Mobile fading channels*. John Wiley & Sons Ltd, 2002.
- [PGL⁺97] R. Pandya, D. Grillo, E. Lycksell, P. Mieybegue, H. Okinaka, and M. Yabusaki, "IMT-2000 standards: Network aspects," *IEEE Personal Commun. Mag.*, vol. 4, no. 4, pp. 20 – 29, Aug. 1997.
- [PKM06] A. Pokhariyal, T. E. Kolding, and P. E. Mogensen, "Performance of down-link frequency domain packet scheduling for the utran long term evolution," in *Proc. of International Symposium on Personal, Indoor and Mobile Radio Communications*, Helsinki, Finland, Sep. 2006.
- [Pos80] J. Postel, "User datagram protocol," RFC 768, Aug. 1980.
- [Pro01] J. G. Proakis, *Digital communications*, 4th ed. McGraw Hill, 2001.

- [PY04] G. Parsaee and A. Yarali, "OFDMA for the 4th generation cellular networks," in *Proc. of Canadian Conference on Electrical and Computer Engineering*, Niagara Falls, Canada, May 2004.
- [Rap02] T. S. Rappaport, *Wireless Communications Principles and Practice*, 2nd ed. Prentice Hall PTR, 2002.
- [RC00] W. Rhee and J. M. Cioffi, "Increase in capacity of multiuser OFDM system using dynamic subchannel allocation," in *Proc. Vehicular Technology Conference*, Tokyo, Japan, May 2000.
- [RGC⁺99] A. Reyes-Lecuona, E. González-Parada, E. Casilari, J. C. Casasola, and A. Díaz-Estrella, "A page-oriented WWW traffic model for wireless system simulations," in *Proc. of International Teletraffic Congress*, Edinburgh, UK, Jun. 1999.
- [Sam98] A. Samukic, "UMTS universal mobile telecommunications system: Development of standards for the third generation," *IEEE Trans. Veh. Technol.*, vol. 47, no. 4, pp. 1099 – 1104, Nov. 1998.
- [SBEM90] S. C. Swales, M. A. Beach, D. J. Edwards, and J. P. McGeehan, "The performance enhancement of multibeam adaptive base-station antennas for cellular land mobile radio systems," *IEEE Trans. Veh. Technol.*, vol. 39, no. 1, pp. 56 – 67, Feb. 1990.
- [SCFJ03] H. Schulzrinne, S. L. Casner, R. Frederick, and V. Jacobson, "RTP: A transport protocol for real-time applications," RFC 3550, Jul. 2003.
- [SDLY00] K. Samaras, C. Demetrescu, C. Luschi, and R. Yan, "Capacity calculation of a packet switched voice cellular network," in *Proc. of IEEE Vehicular Technology Conference*, Tokyo, Japan, May 2000.
- [SFF⁺07] T. Svensson, T. Frank, D. Falconer, M. Sternad, E. Costa, and A. Klein, "B-IFDMA - a power efficient multiple access scheme for non-frequency-adaptive transmission," in *Proc. of IST Mobile and Wireless Communications Summit*, Budapest, Hungary, Jul. 2007.
- [SGLV09] I. Stupia, F. Giannetti, V. Lottici, and L. Vandendorpe, "A novel exponential link error prediction method for OFDM systems," *Lecture Notes in Electrical Engineering*, vol. 41, pp. 291 – 300, 2009.
- [SP01] P. Stuckmann and O. Paul, "Dimensioning GSM/GPRS networks for circuit- and packet-switched services," in *Proc. of International Symposium on Wireless Personal Multimedia Communications*, Aalborg, Denmark, Sep. 2001.
- [Ste94] W. R. Stevens, *TCP/IP illustrated: The protocols*. Addison-Weasley, 1994.
- [tBKA04] S. ten Brink, G. Kramer, and A. Ashikhmin, "Design of low-density parity-check codes for modulation and detection," *IEEE Trans. Commun.*, vol. 52, no. 4, pp. 670 – 678, Apr. 2004.

- [TH01] K. Tigerstedt and K. Heiska, "Static WCDMA system simulator for indoor environments," in *Proc. of IEEE Vehicular Technology Conference*, Rhodes, Greece, May 2001.
- [Tim05] B. Timus, "Cost analysis issues in a wireless multihop architecture with fixed relays," in *Proc. of IEEE Vehicular Technology Conference*, Stockholm, Sweden, May 2005.
- [TW05] E. Tuomaala and H. Wang, "Effective SINR approach of link to system mapping in OFDM/multi-carrier mobile network," in *Proc. of International Conference on Mobile Technology, Applications and Systems*, Guangzhou, China, Nov. 2005.
- [UMT99] UMTS Forum, "UMTS/IMT-2000 spectrum," Report from the UMTS Forum No. 6, Jun. 1999.
- [vNP00] R. van Nee and R. Prasad, *OFDM for wireless multimedia communications*. Artech House, 2000.
- [VTL02] P. Viswanath, D. N. C. Tse, and R. Laroia, "Opportunistic beamforming using dumb antennas," *IEEE Trans. Inform. Theory*, vol. 48, no. 6, pp. 1277 – 1294, Jun. 2002.
- [WDK⁺08] C. Wijting, K. Doppler, K. Kalliojärvi, N. Johansson, J. Nystrom, M. Olsson, A. Osseiran, M. Döttling, J. Luo, T. Svensson, M. Sternad, G. Auer, T. Lestable, and S. Pfletschinger, "WINNER II system concept: Advanced radio technologies for future wireless systems," in *Proc. of ICT-Mobile Summit*, Stockholm, Sweden, Jun. 2008.
- [WDK⁺09] C. Wijting, K. Doppler, K. Kalliojärvi, T. Svensson, M. Sternad, G. Auer, N. Johansson, J. Nystrom, A. Osseiran, M. Döttling, J. Luo, T. Lestable, and S. Pfletschinger, "Key technologies for IMT-Advanced mobile communication systems," *IEEE Wireless Commun. Mag.*, vol. 16, no. 3, pp. 76 – 85, Jun. 2009.
- [WGL⁺05] F. Wang, A. Ghosh, R. Love, K. Stewart, R. Ratasuk, R. Bachu, Y. Sun, and Q. Zhao, "IEEE 802.16e system performance: analysis and simulations," in *Proc. of International Symposium on Personal, Indoor and Mobile Radio Communications*, Berlin, Germany, Sep. 2005.
- [WiM07] WiMAX Forum, "WiMAX system evaluation methodology," Version 2.01, Dec. 2007.
- [WIN06] WINNER Project, "Deliverable D6.13.7: Test scenarios and calibration cases issue 2," Dec. 2006.
- [WIN08] ———, "Deliverable D6.13.14: WINNER II system concept description," Jan. 2008.
- [WLSJ99] A. Wacker, J. Laiho-Steffens, K. Sipilä, and M. Jäsberg, "Static simulator for studying WCDMA radio network planning issues," in *Proc. of IEEE Vehicular Technology Conference*, Houston, USA, May 1999.

-
- [Yac93] M. D. Yacoub, *Foundations of mobile radio engineering*. CRC Press, 1993.
- [YL00] H. Yin and H. Liu, “An efficient multiuser loading algorithm for OFDM-based broadband wireless systems,” in *Proc. of Global Telecommunications Conference*, San Francisco, USA, Dec. 2000.
- [Zim80] H. Zimmermann, “OSI reference model - ISO model of architecture for open systems interconnection,” *IEEE Trans. Commun.*, vol. 28, no. 4, pp. 425 – 432, Apr. 1980.
- [ZK01] J. Zander and S.-L. Kim, *Radio Resource Management for Wireless Networks*. Artech House, 2001.
- [ZL04] Y. J. Zhang and K. B. Letaief, “Multiuser adaptive subcarrier-and-bit allocation with adaptive cell selection for OFDM systems,” *IEEE Trans. Wireless Commun.*, vol. 3, no. 5, pp. 1566 – 1575, Sep. 2004.

Curriculum Vitae

Name: Andreas Fernekeß
Anschrift: Auf der Hardt 63, 64291 Darmstadt
Geburtsdatum: 03.07.1977
Geburtsort: Frankfurt am Main, Deutschland
Familienstand: ledig

Schulbildung

08.1984 - 07.1988 August-Jaspert Grundschule in Frankfurt, Deutschland
08.1988 - 07.1997 Ziehen-Gymnasium in Frankfurt, Deutschland
Schulabschluss: Allgemeine Hochschulreife

Studium

10.1998 - 07.2004 Studium der Elektro- und Informationstechnik an Technische Universität Darmstadt,
Studienabschluß: Diplom-Ingenieur

Berufstätigkeit

seit 02.2005 wissenschaftlicher Mitarbeiter am Fachgebiet Kommunikationstechnik, Institut für Nachrichtentechnik, Technische Universität Darmstadt
07.2004 - 01.2005 Werkstudent bei Panasonic R & D Center Germany GmbH
08.1997 - 08.1998 Zivildienstleistender bei Caritas Sozialstation

Darmstadt, 26.03.2010

Erklärung laut §9 der Promotionsordnung

Ich versichere hiermit, dass ich die vorliegende Dissertation allein und nur unter Verwendung der angegebenen Literatur verfasst habe. Die Arbeit hat bisher noch nicht zu Prüfungszwecken gedient.

Darmstadt, 26. März 2010,

